



CENTRO INTERNACIONAL DE ESTUDOS
DE DOUTORAMENTO E AVANZADOS
DA USC (CIEDUS)

TESE DE DOUTORAMENTO

**THEORETICAL AND
COMPUTATIONAL**

**STUDY OF THE STRUCTURE AND
DYNAMICS OF IONIC LIQUID
MIXTURES: THERMODYNAMICAL
AND INTERFACIAL PROPERTIES**

Borja Docampo Álvarez

ESCOLA DE DOUTORAMENTO INTERNACIONAL
PROGRAMA DE DOUTORAMENTO EN CIENCIA DE MATERIAIS

SANTIAGO DE COMPOSTELA

2018





DECLARACIÓN DO AUTOR/A DA TESE

**Theoretical and Computational Study of the Structure and Dynamics of
Ionic Liquid Mixtures: Thermodynamical and Interfacial Properties**

D. Borja Docámpo Álvarez

Presento a miña tese, seguindo o procedemento axeitado ao Regulamento, e declaro que:

- 1) A tese abarca os resultados da elaboración do meu traballo.
- 2) De selo caso, na tese faise referencia ás colaboracións que tivo este traballo.
- 3) A tese é a versión definitiva presentada para a súa defensa e coincide coa versión enviada en formato electrónico.
- 4) Confirmo que a tese non incorre en ningún tipo de plaxio doutros autores nin de traballos presentados por min para a obtención doutros títulos.

En Santiago de Compostela, a 15 de Outubro de 2018

Asdo: Borja Docampo Álvarez.





AUTORIZACIÓN DO DIRECTOR / TITOR DA TESE

Theoretical and Computational Study of the Structure and Dynamics of Ionic Liquid Mixtures:
Thermodynamical and Interfacial Properties

D. Luis Javier Gallego del Hoyo e D. Luis Miguel Varela Cabo, catedráticos da área de Física da Materia Condensada, do Departamento de Física de Partículas da Universidade de Santiago de Compostela,

INFORMAN:

Que a presente tese, correspóndese co traballo realizado por D. Borja Docampo Álvarez, baixo a nosa dirección, e autorizamos a súa presentación, considerando que reúne os requisitos esixidos no Regulamento de Estudos de Doutoramento da USC, e que como directores desta non incorre nas causas de abstención establecidas na Lei 40/2015.

De acordo co artigo 41 do Regulamento de Estudos de Doutoramento, declaramos tamén que a presente tese de doutoramento é idónea para ser defendida en base á modalidade de COMPENDIO DE PUBLICACIÓNS, nos que a participación do/a doutorando/a foi decisiva para a súa elaboración.

A utilización destes artigos nesta memoria, está en coñecemento dos coautores, tanto doutores como non doutores. Ademais, estes últimos teñen coñecemento de que ningún dos traballos aquí reunidos poderá ser presentado en ningunha outra tese de doutoramento.

En Santiago de Compostela, a 15 de Outubro de 2018

Asdo: D. Luis Javier Gallego del Hoyo

D. Luis Miguel Varela Cabo



Summary

Ionic liquids (ILs) are amphiphilically nanostructured ionic compounds with a characteristically low melting point, under 100 °C, that have been the focus of intense scientific study in recent years. Their highly uncommon combination of properties (low volatility, good electrochemical properties and stability, as well as their nanostructured solvation mechanisms) make them a viable, more eco-friendly alternative to traditional solvents. Furthermore, due to the great number of anion-cation combinations that will result in an IL, it is theoretically possible to fine-tune their properties for specific applications, leading the scientific community to refer to them as “designer solvents”. To achieve this tunability, a deep, systematic study of ionic liquids is first required, as no comprehensive theory that can explain their final properties from the initial choice of anion and cation (a structure-property relationship) exists yet. This is doubly important for mixtures of two or more ILs, the result of which is a new IL with properties that do not necessarily follow ideal mixing rules.

Many of the properties of ILs are difficult to access experimentally. Furthermore, the large number of possible ILs, combined with the cost of synthesizing them, make large scale experimental studies of ILs initially unapproachable. Fortunately, development of ILs as a field of research was concurrent with the increasingly widespread availability of computational power. Computer simulations allow for fast, systematic and relatively inexpensive studies of ILs under arbitrary conditions, with full access to the microstates of the system at every moment, making them a powerful tool both to further theoretical research and to plan experimental studies with.

The focus of this thesis is studying and understanding the mixing

mechanisms of ILs, with water, short chained alcohols, and, primarily, with other ILs; and their impact on bulk and interfacial properties. Understanding the behavior of these mixtures is key for designing application-specific ILs, but this knowledge has other, more immediate uses. In the case of water, due to the highly hygroscopic nature of ILs, a degree of water contamination should be expected in most cases, and understanding its impact, especially for highly sensitive and application-critical properties such as conductivity, is extremely important. Additionally, with water, but also with alcohol, the nanoscale structure of the resulting mixture allows us to better understand the role of hydrogen bonding mechanisms in protic ionic liquids (PILs), a subset of ILs with hydrogen acceptor and donor sites that lead to their self-assembly into hydrogen bonded networks. For this, extensive molecular dynamics (MD) simulations of the involved systems were performed using the GROMACS simulation suite and the OPLS-AA force field. This force field, optimized for simulations of organic liquids, allows for accurate predictions of most structural properties, and, despite its non-polarizable nature, has also been shown to qualitatively predict trends for transport properties.

The first part of this work deals with mixtures of molecular co-solvents with ILs. In the first article of the six composing this thesis, mixtures of the PIL ethylammonium nitrate (EAN) with water, methanol and ethanol were characterized. EAN is peculiar among ILs in that its three-dimensional hydrogen bonded network is similar to that of water. By means of MD simulations, mixtures with all three co-solvents with concentrations throughout the entire mixing range were studied. These mixtures were prepared in the laboratory too, and their density measurements compared to the values obtained from the simulations to validate the parametrizations used, finding that deviations were small in all cases, below 2%. Density behavior with concentration was observed to be different for both alcohols and water, with the former varying progressively along the entire concentration range and the latter showing slow changes with small water concentrations and a more pronounced variation near pure water. The microscopic

structure of the mixtures was studied by means of radial distribution functions (rdfs), coordination numbers, number of hydrogen bonds, and spatial distribution functions (sdfs). From this data, a progressive, homogeneous mixing process was deduced, in which cosolvents accommodate themselves in the hydrogen bonded network formed by the liquid. These mixing dynamics stand in opposition to what had been previously observed for water in aprotic ionic liquids (AILs), where a tendency towards clustering was detected. In the case of water, an inversion of the height of the two first cation-water rdf peaks around 60% water concentration was found, indicating the replacement of $[\text{NO}_3]^-$ anions by water molecules on the cation's polar head, with the anions being displaced closer towards the ethyl carbon chain. This image of progressive integration in the PIL hydrogen bond network was reinforced by the monotonical variation of coordination numbers and hydrogen bonds per molecule. Furthermore, an inflection point can be observed for cation-water coordination numbers at intermediate concentrations, highlighting the point at which the aforementioned replacement process is finished. Around the $[\text{NO}_3]^-$ anion, sdfs showed two very different coordination structures for water and alcohols: while alcohols coordinate with oxygen atoms in a monodentate way, water coordinates between oxygen pairs, in a bidentate way. Finally, the tighter integration of water into the PIL hydrogen bond network was confirmed by means of their velocity autocorrelation functions (vacf), where an oscillatory behavior, indicative of a rattling motion, was found for water but not for alcohols. This suggests a certain degree of caging by the water molecules' nearest neighbors, especially at lower concentrations.

The second article deals with water contamination in ILs near graphene surfaces, and, more specifically, its evolution under nanoconfinement. As IL confinement has been shown to be advantageous for certain electrochemical applications, and water strongly affects the electrochemical properties of ILs, knowledge of how confinement impacts the distribution of residual water inside the cell is a key consideration. Simulation boxes with the AIL 1-butyl-3-methyl-imidazolium

tetrafluoroborate ([BMIM][BF₄]) and a 5% molar content of water, equivalent to about 4200 ppm in weight, and slit distances ranging between 1.5 nm to 12 nm were investigated. For each distance, both neutral and charged walls (with electrode surface charge densities of $\pm 1 \text{ e/nm}^2$) were considered. The results from these simulations were analyzed by means of number density profiles of each species in the direction perpendicular to the wall, the lateral density maps for the innermost layer of the electric double layer (EDL), the angular orientation of water molecules, and their vibrational states. In neutral systems, the interfacial structure of the IL reached 1.5 to 2 nm deep. In systems under 4 nm of size, and therefore no proper bulk region, this interfacial ordering is reinforced, with water settling at the low ion density regions near the second layer. For charged systems, the characteristic structure of alternating anion and cation layers in the EDL was observed for systems of all sizes, and water was found predominantly at the positively charged electrode, with only residual amounts near the negatively charged one. Careful analysis, by means of the potential of the mean force (PMF), showed that part of the reason for this is a much higher energy barrier to move through the first cation layer near the negatively charged electrode, making water adsorption more difficult. However, this barrier was also found to decrease under confinement conditions, while for neutral and positive surface it remained roughly the same.

Regarding the lateral structure of the liquid, close to the positively charged electrode, a transition from ordered long stripes to a hexagonal distribution of anions was observed when comparing to the pure IL and attributed to the addition of water. The orientation of water molecules was recorded and histogrammed, and it was found that, while it was random across the bulk region, near interfaces water shows strong preferences, towards the surface near negatively charged surfaces and towards nearby anions near positively charged surfaces. Regarding the vibrational densities of states (vdos) of water molecules, a blue-shift of their vibrational spectrum was reported under confinement conditions, indicating that they are more strongly bound in their positions by the

surrounding molecules. Finally, using this simulation data, a simple adsorption model of energy levels (one for the bulk and another for each interfacial region) was introduced. A fit of model parameters to estimations of the energy levels obtained from the PMF of the simulated systems was made, and it was shown that simulations indeed follow the predictions of the model to a reasonable degree, except for the case of extremely confined neutral systems, in which the restructuring of the IL shifts water towards the second ionic layer, causing a sharp depletion beyond what the model predicts.

The third and final article in this section focuses on experimental measurements, supported by MD simulations, of mixtures of EAN, propylammonium nitrate (PAN), and butylammonium nitrate (BAN) with water and ethanol in order to better understand the influence of the alkyl chain length on the properties of the mixture, as well as its interaction with hydrogen bonds. This experiment-focused work was proposed with the main goal of validating theoretical conclusions about nanostructured solvation in PILs drawn from the work presented in the first article. Surface tensions, densities and refractive indexes were measured at room temperature and atmospheric pressure for the entire concentration range of the six mixtures studied. In all cases, density decreases when cationic alkyl chain length increases. Furthermore, excess molar volumes were calculated and found to be small but always negative. Refraction indices were also obtained from these measurements by means of the phenomenological Gladstone-Dale model and compared to experimental data. Both sets were found to be in good agreement, showing a close relationship between both magnitudes and making refractive indices of these mixtures easy to obtain. Surface tension results with water showed a rapid decrease with small concentrations of PIL, indicating that the PIL occupies the interfacial region preferentially at low concentrations, similar to a surfactant. This trend was found to be more pronounced with longer alkyl chain lengths, and more gradual in mixtures with ethanol, with little variation until equimolar concentrations. Finally, these results were compared to the rdfs obtained from simulations of these mixtures.

The differences shown between water and ethanol mixtures, with water molecules inside the polar region of the liquid and the alcohol group of ethanol in the border between polar and apolar regions, were related to the different behavior for surface tensions, as ethanol molecules will be more likely to be found at the interface.

In the second part of this work, two articles dealing with bulk mixtures of ILs and one with mixtures of ILs near interfaces are presented. In particular, the focus was the study of mixtures of one PIL (an alkylammonium nitrate) and one AIL (a 1-alkyl-3-methylimidazolium tetrafluoroborate). The choice of two well known but dissimilar ILs was intentional, since the different structural organization of the liquids, and especially the hydrogen bonding present in PILs, is expected to lead to novel nonideal behaviors beyond those observed in mixtures of similar ILs. Indeed, in the fourth article of this thesis, a novel behavior for conductivity was reported in mixtures of [EMIM][BF₄] and EAN. This experimental curve shows a local maximum, upon initial addition of EAN to pure [EMIM][BF₄], as well as a global minimum at intermediate, almost equimolar concentrations. To reproduce this, MD simulations of the mixtures were made, and analyzed by means of their rdfs, sdfs, vacfs, and vdos, as well as structure factors, mean square displacements (MSDs) and diffusion coefficients for each species.

Initially, the density of simulated systems was compared to experimental measurements and a good agreement was found, with differences no higher than 1.25%. The excess molar volume of the mixtures was also calculated, with very small positive excess volumes found. These excess volumes are larger than other reported values for mixtures of ILs, but still small enough to make density behave almost ideally in these mixtures. EAN addition leads to a tighter packing of [EMIM]⁺ and [BF₄]⁻, reflected in a shift of the second and following peaks of the corresponding rdf towards closer positions, until 70% EAN concentration, where this effect stops and long range ordering between both species starts to collapse. EAN, on the

other hand, maintains its characteristic anion-cation distribution until extremely diluted concentrations. The restructuring of the AIL component was highlighted by calculating their partial structure factor, the corresponding representation in the spatial frequency domain of the rdfs. Here, the difference between low and high PIL concentrations is made evident for EAN too, showing both protic ions settling at closer distances as their concentration increases. Finally, with regards to rdfs, atomic rdfs were also obtained for the three hydrogens of the imidazolium ring, showing, as expected, a preference for $[\text{NO}_3]^-$ anions near the more acidic hydrogen that is bound to the carbon between both nitrogen atoms in the ring, but also that these anions are in general more favored around the ring than $[\text{BF}_4]^-$. Therefore, $[\text{EMIM}]^+ - [\text{BF}_4]^-$ interactions are expected to occur outside the ring plane, leading to vertical association between $[\text{EMIM}]^+$ cations being favored. This preference was visualized by means of the sdfs around $[\text{EMIM}]^+$ cations, in which the competition for the more acidic hydrogen between both anions can also be appreciated. Coordination numbers were calculated for anions around both cations, and, considering the total number of anions around each cation, it was found that for $[\text{EA}]^+$ this number remains almost constant, while, for $[\text{EMIM}]^+$, it gradually converges towards that of $[\text{EA}]^+$, suggesting that the previously mentioned tighter packing is caused by the PIL component gradually imposing its structural behavior on the AIL. Indeed, when studying the number of hydrogen bonds per PIL ionic pair, it was found that they were directly proportional to PIL concentration, implying that the onset of the hydrogen bond network happens at very low concentrations and extends gradually as the PIL becomes more dominant.

With regards to single particle dynamics, MSDs, and from them, diffusion coefficients, were calculated for each species. While for anions and $[\text{EA}]^+$ diffusion coefficients remained mostly the same across the entire concentration range, $[\text{EMIM}]^+$ showed an increase upon initial mixing, followed by a gradual decrease as PIL concentration becomes higher. This, combined with the detailed microscopic

understanding of the structure, allowed us to explain the conductivity phenomena in the mixture, with the minimum being an effect of the decreased mobility of the $[\text{EMIM}]^+$ cation, which is in turn caused by the gradual but early onset of the PIL hydrogen bonded network. This causes conductivity to decrease until protic species are the dominant charge carriers, the point from which conductivity starts to converge towards the values of the pure PIL. Even though non-polarizable simulations cannot model transport properties precisely, the behavior trends of the experimental conductivity curve were qualitatively reproduced from simulation data, both with an Einstein-Helfand fit and with the Kohlrausch law. The validity of the second approach relies on assuming independent ionic motion, therefore implying that ionic association is not predominant in the mixture. But more importantly, being able to reproduce the mixture's conductivity behavior strictly from ionic motion implies that proton transfer mechanisms, hypothesized to be important in some transport phenomena involving PILs, do not play a significant role in determining the conductivity of the IL mixture.

After this, the effect of the alkyl chain length of both protic and aprotic cations in the mixture was analyzed in the fifth article. For this, mixtures of EAN, PAN and BAN with $[\text{EMIM}][\text{BF}_4]$ and $[\text{BMIM}][\text{BF}_4]$ were considered and studied with MD simulations, and their densities and conductivities measured experimentally. While in previous articles density had been used mainly as a means to validate the link between simulation and experiment, in this case unexpected deviations from ideality were found for high PIL concentrations in $[\text{EMIM}][\text{BF}_4]$ -PAN and $[\text{EMIM}][\text{BF}_4]$ -BAN mixtures. These larger deviations, studied in regards to in excess volume, had a negative sign, and hinted at the presence of stronger interactions between both components of the mixture. This was also reflected on the excess molar enthalpies of mixing, which were calculated for all systems and showed a pronounced peak for $[\text{EMIM}][\text{BF}_4]$ – PAN and $[\text{EMIM}][\text{BF}_4]$ – BAN mixtures upon initial AIL addition. This stood in opposition to $[\text{EMIM}][\text{BF}_4]$ – EAN and $[\text{BMIM}][\text{BF}_4]$ – EAN, which

behaved like regular mixtures (non-ideal enthalpy of mixing, but ideal entropy of mixing). An unsuccessful attempt to fit the former group to the subregular mixture model was made, after which it was concluded that some structural change was occurring to the pure PIL upon initial mixing, possibly the formation of intermolecular complexes. A study of the rdfs of the mixtures revealed that $[\text{BF}_4]^-$ anions were occupying positions near the PIL cation alkyl chains with little variation in rdf values over the entire concentration range. This was confirmed in $[\text{BA}]^+$ sdfs, where, additionally, it was shown that $[\text{EMIM}]^+$ cations occupy positions around the butyl chain. Comparison with pure BAN sdfs showed that this region was unoccupied in the pure liquid, surrounded only by other butyl chains. The disappearance of this ordering upon mixing with an AIL, whose ions preferentially occupy regions around the tail forming intermolecular complexes, was concluded to be the cause of the observed deviations from ideal behavior in the longer-chained PILs. This was further confirmed by EAN sdfs, where this region was already occupied in the pure IL and no structural reorganization occurred upon mixing. Additionally, sdfs around $[\text{EMIM}]^+$ and $[\text{BMIM}]^+$ cations were calculated, showing that vertical stacking happened on both, but was further reinforced by the presence of a longer, freely rotating butyl chain on $[\text{BMIM}]^+$.

Hydrogen bonds per PIL pair and coordination numbers were also obtained. Hydrogen bonds were the same for all mixtures at equivalent concentrations, and decreased exactly the same way; however, coordination numbers around PIL cations were shown to decrease slower for the longer chained PIL cations, highlighting again the association with AIL ions occurring in those mixtures. Structure factors were calculated, and by means of the polar-apolar partial structure factors, it was shown that the polar-apolar order faded with the addition of shorter-chained ILs. Evidence of some degree of clustering was also found; this was studied by converting the cations' distance matrix into a graph by means of a cut-off distance equal to the distance of their first rdf maxima. By extracting and analyzing the size of the connected components of this graph, it was determined that the onset

of the hydrogen bonded network happened at a concentration between 20% and 30%. Finally, velocity autocorrelation functions for protic cations were obtained, showing that while the smaller $[EA]^+$ cation was prone to short-term “caging”, this effect was not present for the larger PIL cations.

In the sixth and final article composing this thesis, the behavior near graphene surfaces of the IL mixtures previously studied was described, with an eye towards their possible applications in electrochemical devices. More specifically, $[EMIM][BF_4]$ -EAN, $[EMIM][BF_4]$ -BAN, $[BMIM][BF_4]$ -EAN and $[BMIM][BF_4]$ -BAN mixtures, at concentrations of 10%, 50% and 90% PIL as well as the corresponding pure IL components, were simulated in a box between two parallel graphene sheets separated 8 nm, under neutral and charged conditions. These systems were analyzed by means of calculating their number density profiles for each species in the direction perpendicular to the walls, the lateral density maps near the graphene surfaces, and the integral capacity of the EDL for both positively and negatively charged electrodes. The number densities showed two important phenomena taking place in the mixtures. Firstly, protic cations in charged simulations showed a marked preference towards the positive electrode, leaving the negative electrode with a prevalence of aprotic cations. This was interpreted as a consequence of hydrogen bonding between protic cations and the $[NO_3]^-$ anions in the first ionic layer being energetically favorable. Secondly, a restructuring of the EDL near negatively charged electrodes was detected. The first cationic layer splits into multiple maxima, some of them overlapping with the first anionic layer, which leads to an anion depletion in this region upon AIL addition. This effect was found to be nonlinear, with mixtures with 10% AIL being halfway in-between pure PIL systems and equimolar mixtures. The uneven distribution of cations had an effect on the lateral surface patterns found, as two-dimensional protic-aprotic (as well as polar-apolar) segregation was found near the electrodes. In aprotic-dominated mixtures, a gradual transition from stripe (fluid-like) to hexagonal (solid-like) patterns upon PIL addition

was found. This is related to a decrease in the mobility of $[\text{BF}_4]^-$ anions in the presence of PIL by means of the Minkowski parameters of the mixture. From this and from the orientation of the protic cation, it was concluded that hydrogen bonding has a key influence on the interfacial structure of the mixtures. Finally, integral capacitance was calculated for both positively and negatively charged electrodes. It was found that capacitance near the positively charged electrode varies smoothly and only by a small amount. However, near the negatively charged electrode, capacitance remains almost constant from 0% to 50% PIL and then increases sharply. This nonlinear behavior was found to be the consequence of the previously discussed replacement of PIL cations by AIL cations near the electrode. This has a marked effect on both charge density and contact distance, and its influence on the inner structure of the EDL also impacted capacitance. The impact of this inner structure on capacitance was shown by means of a simple theoretical model featuring a dampened oscillating charge density.

Finally, a brief summary of the main conclusions extracted from this work, as well as some discussion on possible future research lines, can be found at the end of this thesis.



Resumen

Los líquidos iónicos (ILs) son compuestos iónicos anfifilicamente nanoestructurados con un punto de fusión bajo, inferior a $100\text{ }^{\circ}\text{C}$, que han sido objeto de atención por parte de la comunidad científica en los últimos años. Su peculiar combinación de propiedades tales como su baja volatilidad, ventajosas características electroquímicas y elevada estabilidad, así como sus mecanismos de solvatación nanoestructurada, los hacen una posible alternativa “verde” respecto a disolventes convencionales. Además, gracias al gran número de combinaciones anión-cación que dan lugar a un IL, es teóricamente posible ajustar sus propiedades para usos específicos, hecho que ha llevado a la comunidad científica a referirse a ellos como “disolventes de diseño”. Para hacer posible este proceso de diseño, es necesario realizar previamente un estudio extenso y sistemático de estos disolventes, ya que aún no ha sido desarrollada una teoría general que permita explicar las propiedades finales del líquido a partir de la elección inicial de anión y catión (es decir, una relación estructura-propiedad). Esto es doblemente importante en el caso de mezclas de dos o más ILs, que forman un nuevo IL con propiedades que no necesariamente tienen por qué seguir reglas de mezcla ideales.

Muchas de las propiedades de los ILs son difíciles de explorar experimentalmente. No solo eso, sino que el gran número de ILs posible, combinado con los costes asociados a su síntesis, hacen estudios experimentales a gran escala en principio inviables. Afortunadamente, el desarrollo de los ILs como campo de investigación ha coincidido en el tiempo con los progresivos avances en recursos computacionales, así como su mayor disponibilidad. Las simulaciones por ordenador permiten realizar estudios rápidos, sistemáticos y relativamente asequibles de ILs bajo condiciones arbitrarias, con pleno acceso a los

microestados del sistema en cualquier instante temporal, convirtiéndolos en una potente herramienta tanto para realizar avances en estudios teóricos como para planificar estudios experimentales.

El tema principal de esta tesis es el estudio y comprensión de los mecanismos de mezcla de los ILs, con agua, alcoholes de cadena corta, y, principalmente, con otros ILs, y el impacto que estos tienen en sus propiedades de *bulk* e interfase. Un conocimiento *a priori* del comportamiento de estas mezclas es clave para el diseño de ILs para casos específicos, pero, además, estos resultados tienen otras aplicaciones mucho más inmediatas. En el caso específico del agua, dada la naturaleza altamente higroscópica de los ILs, su presencia, en grado residual, es en muchos casos inevitable. Entender el impacto que este contenido de agua tiene, especialmente en propiedades críticas y altamente sensibles a ella como la conductividad eléctrica, es sumamente importante. Además, no solo con el agua sino también con el alcohol, la nanoestructura de la mezcla nos permite entender mejor el rol de los mecanismos de enlace de hidrógeno en la estructura de los líquidos iónicos próticos (PILs), una clase de ILs con sitios aceptores y donores de hidrógeno que dan lugar a su autoensamblado en redes enlazadas por hidrógenos. Para ello, se realizaron numerosas simulaciones de dinámica molecular (MD) de los sistemas estudiados, mediante el *software* de simulación GROMACS y el campo de fuerzas OPLS-AA. Este campo de fuerzas, optimizado para la simulación de líquidos orgánicos, permite realizar predicciones precisas de propiedades estructurales, y, aún siendo un campo de fuerzas no polarizado, ha sido empleado con éxito en diversos trabajos para realizar predicciones cualitativas sobre propiedades de transporte.

La primera parte de este trabajo trata sobre mezclas de ILs con cosolventes moleculares. En el primer artículo de los seis que constituyen esta tesis, mezclas de un PIL, el nitrato de etilamonio (EAN), con agua, metanol y etanol fueron estudiadas y caracterizadas. El EAN es peculiar entre los PILs en que su red de enlaces de hidrógeno se asemeja en cierta medida a la del agua. Mediante simulaciones de

MD, se estudiaron mezclas de este líquido con los tres cosolventes en concentraciones que comprendían la totalidad del rango de mezcla. Estas mezclas fueron, además, preparadas en laboratorio, y sus densidades medidas experimentalmente para su comparación con los valores obtenidos mediante simulación, con el objetivo de validar los parámetros empleados. Las desviaciones sobre estos valores experimentales fueron pequeñas, menores al 2% en todos los casos. Se encontró que la respuesta de la densidad frente a la concentración variaba entre las mezclas con alcoholes y con agua, con las primeras mostrando una progresión lenta a lo largo del rango de mezcla y la segunda sufriendo pequeños cambios a bajas concentraciones de agua y variaciones más fuertes a concentraciones más altas. La estructura microscópica de las mezclas fue estudiada mediante sus funciones de distribución radial (rdfs), números de coordinación, número de enlaces de hidrógeno por par iónico y funciones de distribución espacial (sdfs). A partir de estos datos, se concluyó que se trata de un proceso de mezcla homogéneo, en el que los cosolventes se incorporan progresivamente en la red de enlaces de hidrógeno del líquido. Esta dinámica contrasta con lo que había sido observado previamente para el agua en mezclas con líquidos iónicos apróticos (AILs), donde se detectó una tendencia a formar pequeños *clusters*. En el caso concreto del agua en PILs, se detectó además una inversión en la altura relativa de los dos primeros máximos de la rdf catión-agua, indicando que en torno a esta concentración se produce una sustitución de aniones por moléculas de agua en torno a la cabeza polar del catión, siendo los aniones desplazados a posiciones más próximas a la cola. Esta imagen de una integración progresiva del cosolvente en la red de enlaces de hidrógeno del PIL se ve reforzada por la variación monótona tanto de números de coordinación como del número de enlaces de hidrógeno por molécula. Además, se puede observar un punto de inflexión, a concentraciones intermedias, en los números de coordinación catión-agua, indicando el punto en el que el proceso de sustitución mencionado anteriormente ha finalizado. Alrededor del anión $[\text{NO}_3]^-$, las sdfs revelaron dos estructuras de coordinación distintas para agua y alcoholes: los alcoholes coordinan con los átomos de oxígeno de

forma monodentada, mientras que, en el caso del agua, las moléculas se sitúan en los puntos intermedios de cada par de átomos de oxígeno, coordinando de forma bidentada. Finalmente, se verificó de nuevo que el agua se integra más intensamente en la red de enlaces de hidrógeno mediante sus correspondientes funciones de autocorrelación de velocidades (vacfs), donde se detectó, en el caso del agua pero no de los alcoholes, un comportamiento oscilatorio. Esto sugiere la presencia, especialmente a bajas concentraciones de agua, de un “efecto caja”, en el que la molécula de agua se ve temporalmente atrapada entre sus vecinos cercanos.

El segundo artículo se centra en la contaminación por agua residual en ILs en las proximidades de una superficie de grafeno, y, en particular, su evolución en situaciones de nanoconfinamiento. Ya que varios estudios han mostrado que el confinamiento de ILs es beneficioso para su uso en ciertos procesos electroquímicos, y dado que el agua puede alterar fuertemente las propiedades electroquímicas del IL, saber cómo una situación de nanoconfinamiento influye en la distribución del agua en la celda es clave a la hora de considerar su uso práctico. Se prepararon cajas de simulación con el AIL tetrafluoroborato de 1-butil-3-metil-imidazolio ([BMIM][BF₄]) y un contenido en agua de un 5 % molar, el equivalente a unas 4200 ppm en peso, confinadas entre dos láminas de grafeno a distancias que variaban desde 1.5 nm a 12 nm. Para cada distancia, se estudió el caso de una celda neutra y el caso cargado, para el cual se tomaron densidades de carga superficiales de $\pm 1 \text{ e/nm}^2$ en los electrodos. Los resultados obtenidos de las simulaciones fueron analizados a través de los perfiles de densidad numérica de cada especie en la dirección perpendicular a las paredes, los mapas de densidad lateral (superficial) de la primera capa de la doble capa eléctrica (EDL), la orientación angular de las moléculas de agua y sus estados vibracionales. En los casos neutros, la estructura interfacial del IL alcanzaba de 1.5 a 2 nm de profundidad. En sistemas de tamaños menores a 4 nm, y por tanto sin región de *bulk* definida, esta estructura interfacial se ve reforzada, con el agua situándose predominantemente en las regiones de baja

densidad iónica cerca de la segunda capa. En sistemas cargados, se observa la presencia de la estructura de capas alternas de aniones y cationes característica de la EDL para todos los tamaños, con el agua apareciendo predominantemente en el electrodo positivo, mostrando solo una presencia residual en el negativo. Un análisis detallado a través del potencial de la fuerza media (PMF) mostró que uno de los motivos detrás de este fenómeno es una barrera de energía mucho más alta en la capa catiónica próxima al electrodo negativo, dificultando la adsorción de agua a este. Esta barrera, sin embargo, decrece progresivamente bajo condiciones de confinamiento, mientras que las barreras de potencial en electrodos neutros y positivos se mantiene relativamente constante.

Estudiando la estructura lateral del líquido, se detectó, para el electrodo positivo, una transición de patrones lineales a una distribución hexagonal de aniones una vez se añadía agua al IL. La orientación de las moléculas de agua fue grabada e histogramada, encontrándose que, si bien es aleatoria en la región de *bulk*, el agua de las regiones interfaciales muestra preferencias marcadas, orientándose hacia la pared en la región próxima al electrodo negativo y hacia aniones cercanos en la región próxima al electrodo positivo. En cuanto a las densidades de estado vibracionales (vDOS) de las moléculas de agua, se encontró un desplazamiento hacia el azul de su espectro vibracional bajo condiciones de confinamiento, indicando mayores restricciones en su movimiento debido al efecto de moléculas cercanas. Por último, usando los datos obtenidos mediante estas simulaciones, se planteó un modelo simple de adsorción basado en niveles energéticos, uno para la región de *bulk* y otro para cada una de las regiones interfaciales, y realizando un ajuste de los parámetros del modelo a estimaciones de los niveles de energía basados en los PMF, se obtuvo que las simulaciones cumplen en un grado razonable las predicciones del modelo, con la notable excepción de los sistemas neutros extremadamente confinados, en los que la reestructuración del IL desplaza las moléculas de agua a la segunda capa iónica, causando una disminución en la cantidad de agua más allá de las predicciones del modelo.

El tercer y último artículo de esta primera parte se centra en medidas experimentales, apoyadas por simulaciones MD, de mezclas de EAN, nitrato de propilamonio (PAN) y nitrato de butilamonio (BAN) con agua y etanol, con el objetivo de entender mejor la influencia de la longitud de la cadena del catión en las propiedades de la mezcla, así como su interacción con los enlaces de hidrógeno. Este ejercicio de corte experimental se propuso, también, con vistas a validar las conclusiones teóricas sobre la solvatación nanoestructurada en PILs obtenidas en el primer artículo. Se midieron, a lo largo de todo el intervalo de mezcla de las seis mezclas estudiadas, densidades, tensiones superficiales e índices de refracción, a temperatura ambiente y presión atmosférica. En todos los casos, una mayor longitud de cadena lleva a un descenso en la densidad. Los volúmenes de exceso asociados fueron calculados, siendo, en todos los casos, pequeños y siempre negativos. Además, a partir de las densidades se calcularon los índices de refracción de las mezclas mediante el modelo de Gladstone-Dale. Los valores obtenidos son próximos a los índices de refracción obtenidos experimentalmente, mostrando una relación cercana entre las dos magnitudes. Los resultados de las medidas de tensión superficial en mezclas con agua muestran un rápido descenso con bajas concentraciones de PIL, indicando que este ocupa preferentemente la región interfacial como lo haría un surfactante. Esta tendencia es más marcada para longitudes de cadena más largas, y mucho más gradual para mezclas con etanol, en las que se aprecia muy poca variación hasta llegar a concentraciones equimolares. Por último, los resultados experimentales fueron contrastados con las rdfs obtenidas mediante simulaciones MD de estas mezclas. Las diferencias encontradas entre mezclas con agua y con etanol, con las moléculas de agua situándose en la región polar del líquido y los grupos alcohol del etanol situándose en las zonas limítrofes entre las regiones polar y apolar, fueron asociadas al comportamiento de la tensión superficial y la mayor afinidad del etanol por situarse en la interfase.

En la segunda mitad de esta tesis se presentan dos artículos sobre mezclas en *bulk* de ILs y un tercero sobre estas mezclas en presencia

de interfases. En concreto, el objeto de estudio de estos trabajos fueron mezclas de un PIL (de la familia de los nitratos de alquilamonio) y un AIL (de los tetrafluoroboratos de 1-alquil-3-metilimidazolio). Esta elección de dos ILs bien conocidos pero con marcadas diferencias entre ellos fue realizada con la intención de que sus diferencias a nivel estructural, y en concreto las interacciones por enlace de hidrógeno presentes en los PILs, lleven a la aparición de comportamientos no ideales novedosos, no presentes en las mezclas de ILs con características similares. En el cuarto artículo de esta tesis se presenta uno de estos comportamientos, una novedosa respuesta no ideal de la conductividad frente a la concentración en mezclas de [EMIM][BF₄] con EAN. Esta curva, obtenida experimentalmente, muestra un máximo local al añadir pequeñas cantidades de EAN a [EMIM][BF₄], así como un mínimo global a concentraciones intermedias, casi equimolares. Para reproducir estos resultados, se realizaron simulaciones mediante MD de estas mezclas, y los resultados fueron estudiados a través de sus rdfs, sdfs, vacfs, vdos, factores de estructura, desplazamientos cuadráticos medios (MSDs) y coeficientes de difusión de cada especie.

Como primer paso, se compararon las densidades de los sistemas simulados con sus correspondientes medidas experimentales, viéndose que las diferencias eran menores al 1.25 %. Los volúmenes molares de exceso de cada mezcla fueron también calculados, dando en este caso valores pequeños y positivos, mayores que los valores medidos en otros estudios sobre mezclas de ILs, pero aún lo suficientemente pequeños como para que pueda considerarse que la densidad se comporta de manera prácticamente ideal en estos sistemas. La introducción del EAN en el [EMIM][BF₄] conlleva un empaquetamiento más compacto de sus iones constituyentes, hecho que se refleja en un desplazamiento de los picos segundo y posteriores de las correspondientes rdfs, situándose en posiciones más cercanas hasta llegar a una concentración de 70 % EAN, donde este efecto termina y el orden de largo alcance entre los iones apróticos empieza a desaparecer. Los iones del EAN, por otra parte, mantienen su distribución anión-cación característica hasta concentraciones altamente diluidas.

La reestructuración del componente aprótico de la mezcla se puso aún más de manifiesto al calcular los factores de estructura, la representación en el dominio de frecuencia espacial de las rdfs. Mediante ellas se pudo apreciar también la diferencia entre concentraciones altas y bajas de PIL para el EAN, al mostrar cómo los iones próticos se sitúan a distancias progresivamente más cercanas según su concentración aumenta. Por último, en lo que concierne a las rdfs, se calcularon las rdfs atómicas correspondientes a los tres hidrógenos del anillo imidazolio, mostrando, como era de esperar, una preferencia por parte del $[\text{NO}_3]^-$ por situarse cerca del hidrógeno más ácido, es decir, el que se encuentra situado entre los dos nitrógenos del anillo. Pero, además, se apreció que los nitratos eran por lo general más favorecidos a la hora de ocupar posiciones alrededor del plano del anillo que los $[\text{BF}_4]^-$. Por lo tanto, se puede esperar que las interacciones $[\text{EMIM}]^+ - [\text{BF}_4]^-$ ocurran predominantemente fuera del plano del anillo, llevando a favorecer asociaciones verticales. Este hecho se visualizó claramente una vez calculadas las sdfs alrededor de los cationes $[\text{EMIM}]^+$, en las que la competición entre aniones por el hidrógeno ácido se aprecia también de forma evidente. Los números de coordinación de aniones alrededor de ambos cationes fueron calculados. La suma de ambos alrededor del $[\text{EA}]^+$ permanece prácticamente constante, mientras que para el $[\text{EMIM}]^+$ converge gradualmente hacia los valores del $[\text{EA}]^+$, lo que sugiere que el empaquetamiento más compacto es consecuencia del hecho de que el componente prótico impone progresivamente su estructura al componente aprótico. El cómputo del número de enlaces de hidrógeno por par iónico de PIL mostró un resultado directamente proporcional a su concentración, con la implicación de que, efectivamente, la estructura del PIL, con su red de enlaces de hidrógeno asociada, aparece a concentraciones muy bajas y se extiende gradualmente según el PIL se vuelve dominante en la mezcla.

Respecto a la dinámica de las moléculas de la mezcla, se calculó para cada especie su MSD, y, a partir de estos, los coeficientes de difusión. Si bien para ambos aniones y para el $[\text{EA}]^+$ los coeficientes de difusión permanecen estables en todo el intervalo de mezcla, para

el [EMIM]⁺ se observa un ligero aumento al mezclar PIL, seguido de su progresiva disminución según la concentración de PIL aumenta. Esto, combinado con la información que los resultados anteriores ofrecen sobre la estructura de la mezcla, permite explicar los fenómenos detrás de la curva de conductividad encontrada, en la que el mínimo es consecuencia de este descenso en la movilidad del [EMIM]⁺, que a su vez es consecuencia de la aparición gradual pero temprana de la red de enlaces de hidrógeno. Esto lleva a un descenso en la conductividad eléctrica hasta el punto en el que los portadores de carga dominantes pasan a ser los iones próticos, momento en el cual la conductividad vuelve a aumentar convergiendo rápidamente hacia los valores del PIL puro. Aunque los modelos no polarizables no permiten reproducir propiedades de transporte de forma precisa, estos comportamientos fueron reproducidos de forma cualitativa a partir de los datos de las simulaciones, tanto mediante un ajuste Einstein-Helfand como a través de la ley de Kohlrausch. La validez del segundo método se asienta en la hipótesis de que el movimiento de cada especie iónica es independiente, lo que implica que en este caso la asociación entre especies iónicas no es un efecto importante en estas mezclas. Pero una conclusión mucho más importante es que poder reproducir el comportamiento de la conductividad únicamente a través del movimiento iónico implica que los mecanismos de transferencia de protones, considerados potencialmente importantes a la hora de determinar el comportamiento de los PILs y sus propiedades electroquímicas y de transporte, no están jugando un papel relevante a la hora de determinar la conductividad de la mezcla.

Después de esto, en el quinto artículo se estudia el efecto de la longitud de la cadena alquílica en la mezcla, tanto en cationes próticos como apróticos. Para este trabajo, mezclas de EAN, PAN y BAN con [EMIM][BF₄] y [BMIM][BF₄] fueron estudiadas mediante simulaciones MD, y sus densidades y conductividades medidas experimentalmente. Si bien en los artículos anteriores la densidad había mostrado comportamientos cerca de la idealidad y su estudio se había usado principalmente como una forma de validar experimentalmente

los resultados obtenidos por simulación, en este caso se encontraron inesperadamente desviaciones de la idealidad en las mezclas con [EMIM][BF₄]-PAN y [EMIM][BF₄]-BAN. Estas desviaciones, en el contexto del volumen de exceso, toman valores negativos, sugiriendo la aparición de interacciones entre ambos componentes de la mezcla. Las desviaciones también se pudieron observar en las entalpías molares de exceso de mezcla, calculadas para todos los sistemas, en las que aparece un pico pronunciado para mezclas con [EMIM] [BF₄] – PAN y [EMIM] [BF₄] – BAN en el momento en el que se añade AIL al PIL puro. Por otra parte, tanto la mezcla [EMIM] [BF₄] – EAN como la mezcla [BMIM] [BF₄] – EAN se comportan como mezclas regulares, con una entalpía de mezcla no ideal pero una entropía de mezcla ideal. Tras un intento infructuoso de ajustar estas dos primeras mezclas al modelo subregular, se concluyó que algún cambio estructural estaba ocurriendo en el seno del líquido en el momento de la mezcla, posiblemente la formación de complejos intermoleculares. Un estudio de las rdfs de las mezclas reveló que los aniones [BF₄]⁻ ocupan posiciones cerca de las cadenas de carbono del catión prótico, con poca variación en los valores de la rdf a lo largo del intervalo de mezcla. Este hecho fue corroborado mediante las sdfs en torno al [BA]⁺, donde además se pudo observar que el catión [EMIM]⁺ ocupa posiciones cercanas al grupo butil. Esta región se encuentra vacía en el BAN puro, estando las cadenas alquílicas rodeadas únicamente de otras cadenas. La desaparición de este orden polar-apolar al mezclar los dos líquidos, y la asociación de los iones de ambos componentes formando complejos multi-iónicos se tomó como causa fundamental tras las desviaciones de la idealidad observadas en estos líquidos. Añadiendo peso a esta hipótesis, se observó en las sdfs del EAN que este proceso no tiene lugar en el caso de este líquido, ya que la región en torno a la cadena se encuentra ya rodeada de centros polares en su estado puro. También se calcularon sdfs centradas alrededor de los cationes [EMIM]⁺ y [BMIM]⁺, mostrando los fenómenos de asociación vertical mencionados anteriormente, que, en el caso del [BMIM]⁺, se veían reforzados por la presencia de una cadena de longitud más larga y con libertad de movimiento para rotar.

También se calcularon tanto el número de enlaces de hidrógeno por par iónico de PIL como los números de coordinación. El número de enlaces de hidrógeno obtenido fue el mismo para todas las mezclas a concentraciones similares, mostrando la misma evolución; sin embargo, se observó que los números de coordinación en torno a cationes próticos disminuyen más lentamente, apuntando de nuevo a la asociación con iones apróticos en estas mezclas. Se obtuvieron los factores de estructura, y, mediante los parciales correspondientes a la organización polar-apolar, se mostró que esta nanoheterogeneidad desaparece al añadir LIs de cadena más corta. Ante indicios de clustrización a bajas concentraciones, se estudió este fenómeno creando un grafo mediante la aplicación de una distancia de corte, igual a la posición del primer máximo de la rdf, a la matriz de distancias entre cationes. Del tamaño de las componentes conexas de este grafo se pudo determinar que la red de enlaces de hidrógeno se establecía a lo largo del líquido en concentraciones entre el 20 % y el 30 %. Por último, las funciones de autocorrelación de velocidades de los cationes fueron obtenidas, mostrando que el “efecto caja” se da en el caso del catión $[EA]^+$ pero no para los cationes próticos de mayor tamaño.

En el sexto y último artículo de esta tesis, se describe el comportamiento de estas mezclas de dos ILs cerca de superficies de grafeno, con vistas a su posible aplicación en dispositivos electroquímicos. En concreto, se realizaron simulaciones de mezclas $[EMIM][BF_4]$ -EAN, $[EMIM][BF_4]$ -BAN, $[BMIM][BF_4]$ -EAN y $[BMIM][BF_4]$ -BAN, a concentraciones de 10 %, 50 % y 90 %, así como los líquidos puros, en cajas de 8 nm de ancho confinadas entre dos superficies de grafeno paralelas, bajo condiciones neutras y cargadas. De nuevo, el análisis de estos sistemas se realizó mediante los perfiles de densidad numérica de las distintas especies en la dirección normal a las paredes, los mapas de densidad lateral cerca de las superficies de grafeno, y la capacitancia integral de la EDL para los electrodos positivo y negativo. El estudio de las densidades numéricas reveló dos fenómenos importantes en estas mezclas. En primer lugar, los cationes próticos muestran una fuerte preferencia por regiones cercanas al electrodo

positivo, dejando el electrodo negativo con una abundancia de cationes apróticos. Este fenómeno se interpretó como una consecuencia de la posibilidad de formar enlaces de hidrógeno con los aniones $[\text{NO}_3]^-$ de la primera capa, lo que convierte estas posiciones en energéticamente más favorables. En segundo lugar, se detectó una peculiar evolución de estructura de la EDL cerca del electrodo negativo. La primera capa catiónica se divide en múltiples máximos de la densidad iónica, algunos de ellos solapándose con regiones propias de la primera capa aniónica, lo que lleva a un vaciamiento de aniones en la región según se añade AIL. Este efecto es no lineal, con mezclas con un 10 % de AIL encontrándose a medio camino entre el PIL puro y las mezclas equimolares. La distribución asimétrica de los aniones tiene consecuencias claras en los patrones de la estructura lateral en la interfase del sistema, en la que se encontró segregación planar, tanto prótica-aprótica como polar-apolar. En las mezclas con predominancia aprótica, se observa una transición gradual entre patrones lineales (más fluidos) y hexagonales (más rígidos) al añadir PIL. Este efecto se relacionó, por medio de la obtención de los parámetros de Minkowski de los patrones, con una reducción de la movilidad de los aniones $[\text{BF}_4]^-$. A partir de esta observación y de la orientación del catión prótico, se pudo concluir que los enlaces de hidrógeno también juegan un papel clave en la estructura interfacial de las mezclas. Por último, se calculó la capacitancia integral en los electrodos positivos y negativos. Se observó cómo la capacitancia cerca del electrodo positivo varía suavemente y en pequeñas cantidades. Sin embargo, cerca del electrodo negativo la capacitancia permanece casi constante entre 0 % y 50 % PIL para luego aumentar bruscamente. Este comportamiento no lineal se atribuyó a la anteriormente mencionada sustitución, en este electrodo, de cationes próticos por su contrapartida aprótica. Este fenómeno conlleva cambios importantes tanto en la densidad de carga como en la distancia de contacto, además de su influencia en el resto de la estructura de la EDL, alterando así la capacitancia en el electrodo. El impacto de la estructura interior de la EDL en la capacitancia fue discutido a través de un modelo teórico consistente en una densidad de carga oscilatoria y amortiguada.

Esta tesis concluye con un breve resumen de las conclusiones principales extraídas de este trabajo, así como una perspectiva sobre posibles líneas de trabajo futuras.





Agradecimientos

Durante el desarrollo de esta tesis, he recibido el ánimo, apoyo y afecto de una gran cantidad de personas a las que me gustaría dedicar una breve mención. Este trabajo no habría, sin su presencia, llegado a ser lo que hoy es, y quiero por tanto agradecerles su aportación a esta etapa de mi vida. Gracias, porque esta tesis es tan vuestra como mía.

- A mi padre y mi madre, cuyo apoyo, económico pero sobre todo anímico, resultó determinante para animarme a embarcarme en estos estudios.
- A Luis, mi director de tesis, que estuvo ahí cuando otros no estuvieron.
- A Javier, mi otro director de tesis, con quién es imposible tener una conversación sin aprender algo nuevo.
- A Julio, compañero de desventuras en el laboratorio. Es difícil no acordarse con una sonrisa de todas las vueltas que dábamos a cada experimento hasta encontrar la forma perfecta de realizarlo.
- A Víctor, Hadrián y Txema, compañeros del día a día. Sus contribuciones a esta tesis son demasiadas para enumerar, pero entre ellas siempre destacará la cafetera del despacho.
- A Trini, Jesús y Silvia, que me enseñaron el día a día del grupo, aguantando pacientemente hasta que entendí por fin cómo funciona esto de la ciencia.
- A Óscar, y con él a todos nuestros colaboradores de la Universidad de Coruña. Espero tener la oportunidad de volver a pasar

por allí algún día (aunque solo sea para disfrutar de los bocatas de jamón serrano de su cafetería...)

- A mis compañeros y profesores del Máster de Finanzas de la Universidad de Vigo. El sacrificio de tener que ir a clases todos los fines de semana mereció la pena gracias a vosotros.
- A Ruth, Vladislav, y todos nuestros colaboradores de otras universidades. Siempre ha sido y será un placer encontrarme con vosotros en el congreso de turno.
- A Christian. Nunca me olvidaré de mis tres meses en Viena en tu compañía. Espero que algún día pueda devolverte la hospitalidad que me mostraste. Idealmente con un *Wild Ricochet*.
- Y, por supuesto, a Justin, Valerie, Christopher, Paul, Sahil... Algunos desde hace mucho, otros desde hace menos, pero todos estuvisteis ahí conmigo, esas largas noches, jugando, charlando, riendo. Y las que aún nos quedan.

Por último, mencionar que esta tesis fue realizada con las ayudas de los proyectos AGRUP2015/11, GRC ED431C 2016/001 y ED431-D 2017/06 (Xunta de Galicia), y de los proyectos MAT2014-57943-C3-1-P, MAT2014-57943-C3-2-P, MAT2014-57943-C3-3-P, MAT-2017-89239-C2-1-P, MAT2017-89239-C2-2-P, CTQ2015-65816-R y FIS2014-59279-P (Ministerio de Economía e Innovación) y FIS2012-33126 (Ministerio de Ciencia e Innovación); todos estos proyectos fueron financiados parciamente con fondos FEDER. Las acciones COST CM1206 y MP1303 (Unión Europea) también financiaron esta tesis.



A Antonio Docampo



Contents

1	Introduction	1
1.1	Motivation and purpose	1
1.2	Ionic liquids	6
1.3	Methodology	12
2	Results and Discussion	19
2.1	Mixtures of protic ionic liquids and molecular co-solvents: a molecular dynamics simulation	21
2.2	Molecular dynamics simulation of the behaviour of water in nano-confined ionic liquid-water mixtures	45
2.3	Surface and bulk characterisation of mixtures containing alkylammonium nitrates and water or ethanol: Experimental and simulated properties at 298.15 K	67
2.4	Molecular Dynamics Simulations of Mixtures of Protic and Aprotic Ionic Liquids	88
2.5	Effect of Alkyl Chain Length on the Structure and Thermodynamics of Protic-Aprotic Ionic Liquid Mixtures: A Molecular Dynamics Study	119
2.6	Molecular dynamics simulations of novel electrolytes based on mixtures of protic and aprotic ionic liquids at the electrochemical interface: structure and capacitance of the electric double layer	148
3	Conclusions and future perspectives	169
	Bibliography	175
	List of Tables	212
	List of Figures	214
	List of publications related to this thesis	223



1 Introduction

Before being a pirate, you should be a sailor.

The Secret of Monkey Island

1.1 MOTIVATION AND PURPOSE

Ionic liquids are considered by the scientific community one of the key materials of the 21st century. The increased ecological awareness developed by society during the second half of the 20th century has led to an urge to review and reinvent many of the industrial processes our economy is based on, resulting, among other significant changes, in the advent of the so-called “green chemistry”. Ionic liquids are uniquely positioned to replace traditional industrial solvents, many of which are massively produced, toxic volatile, organic compounds, due to properties such as their negligible vapor pressure or the possibility of recovering and reusing the liquid after each use. This ultimately means that, while ionic liquids are not intrinsically harmless (depending on the specifics, they can be highly toxic), they can be *designed* to be “eco-friendly”, a rationale that has led to the moniker “green solvents” being commonly employed when discussing these new materials.¹

“Design” is not a casually chosen word, and has a key meaning in the field of ionic liquids. The number of anion-cation combinations that can result in an ionic liquid is notoriously high. Additionally, most cations and a considerable amount of anions are organic molecules, in which the addition of new functional groups (such as -OH groups) or a variation in the length of alkyl chains leads to new, different ions. Each anion-cation combination will present a different set of

properties (discussed at length in the following subsection) which might range from helpful to hindrances, depending on the situation at hand. It is therefore often said that ionic liquids are *designer solvents*,² materials purposely tailor-made to fit the requirements of each specific application, prepared by cherry-picking a proper combination of anions and cations from those available that fits the desired properties.

This wide range of tunable properties makes ionic liquids have a great number of potential applications. Besides solvents, ionic liquids have seen use as catalysts, electrolytes, thermal fluids, lubricants, waste separators or nuclear material recovery media.²⁻⁸ Their use as electrolytes is an active research topic and one of the main motivations behind this thesis, as ionic liquids have some of the largest electrochemical windows known for solvents. This, combined with their aforementioned low vapor pressure, high thermal stability and wide liquidus range, makes the prospect of using them in batteries and capacitors attractive.

A systematic study of all ionic liquids is a challenging proposition, to say the least. This challenge is magnified to unrealistic dimensions after a simple realization: a mixture of two or more ionic liquids is also an ionic liquid. The estimated number⁹ of possible ternary mixtures of ionic liquids is of the order of 10^{18} , and we do not currently have an understanding of how the mixing process changes the properties of the mixture when compared to those of its pure components. In fact, generally speaking, it is not possible to know, before synthesising it, the properties of an ionic liquid with an arbitrary cation-anion combination. The ultimate goal of theoretical ionic liquid studies is developing a predictive framework that allows applied scientists and prospective users of ionic liquids to know which liquid(s) would suit their needs. Meanwhile, research must proceed on a case by case basis, studying the properties of specific ionic liquids.

This thesis is an attempt to contribute to the understanding of ionic liquids and their mixing mechanisms. Computer simulations, and in particular molecular dynamics, were the tool of choice for this study,

having proved themselves useful time and time again for the study of liquid systems, allowing easy access to microscopic features (such as their structure near graphene interfaces), and, more importantly, allowing large-scale studies limited only by the computational power available, a key consideration when approaching mixtures over their entire mixing range (which multiplies the number of systems to study).

The first half of this thesis studies mixtures of ILs with molecular cosolvents, namely water, methanol and ethanol, in an effort to better characterize nanostructured solvation, a fundamental property of these systems, and its interaction with hydrogen bonding. A number of previous efforts to describe the behavior of ILs with water and short-chained alcohols can be found in the literature.¹⁰⁻¹³ Many focus on the stability of specific ILs under different conditions, as well as their miscibility with water and the corresponding phase diagrams.¹¹ Cammarata *et al.* found experimentally, by means of spectroscopy studies, that water in $[\text{C}_n\text{MIM}]^+$ -based ILs associated preferentially with anions.¹² Gutowski *et al.* found that the water miscibility of $[\text{C}_n\text{MIM}]^+$ -based ILs could be controlled by means of mixtures with water-structuring salts.¹⁴ Mendez-Morales *et al.* studied, by means of MD simulations, the effect of anion hydrophobicity and cation chain length on the miscibility and microscopical structure of $[\text{C}_n\text{MIM}]^+$ -based ILs with water, reporting their velocity autocorrelation functions (vacf) for the first time.¹⁵ However, only a few studies of mixtures of PIL with water could be found.¹⁶⁻²² These reports were experimental in nature. For example, Greaves *et al.*^{23,24} used X-ray scattering to find that water molecules placed themselves around the polar region in several PILs, integrating with their hydrogen bonded network without greatly disturbing their structure. For alcohols, they found that the impact of the cosolvent on PIL structure was highly dependent on the relative length of the alkyl chains of alcohol and cation. No computational studies regarding the nanostructure of PIL and water mixtures could be found, however. Given the importance of hydrogen bonding to understand the structure of PILs, and, in particular, the similarity of EAN and its three-dimensional network with that of water, the case of mixing PILs

with water and short-chained alcohols (methanol and ethanol) was a natural first step in this thesis. As well as pure molecular dynamics (MD) studies, an analysis of their experimental properties and their interpretation is presented in this section.

The effect of low amounts of water in AILs near graphene surfaces was also studied. In many real-world applications, and in particular, for electrochemical and energy storage devices, ILs will be confined and exposed to neutral and charged surfaces. Interaction with confined geometries can change, sometimes dramatically, the properties of the IL,^{25,26} and understanding what affects these interactions lets engineers optimize both the IL and the device for better performance.²⁷ Many properties of both the interface (material, charge) and the IL (amphiphilicity) have been found to influence the resulting IL structure near the interface.^{28,29} In particular, a key property of ILs as dense ionic media is the appearance of a structure of alternating layers of anions and cations near charged interfaces, known as the electric double layer (EDL).³⁰⁻⁴³ Computer simulations are a helpful when approaching these systems. Indeed, a number of MD studies exist, detailing IL behavior in porous carbon²⁷ or graphene nanopores,⁴⁴ describing the structure of the EDL and analyzing the effect that monovalent^{45,46} and multivalent^{47,48} inorganic salts have on it. As mentioned before, water contamination is expected to some degree in ionic liquids.^{49,50} This is doubly important here, as water not only greatly alters some of the properties of ILs as described later in this chapter, but it can also impact electrochemical processes taking place near electrodes. Feng *et al.* described by means of MD simulations the adsorption of water molecules in imidazolium-based ILs near graphene surfaces.⁵¹ Chapter 2.2 follows up on this study by describing the effect of nanoconfinement on these mixtures as well as by providing a simple theoretical model for water adsorption. This research also showed, for the first time, that the lateral pattern formed by the ionic liquid near the graphene wall changes when water is added. Voltage-driven structural changes had previously been observed by Salanne *et al.*,^{52,53} this result and later research⁵⁴ generalize these

transitions as a consequence of changes in the charge density in the interfacial layer.

The second half of the results presented here focus on previously uncharted territory: mixtures of two dissimilar families of ionic liquids, in this case, alkylammonium nitrates (protic ionic liquids) and alkylmethylimidazoles (aprotic ionic liquids). Most studies of ionic liquid mixtures, as will be discussed in the next section, focus on two similar ionic liquids sharing a common anion or cation. Therefore, mixtures will show a larger degree of ideality and, in many cases, differing properties will simply be a direct result of the size difference between the original ion and the one replacing it. Our chosen protic and aprotic ionic liquids have not only notably different sizes and geometries, but also different intermolecular interactions, of which the strong hydrogen bonding present on protic ionic liquids is the most important. These differences make studying these systems a more complicated task, but, as presented in this thesis, have also been found to lead to rich and varied nonideal behavior in some of the resulting mixture's properties.

A number of studies on IL mixtures can be found on the literature,^{55,56} most of them focusing on imidazolium-based AILs.⁵⁷⁻⁶³ The fundamental question in most of these studies revolves about the ideality of the resulting mixture.⁶¹ Quitevis *et al.* performed an Optical Kerr Effect spectral analysis on mixtures containing different anions and found that, depending on the combination, the resulting spectra could be additive or nonadditive, implying, in the second case, that nanostructural changes from the pure components were occurring.^{57,58} Computational studies also exist. For example, Brüssel *et al.*^{59,60} used *ab initio* MD simulations to study mixtures of common-ion imidazolium-based ILs and concluded that they were quasi-ideal systems whose behavior was controlled by weak interactions related, for the most part, to competition between ions for specific sites. Lian *et al.* performed MD simulations of [EMIM] [BF₄]_x [TFSI]_{1-x} mixtures near carbon electrodes and found that ca-

capitance could be increased by means of mixing both anions.⁶⁴ Few studies on PIL mixtures with a second IL exist. Zheng *et al.*⁶⁵ and Kunz *et al.*⁶⁶ studied the surface properties on aggregates of long alkyl chain imidazolium-based ILs, using EAN as a surfactant. Russina *et al.*⁶⁷ studied mixtures of EAN and [EMIM][NO₃], reporting a smooth evolution with concentration as ions gradually redistributed into their favored structures while maintaining local electroneutrality. For this work, the choice of mixing a PIL with an AIL was made, expecting that their dissimilarities would give rise to novel, nonideal behavior in the studied mixtures. Chapter 2.4 starts describing mixtures of EAN and [EMIM][BF₄], for which a unique conductivity-concentration curve was experimentally found, and for which computer simulations showed the underlying structural phenomena behind this behavior, namely, changes in ionic mobility and the gradual onset of the hydrogen bonded network. Next, a study on the effect of longer alkyl chains in both PIL and AIL cation was made, finding that the presence of longer alkyl chains on the protic component of the mixture leads to the formation of intermolecular complexes. And, as a final step, the behavior of all these mixtures at the electrochemical interface, specifically near graphene electrodes, was studied and described, relating concentration-dependent changes in the aforementioned lateral distribution of the liquid to the capacitance of the IL cell.

The rest of this chapter reviews past and current research on the field of ionic liquids as well as their most important characteristics, and introduces the simulation techniques used. Afterwards, in Chapter 2, results obtained are analyzed and discussed in detail. Finally, Chapter 3 summarizes the main conclusions of this thesis and suggests future lines of work.

1.2 IONIC LIQUIDS

Ionic liquids (ILs) are, as their name indicates, purely ionic compounds with low melting points, making them liquid at close to am-

bient temperatures. Traditional salts (e.g. NaCl) in liquid state are denominated *molten salts* instead, while an IL is considered as such if it has a melting point below 100 °C (the term *room temperature molten salts* is also common). While this may seem an arbitrary limit at first, it means the IL will coexist with water in its liquid form, something which has major implications that will be discussed later in this section. A more immediate consequence is that, unlike traditional molten salts, ILs are not limited in application to high temperature industrial processes.

This low melting point can be attributed to component anions and cations. Instead of the small - sometimes monoatomic - and roughly equivalent sized ions present in molten salts, IL component ions can vary greatly in size and shape (Figure 1.1). The archetypical IL is usually formed by a large, organic cation with one or more alkyl chains of varying length, and a much smaller inorganic anion such as a nitrate or a phosphate. This is not always the case; however, a large size difference between anion and cation is frequent,⁶⁸ and it has been suggested that this asymmetry, and not just the larger ion size, might be a key factor behind the resulting liquids' low melting points, due to the decrease in free lattice energies and the large entropy change associated with the phase transition.^{10,69}

An important property of ILs is that their structure, on a nano-scale level, is heterogeneous. In 2006, by means of MD simulations, Canongia-Lopes and Pádua predicted that alkylmethylimidazolium--based ILs with an alkyl chain length of four carbon atoms (1-butyl-3-methylimidazolium, [BMIM]⁺) or longer would show segregation into polar (charged) and apolar (alkyl chain) domains.⁷⁰ This prediction was experimentally confirmed the following year by Triolo *et al.* by means of X-ray diffraction.⁷¹ Similarly, Atkin *et al.* reported, in 2008, experimental evidence of polar-apolar nanodomain segregation for EAN and its C₃-sized cousin, propylammonium nitrate (PAN).⁷² The nanostructured nature of these compounds is key to understand their behavior and beneficial properties as solvents, as described later

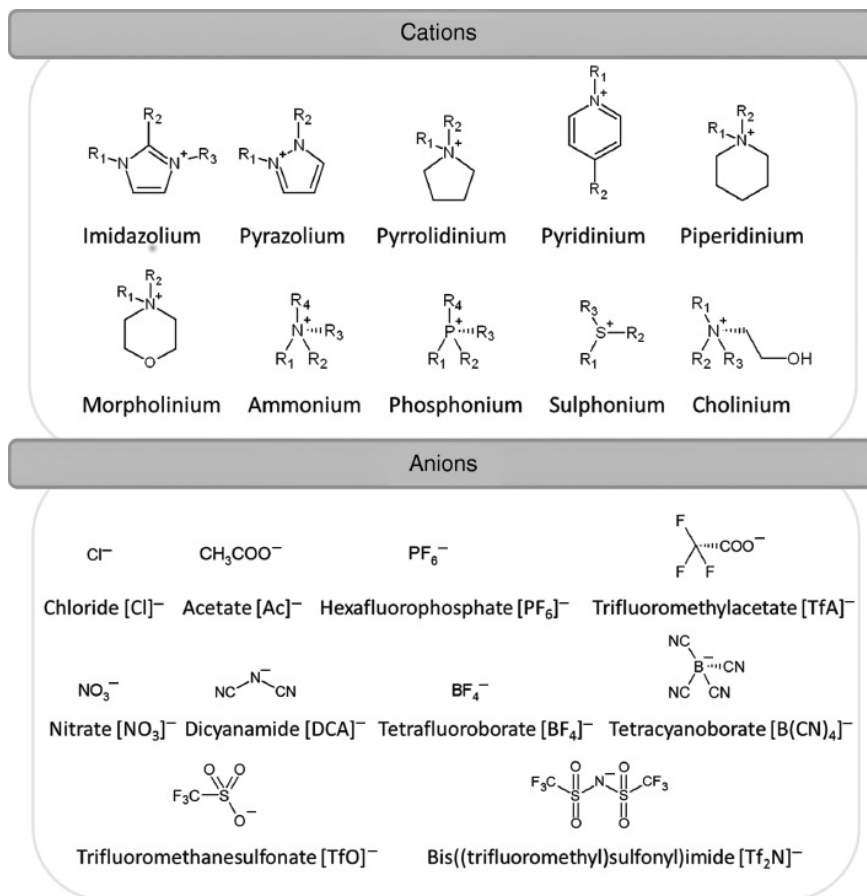


Figure 1.1: Examples of commonly found IL cations and anions. Figure taken from Ref. 5.

in this section.

A key phenomenon that might be present for a given anion-cation pair is proton transfer, that is, the presence of hydrogen donor sites on the cation and hydrogen acceptor sites on the anion. In those cases, the resulting IL is called a *protic ionic liquid* (PIL) that will exist in an acid-base equilibrium with its conjugate pair (the presence of a small number of neutral species is considered part of the “pure” IL⁷³) and show a tendency to form hydrogen bonded networks.⁷⁴ Those who do not are correspondingly called *aprotic ionic liquids*, or AILs. ILs are thus divided in two big families with a few notable differences. AILs lack the aforementioned proton transfer mechanisms and usually have a much lower, almost negligible vapor pressure. This has led to the long held viewpoint that AILs are the “stable” subset of ILs, and therefore the “interesting” ones. AILs have been the focus of the scientific community for nearly three decades, starting in 1992, when Wilkes *et al.* published an article describing the synthesis of 1-ethyl-3-methyl-imidazolium ([EMIM]⁺) based ionic liquids. During that period, most aspects of AILs have been the subject of academic research, with extensive work being done on their possible applications in electrochemistry and catalysis, all while articles discussing the synthesis of new AILs continued to be released. On the other hand, PILs at large have been almost completely ignored until recent years. This is despite them having been known for more than a century: in 1888, Gabriel and Weiner described ethanolanmonium nitrate, a salt with a melting point of 55-55° C, which can exist as a metastable liquid at ambient temperatures and even lower, following a thermal transition at -25. °C. In 1914, in an article commonly cited as the starting point of ionic liquid research, Walden reported the synthesis of the first true room-temperature IL (RTIL), ethylammonium nitrate (EAN).

In spite of this early start, PILs remained a curiosity during the 20th century. This changed recently, and, in the last decade, the properties that until then made PILs “uninteresting” started to be mentioned

instead as unique characteristics enabling new and interesting uses of ILs, lithium-ion batteries⁸ and hydrogen-based fuel cells⁷⁵⁻⁷⁷ being notable among them. It also bears reminding that, unlike AILs, PILs are extremely simple to synthesize, being the product of the reaction between a Brønsted acid and a Brønsted base. EAN in particular stands out among ILs due to its ability to form a three-dimensional hydrogen-bonded network, making it an unique solvent with many “water-like” properties while still showing the properties that make ILs interesting in the first place.^{6,78}

As for other properties, while a few common characteristics may be found, due to the large amount of possible anion-cation combinations, it is more accurate to discuss them in terms of *possible properties* and *property ranges*. Following is a list with the most notable properties found on ILs, both generally and for certain specific ILs:

- **Liquidus range and thermal stability:** By definition, ILs have a low melting point, under 100 °C. RTILs generally have much lower melting points, reaching -50 °C or lower. With higher temperatures, different behavior may be found depending on the IL. Many, especially AILs, do not present a gas phase at normal pressure conditions, instead undergoing thermal decomposition. Some PILs are known to evaporate normally, and a few others, among which 1-methylimidazolium chloride, used in industrial applications, is a notable case, simply neutralize into their conjugate acid-base pair. In both cases the original PIL is recoverable. Therefore, all ILs have, for one reason or another, an effective operating temperature range at which they will be a stable liquid. This liquidus range is generally large, of the order of 200 or 300 °C, and even in worst case scenarios ILs outperform other solvents such as water in this regard, increasing their number of possible applications.
- **Vapor pressure:** Related to the previous point, ILs have a lower vapor pressure than most other solvents. For many AILs,

this vapor pressure is almost negligible. PIL vapor pressure is generally higher,⁷⁴ but still low and within what can be considered non-volatile.

- **Hygroscopy:** On the other hand, a major issue for potential IL applications is their hygroscopic nature. ILs in contact with air will quickly absorb ambient humidity due to the solvophilic nature of their polar regions. Water content is known to impact IL mixtures in a significant way, especially regarding transport properties, so special care must be taken to isolate the liquid from the outside. Water solvation on PIL, as well as the effects of water contamination on AIL-based capacitors, are analyzed in detail as part of this thesis.
- **Electrochemical properties:** Being liquids entirely composed of charged particles, ionic conductivity is an intrinsic property of ILs. The high number of charge carriers compensates the relatively low mobility of ions. This results on conductivities of the order of 0.1 S/m, halfway between that of pure water (10^{-6} S/m) and metals (10^6 S/m), but lower than conventional electrolytes.⁷⁹ However, ILs also possess much larger electrochemical windows, between 2 and 6 V, making them more versatile for use in electrochemical applications. Furthermore, circumventing the lower conductivity can be possible by means of IL-cosolvent solutions, making the study of this systems an active research topic.^{80,81} Finally, PILs are considered materials of high interest for certain redox reactions and for processes involving proton capture, transport, and storage, such as fuel cells.⁷⁵⁻⁷⁸
- **Miscibility and solvation properties:** Ionic liquids are notably good solvents due to the presence of polar and apolar regions in the molecular structure of their constituent ions. Hence, they are generally miscible with a large number of liquids, such as water and other ionic liquids, for their entire concentration ranges, although exceptions do exist.^{14,55} The amphiphilically

nanostructured natured following from this gives rise to the selective solvation mechanism known as *nanostructured solvation*.⁸²⁻⁸⁴ polar goes to polar, and apolar goes to apolar. Salts, for example, will form solvation complexes in the polar regions of the liquid, while water behavior will vary depending on the presence of a hydrogen bond network, integrating itself into its structure when one exists or, when it does not and water concentration is low, forming isolated water clusters.

- **Density:** IL densities are one of their most measured properties, with extensive data available on scientific literature. This is partially due to the ease with which it can be measured, but also because of its importance for many potential applications. Data on the effect on density of different additives such as salts or other cosolvents is also readily available in many cases.^{85,86} In general, ILs are denser than water, with typical densities ranging from 1.2 g/ml to 1.4 g/ml.⁸⁷ As a general rule, ions with longer alkyl chains will result in ILs with lower densities. Density values are also relatively stable with temperature, with thermal expansion coefficients around $5-7 \cdot 10^{-4} \text{ K}^{-1}$.⁸⁸
- **Viscosity:** ILs show in general high viscosity, with typical values oscillating between 10 and 1000 cP, compared to water viscosities around 0.89 cP.⁸⁷ Temperature, as well as the presence of impurities, have a strong effect on viscosity. In addition to the obvious implications in practical applications, it bears mentioning that, for computational studies, a high viscosity means that longer computation times are needed to obtain good estimations of dynamic and transport properties.

1.3 METHODOLOGY

The advent of computer-assisted research has been a key development in scientific research since the second half of the 20th century.

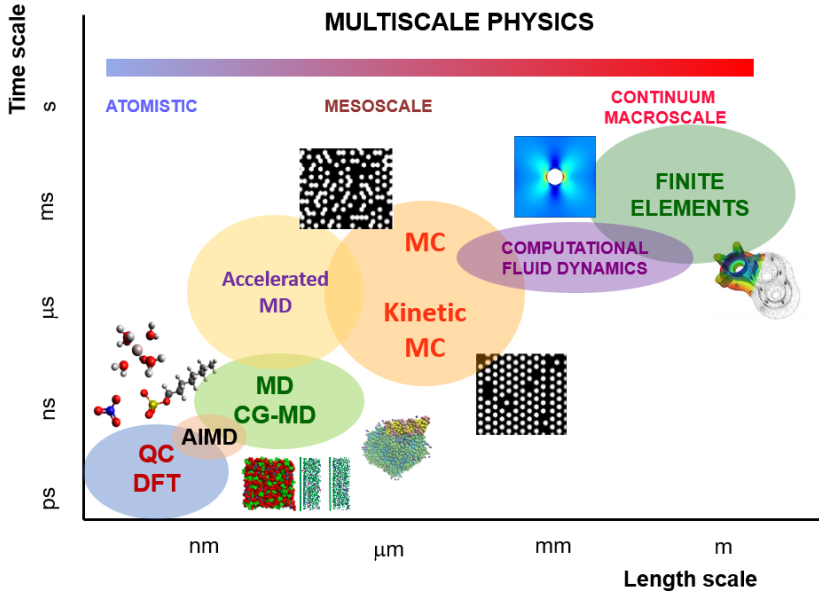


Figure 1.2: Diagram with different commonly employed simulation methods showing the size and time scales they are commonly used for.

In materials science, computer simulations allow scientists to observe and characterize materials at the microscopic level and correlate them to their macroscopic properties. This is particularly important in soft matter and ILs in particular, where experimental analysis of these properties can be difficult to approach. Furthermore, the computing power needed for these simulations is no longer restricted to supercomputers, and is becoming more and more readily available to researchers around the world. These characteristics combine to make computer simulations an ideal tool to investigate the properties of ILs before committing large amounts of money on experimental studies. Experimental results can then feed back into the simulation model, leading to a more refined model for future simulations.

There are different ways to approach computer simulation of a material, based on different theoretical physical and statistical principles.

The choice of method is an important first consideration that will be conditioned by the size of the system studied, the time scale of the phenomena to be observed, and the computational resources available (Figure 1.2). For the purpose of studying the nanoscale properties of ILs, the choice is essentially between *ab initio* quantum chemical methods such as density functional theory (DFT) calculations, or classical molecular dynamics (MD) simulations. DFT and other quantum mechanics-based methodologies can provide deep insights on phenomena involving single ions or complexes formed by a bunch of molecules, but their computationally intensive nature makes them scale poorly for bulk material simulations. As mentioned previously, the structure and single-particle dynamics of ILs and their mixtures is the main goal of this thesis, so MD simulations, the most fitting for the corresponding time and length scales as shown in Fig. 1.2 were used for this work.

Classical MD simulations consist on numerically solving Newton's equations of motion under a specified force field for a number of particles, each typically corresponding to an atom in a molecule, for every step of a discretized time frame. While other important practical applications such as protein dynamics exist, our main concern here are MD simulations of bulk matter, for which calculations are performed for a cell, typically cubic or orthorhombic, full of molecules and subject to periodic boundary conditions, so that a succession of exact replicas of the box exist in every direction. A number of software implementations, free and commercial, implementing algorithms to perform these calculations efficiently, are readily available, such as CHARMM or LAMMPS. In our case, we opted for the GROMACS suite, versions 5.1 and 2016.1, for a number of reasons. First, it is a free and open-sourced software regularly maintained and frequently updated. Second, it is easy to operate and provides detailed, well formatted information about each operation performed, making troubleshooting any possible issues much easier. And finally, it is not only fast, but also has been shown to scale better when parallelized.

Prior to simulation, a box containing a random configuration of the desired number of each molecular species is generated. For this, we used the PACKMOL tool.⁸⁹ Although box size can be adjusted later (especially in the case of NPT simulations), it is a good idea to choose dimensions that will result in a system density as close as possible to the liquid's experimental density or, if unknown, to a reasonable estimation of it. This box configuration must then undergo an energy minimization process. GROMACS implements three different algorithms for this purpose: steepest descent, conjugate gradients, and a limited-memory Broyden-Fletcher-Goldfarb-Shanno quasi-Newtonian minimizer. For the work presented on this thesis, the conjugate gradients algorithm was used.

After minimization but prior to the production run, the system must be stabilized by means of a long enough MD simulation to allow its structure and properties such as density to converge and stabilize. Initial velocities are generated here for each particle, following a Maxwell distribution at the temperature selected for the system. Then the system proceeds to stabilization, and, after finishing, a new MD simulation is ran, this time periodically recording particle data (position, velocity, forces) and system data (total kinetic and potential energies) in a number of log files, where analysis will be later performed.

As previously mentioned, each simulation step involves solving Newton's equations of motion for every particle in the system:

$$F_i = m_i a_i, \quad (1.1)$$

which must be integrated in discrete time, so as to calculate the state of the system at $t + \Delta t$ given known values of $x(t)$, $v(t)$ for the previous time step t . Again, GROMACS implements a number of algorithms, most of them based on leap-frog or velocity Verlet methods. For this work the leap-frog integrator⁹⁰ was used. This algorithm receives its name from using $v(t - \frac{1}{2}\Delta t)$ to calculate $v(t + \frac{1}{2}\Delta t)$, effectively making positions and velocities update alternatingly, as depicted in

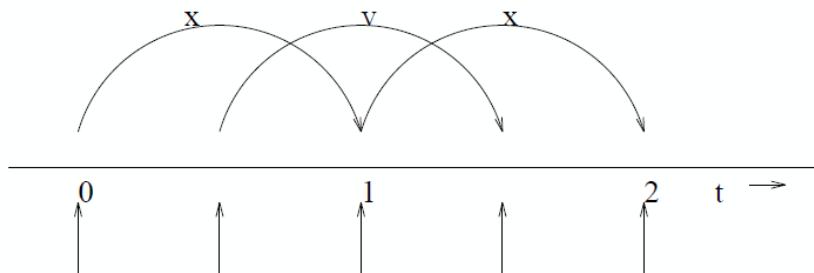


Figure 1.3: Depiction of the leap-frog integration method. Figure taken from Ref. 91

Figure 1.3:

$$\vec{v}(t + \frac{1}{2}\Delta t) = \vec{v}(t - \frac{1}{2}\Delta t) + \frac{\Delta t}{m}\vec{F}(t)$$

$$\vec{r}(t + \Delta t) = \vec{r} + \vec{v}(t + \frac{1}{2}\Delta t)\Delta t \quad (1.2)$$

Interactions between particles are divided into bonded (intramolecular) and non-bonded interactions,

$$V = V_{bonded} + V_{nonbonded}, \quad (1.3)$$

and rely on a set of particle-, bond-, and molecule-specific parameters. Collections of these parameters are denominated “force fields” and are typically obtained by means of quantum chemistry calculations, although other methods such as machine learning optimization are possible. Since the behavior of the atoms’ electronic cloud cannot be replicated by static parameters, parameters will vary depending on what situations the force field has been optimized for. In effect, this means a variety of general-purpose and application-specific force fields exist, with OPLS,⁹² GROMOS,⁹³ AMBER⁹⁴ and CHARMM⁹⁵ being some examples. For this thesis, the OPLS-AA⁹² (Optimized Potentials for Liquid Simulations) force field was employed. This force field was optimized to fit the experimental properties of liquids

and had been already used for ILs with good results prior to the beginning of this thesis.^{83,96} The AA (all-atom) variant explicitly represents every atom, as opposed to OPLS-UA (united atom), where carbon-bound hydrogens are ignored and represented as part of the carbon's parameters.

In OPLS, bonded interactions are modelled in the following manner:

$$V_{bonded} = V_{bonds} + V_{angles} + V_{dihedrals} \quad (1.4)$$

$$V_{bonds} = \sum_{bonds} \frac{1}{2} k_B (r - r_0)^2 \quad (1.5)$$

$$V_{angles} = \sum_{angles} k_\theta (\theta - \theta_0)^2 \quad (1.6)$$

$$V_{dihedral} = \sum_{dihedrals} \frac{1}{2} \sum_{k=1}^4 V_i [1 + (-1)^{k+1} \cos(k\phi)]. \quad (1.7)$$

Bonds and angles are modeled with a linear or angular (respectively) harmonic potential. Dihedrals are modeled as a four term Fourier cosine expansion. Internally, GROMACS implements this potential by using Ryckaert-Bellemans dihedrals, for which equivalent parameters can be easily calculated.

Non-bonded interactions consist in a repulsion term, a dispersion term, and a Coulomb term. The first two are grouped into a Lennard-Jones (or, in other cases, Buckingham) interaction. Adding the classical Coulomb term, the result is the following expression:

$$V_{non-bonded} = \sum_{i>j} \left(\frac{A_{ij}}{r_{ij}^{12}} - \frac{C_{ij}}{r_{ij}^6} + \frac{q_i q_j}{4\pi\epsilon_0 r_{ij}} \right), \quad (1.8)$$

which uses the combination rules $A_{ij} = \sqrt{A_{ii}A_{jj}}$ and $C_{ij} = \sqrt{C_{ii}C_{jj}}$. For the case of the interaction between an atom and a single-layer surface (such as graphene), an integrated 10-4 Lennard-Jones potential can be used instead for faster computation times.

These non-bonded interactions have effectively infinite range; however, for practical purposes a cut-off distance, no greater than half the shortest box side, is introduced. Buffered Verlet lists keep track of which molecules are closer to each other than this threshold. For the rest, a Particle Mesh Ewald sum is made to calculate the remainder of the force and conserve the total energy of the system. In parallel run simulations, this can be done on dedicated threads, allowing for further speed gains.



2 Results and Discussion

This chapter presents the full results obtained in this thesis work. The studies performed were computational in nature, using classical MD simulations; where possible, complementary experimental measurements of density and conductivity were also made to compare with simulation results.

The main topic of research was the evolution of structural, interfacial, and transport properties, both on a microscopic and aggregate (macroscopic) level, of protic and aprotic ILs upon mixing, with either molecular cosolvents, or with each other. This can be important for many reasons: tuning IL properties for optimum performance for a specific application is a given, but one must also consider the case of accidental contamination, notably in the case of water. For this reason, the first three subsections of this chapter present studies of water in ILs. The structure and dynamics of EAN mixtures with water, methanol, and ethanol were analyzed. A progressive, homogeneous accommodation of the molecular cosolvents into the mixture's hydrogen bonded network was found, in contrast to previous findings for AILs. Water was also found to integrate strongly into the PIL structure, displaying short-term caging effects and replacing $[EA]^+$ in the first anionic solvation layer at concentrations over 50%.

Most studies of IL-IL mixtures focus on mixtures of two similar ILs sharing a common ion. In this thesis, the choice of mixing a protic IL with an aprotic IL was intentionally made so as to mix two dissimilar liquids with different internal structures in order to search for possible novel phenomena due to the nonideality of the mixture. Mixtures of $[EMIM][BF_4]+EAN$ were found to display a novel, complex electrical conductivity curve, with both a local maximum at low PIL concentrations and a global minimum at near equimolar concentrations. Analysis of the internal structure of the mixture, by

means such as the radial distribution functions, this effect was attributed to the protic hydrogen bonded network and its dominance in the mixture. Meanwhile, other magnitudes, such as density, showed an almost ideal behavior, even if deviations from ideality were larger than in most IL mixtures reported in the literature. Longer alkyl chain length cations were found to introduce different, additional nonideal behavior in the case of the protic cations, whose mixtures displayed, upon initial addition of [EMIM][BF₄], a large, negative excess molar enthalpy of mixing. This was found to be due to the occupation, by [EMIM][BF₄] ions, of regions near the apolar cation tail, which are empty or surrounded by other tails in the pure liquid.

Due to the potential applications of ILs in batteries, supercapacitors, and other electrochemical devices, ILs and their mixtures were also studied in the presence of neutral, positively charged and negatively charged graphene surfaces. A study on water presence in nanoconfined [BMIM][BF₄] showed that water is found predominantly at the positively charged electrode, with only residual amounts near the negatively charged electrode. Careful analysis, by means of the potential of the mean force (PMF), showed that part of the reason for this is a much higher energy barrier to move through the first cation layer near the negatively charged electrode, making water adsorption more difficult. On the other hand, a study of the aforementioned PIL+AIL mixtures revealed an asymmetrical distribution of cations in charged cells, with protic cations occupying positions near the positively charged electrode so as to form hydrogen bonds with nearby nitrate anions. This means that the first cationic layer near the negatively charged electrode is composed predominantly by imidazolium cations, which in turn affects the capacitance of the cell.

Following are the detailed results of this work. Each subsection includes a brief summary of the research topic and its main conclusions followed by the corresponding published article (reference and figure numbers may differ from the original work).

2.1 MIXTURES OF PROTIC IONIC LIQUIDS AND MOLECULAR COSOLVENTS: A MOLECULAR DYNAMICS SIMULATION

The hydrogen bonded structure of PILs is the key property distinguishing them from AILs. As such, its study is an important step towards understanding the structure and dynamics of this family of ILs. Additionally, water and alcohols, two important molecular solvents, are completely miscible with one of the reference PILs, EAN, and, as discussed previously, water content in ILs is a key concern for many potential applications. Therefore, studying mixtures of EAN with these molecular cosolvents is important for both basic science and applications of PILs.

In the following article, we reported the first, up to our knowledge, MD study of mixtures of EAN with water and short-chained alcohols (methanol and ethanol). Our goal was to understand the solvation of a small amount of these molecules in PIL as well as the evolution of hydrogen bonded structures in the mixture for the entire concentration range. Our findings show the progressive, homogeneous accommodation of cosolvent molecules in the hydrogen bonded network, opposite to previous findings in AILs. Radial distribution functions revealed that water replaces cations in the first solvation shell of the anions for concentrations higher than 50%. Meanwhile, alcohol molecules accommodate themselves in the frontiers of the polar-apolar nanodomains. Different coordinations around the anions (monodentate vs. bidentate) were found in the spatial distribution functions. And when analyzing dynamic properties by means of velocity autocorrelation functions, a caging effect can be observed for water molecules, but not for alcohol.



Mixtures of protic ionic liquids and molecular cosolvents: A molecular dynamics simulation

Borja Docampo-Álvarez,^{1,a)} Víctor Gómez-González,¹ Trinidad Méndez-Morales,¹ Jesús Carrete,^{1,2} Julio R. Rodríguez,¹ Óscar Cabeza,³ Luis J. Gallego,¹ and Luis M. Varela^{1,b)}

¹Grupo de Nanomateriais e Materia Branda, Departamento de Física da Materia Condensada, Universidade de Santiago de Compostela, Campus Vida s/n E-15782, Santiago de Compostela, Spain

²LITEN, CEA-Grenoble, 17 rue des Martyrs, BP166, F-38054, Grenoble, Cedex 9, France

³Facultade de Ciencias, Universidade da Coruña, Campus A Zapateira s/n E-15008, A Coruña, Spain

(Received 26 February 2014; accepted 13 May 2014; published online 2 June 2014)

Mixtures of protic ionic liquids and molecular cosolvents: a molecular dynamics simulation

J. Chem. Phys. **140** (21), 214502

Borja Docampo-Álvarez,^{1,2} Víctor Gómez-González,^{1,2} Trinidad Méndez-Morales,² Jesús Carrete,^{2,3} Julio R. Rodríguez,² Óscar Cabeza,⁴ Luis J. Gallego,² Luis M. Varela²



^aContributed equally to this work.

^bGrupo de Nanomateriais e Materia Branda, Departamento de Física da Materia Condensada, Universidade de Santiago de Compostela, Campus Vida s/n E-15782, Santiago de Compostela, Spain

^cLITEN, CEA-Grenoble, 17 rue des Martyrs, BP166, F-38054, Grenoble, Cedex 9, France

^dFacultade de Ciencias, Universidade da Coruña, Campus A Zapateira s/n E-15008, A Coruña, Spain

2.2 MOLECULAR DYNAMICS SIMULATION OF THE BEHAVIOUR OF WATER IN NANO-CONFINED IONIC LIQUID-WATER MIXTURES

Water content can drastically alter properties of ILs that are key for electrochemical applications such as their electrical conductivity. Water can also interfere with redox reactions taking place near electrodes. Before using ILs as solvents for such reactions, or as part of novel electrolyte compounds for supercapacitors, it is important to understand the behavior of a residual amount of water in the cell interface. Feng *et al.*⁵¹ had previously provided first insights into these systems. As nanoconfinement has been found to be beneficial for the performance of ILs in certain situations, this paper further analyzes the behavior of water molecules in [BMIM][BF₄] confined between graphene layers at different cell sizes.

Results show that water molecules are adsorbed under all conditions studied. However, the potential of mean force for water is lower for positively charged surfaces due to the preferential hydration of anions. Nanoconfinement was found to increase the probability of finding water near the positively charged electrode while causing depletion at neutral and negatively charged surfaces. A simple, two-level statistical model was proposed to predict the degree of water presence near electrodes in these systems. Finally, a novel phase transition, upon water addition, for the distribution of interfacial ions was found, and reported in this article for the first time, with anions changing from a striped pattern to a hexagonal one. This result shows that previously observed voltage-induced phase transitions^{52,53} are a particular case of a group of interfacial structure phase transitions induced by any effect altering surface charge density.

Molecular dynamics simulation of the behaviour of water in nano-confined ionic liquid–water mixtures

B Docampo-Álvarez¹, V Gómez-González¹, H Montes-Campos¹,
J M Otero-Mato¹, T Méndez-Morales¹, O Cabeza², L J Gallego¹,
R M Lynden-Bell³, V B Ivaništšev⁴, M V Fedorov⁵ and L M Varela¹

¹ Departamento de Física da Materia Condensada, Facultade de Física, Universidade de Santiago de Compostela, Campus Vida s/n, E-15782 Santiago de Compostela, Spain

² Departamento de Física, Facultade de Ciencias, Universidade da Coruña, Campus A Zapateira s/n, E-15071 A Coruña, Spain

³ Department of Chemistry, University of Cambridge, Lensfield Road, CB2 1EW Cambridge, UK

⁴ Institute of Chemistry, University of Tartu, Ravila 14a, 50411 Tartu, Estonia

⁵ Department of Physics, Scottish Universities Physics Alliance (SUPA), Strathclyde University, John Anderson Building, 107 Rottenrow East, G4 0NG Glasgow, UK

E-mail: luismiguel.varela@usc.es

Received 28 February 2016, revised 29 March 2016

Accepted for publication 30 March 2016

Published



Molecular dynamics simulation of the behaviour of water in nano-confined ionic liquid–water mixtures

J. Phys. Condens. Matter 28 (46), 464001.

B Docampo-Álvarez¹, V Gómez-González¹, H Montes-Campos¹,
J M Otero-Mato¹, T Méndez-Morales¹, O Cabeza², L J Gallego¹,
R M Lynden-Bell³, V B Ivaništšev⁴, M V Fedorov⁵ and L M Varela¹

^aGrupo de Nanomateriales, Fotónica y Materia Blanda. Departamentos de Física da Materia Condensada y Física Aplicada, Facultade de Física, Universidade de Santiago de Compostela, Campus Vida s/n, E-15782 Santiago de Compostela, Spain

^bDepartamento de Física, Facultade de Ciencias, Universidade da Coruña, Campus A Zapateira s/n, E-15071 A Coruña, Spain

^cDepartment of Chemistry, University of Cambridge, Lensfield Road, CB2 1EW Cambridge, UK

^dInstitute of Chemistry, University of Tartu, Ravila 14a, 50411 Tartu, Estonia

^eDepartment of Physics, Scottish Universities Physics Alliance (SUPA), Strathclyde University, John Anderson Building, 107 Rottenrow East, G4 0NG Glasgow, UK

2.3 SURFACE AND BULK CHARACTERISATION OF MIXTURES CONTAINING ALKYLAMMONIUM NITRATES AND WATER OR ETHANOL: EXPERIMENTAL AND SIMULATED PROPERTIES AT 298.15 K

Following the studies presented in section 2.1, a clear picture of nanostructured solvation mechanisms in EAN started to emerge. The desire to experimentally validate these results, as well as the open question of the effect of cation alkyl chain length on the mixtures, led to a collaboration with the *Mesturas* group of the University of A Coruña with the purpose of experimentally characterizing macroscopic properties of these mixtures and their relation with their microscopic structure as shown in MD simulations. This article presents the results of this work.

Detailed experimental data for density, surface tension and refractive index measurements are presented for mixtures of EAN, PAN and BAN with water and ethanol. The validity of our understanding of nanostructured solvation is shown by the different evolution of surface tension for both cosolvents, as ethanol is more likely to be found closer to the (apolar) liquid interface. This is a consequence of its preference for regions at the frontier between polar and apolar interfaces and leads to a steeper curve for surface tension at high PIL concentrations. Water, meanwhile, occupies places around polar heads, inside the liquid, and its effect on surface tension is therefore minimized until PIL concentration is low enough.



Surface and bulk characterisation of mixtures containing alkylammonium nitrates and water or ethanol: Experimental and simulated properties at 298.15 K



Luisa Segade^{a,*}, Manuel Cabanas^a, Montserrat Domínguez-Pérez^a, Esther Rilo^a, Sandra García-Garabal^a, Mireille Turmine^b, Luis M. Varela^c, Víctor Gómez-González^c, Borja Docampo-Alvarez^c, Oscar Cabeza^a

^a Grupo Mesturas, Departamento de Física, Facultade de Ciencias, Universidade da Coruña, Campus da Zapateira, 15071 A Coruña, Spain

^b Sorbonne Universités, UPMC Univ Paris 06, CNRS, Laboratoire Interfaces et Systèmes Electrochimiques, 4 place Jussieu, F-75005 Paris, France

^c Departamento de Física da Materia Condensada, Universidade de Santiago de Compostela, Campus Vida s/n, 15782 Santiago de Compostela, Spain

Surface and bulk characterisation of mixtures containing alkylammonium nitrates and water or ethanol: experimental and simulated properties at 298.15 K

J. Mol. Liq. 222, 663–670.

Luisa Segade,^a Manuel Cabanas,^a Montserrat Domínguez-Pérez,^a Esther Rilo,^a Sandra García-Garabal,^a Mireille Turmine,^b Luis M. Varela,^c Víctor Gómez-González,^c Borja Docampo-Alvarez,^c Oscar Cabeza^a

^a Grupo Mesturas, Departamento de Física, Facultade de Ciencias, Universidade da Coruña, Campus A Zapateira s/n, 15071 A Coruña, Spain

^b Sorbonne Université, UPMC Univ Paris 06, CNRS, Laboratoire Interfaces et Systèmes Electrochimiques, 4 place Jussieu, F-75005, Paris, France

^c Departamento de Física da Materia Condensada, Universidade de Santiago de Compostela, Campus Vida s/n, 15782 Santiago de Compostela, Spain

2.4 MOLECULAR DYNAMICS SIMULATIONS OF MIXTURES OF PROTIC AND APROTIC IONIC LIQUIDS

Once the properties of mixtures with molecular cosolvents were known and the fundamental details of nanostructured solvation were confirmed, we undertook the characterization of IL-IL mixtures. These mixtures are considered a potential way of fine-tuning ILs for specific applications beyond what is currently possible with combinations of a single cation and a single anion. These mixtures show in most cases close to ideal behavior for relevant magnitudes, and many studies on IL mixtures focus on two ILs sharing a common ion, making their ideality even more pronounced. Following the same logic, choosing two dissimilar ILs with very different properties should magnify nonideal mixing behavior and possibly lead to the appearance of novel phenomena. The following article presents simulation and experimental results of mixtures of the AIL [EMIM][BF₄] and the PIL EAN, the first of its kind, to our knowledge, ever reported.

A complex, novel dependence on concentration was found experimentally for electrical conductivity. Its behavior, featuring a local maximum at low PIL concentrations and a global minimum at close to equimolar concentrations, was reported and qualitatively reproduced by means of MD simulations. Analysis of the simulations revealed a homogeneous mixing process in which hydrogen bonded network becomes the key interaction in the mixture after a certain amount of PIL, around 20%, is present. This result is reminiscent of the ability of water to establish a porous network throughout the liquid in mixtures with AILs.²¹¹ This leads to a progressively tighter structure as PIL concentration increases, and, as a consequence, a decreased mobility for AIL cations.

PCCP



PAPER

[View Article Online](#)

[View Journal](#) | [View Issue](#)



Cite this: *Phys. Chem. Chem. Phys.*,
2016, **18**, 23932

Molecular dynamics simulations of mixtures of protic and aprotic ionic liquids

Borja Docampo-Álvarez,^a Víctor Gómez-González,^a Trinidad Méndez-Morales,^a Julio R. Rodríguez,^a Elena López-Lago,^a Oscar Cabeza,^b Luis J. Gallego^a and Luis M. Varela^{a*}

^a Sorbonne Universités, UPMC Univ Paris 06, UMR, Laboratoire Interfaces et Systèmes Electrochimiques, 4 place Jussieu, F-75005 Paris, France
^b Departamento de Física da Materia Condensada, Universidade de Santiago de Compostela, Campus Vida s/n, 15782 Santiago de Compostela, Spain

Molecular Dynamics Simulations of Mixtures of Protic and Aprotic Ionic Liquids

Phys. Chem. Chem. Phys. 2016, **18**, 23932.

Borja Docampo-Álvarez,^a Víctor Gómez-González,^a Trinidad Méndez-Morales,^a Julio R. Rodríguez,^a Elena López-Lago,^a Oscar Cabeza,^b Luis J. Gallego,^a and Luis M. Varela^a

^a Grupo de Nanomateriales, Fotónica y Materia Blanda. Departamentos de Física da Materia Condensada y Física Aplicada, Facultade de Física, Universidade de Santiago de Compostela, Campus Vida s/n, E-15782 Santiago de Compostela, Spain

^b Departamento de Física, Facultade de Ciencias, Universidade da Coruña, Campus A Zapateira s/n, E-15071 A Coruña, Spain

2.5 EFFECT OF ALKYL CHAIN LENGTH ON THE STRUCTURE AND THERMODYNAMICS OF PROTIC-APROTIC IONIC LIQUID MIXTURES: A MOLECULAR DYNAMICS STUDY

The effect of the length of the alkyl chain on the mixtures described in Section 2.4 was studied next. ILs are nanostructured materials, where the presence of polar and nonpolar regions leads to differentiated polar and apolar domains. This effect depends on the presence of a large enough nonpolar region in the ions, making the length of alkyl chains a key contributing factor. It follows from this that, when mixing two different families of ionic liquids, a different alkyl chain length in any of the two cations may lead to different mixture interactions and resulting structures. The following article presents MD studies of PIL-AIL mixtures involving the PILs EAN, PAN and BAN and the AILs [EMIM][BF₄] and [BMIM][BF₄].

Results show pronounced peaks for excess volume upon initial AIL mixing with PAN and BAN, with corresponding peaks for enthalpy. Detailed analysis, supported by radial and spatial distribution functions, reveals an association between [EMIM]⁺ cations and the apolar regions of [PA]⁺ and [BA]⁺. The polar-apolar bulk ordering present in the pure PIL is disrupted in order to accommodate AIL ions around the apolar region. Mixtures with [BMIM][BF₄] and EAN, on the other hand, behaved similarly to previously studied mixtures of [EMIM][BF₄] and EAN, albeit with slightly larger excess magnitudes.

PCCP



PAPER

View Article Online
View Journal | View IssueCite this: *Phys. Chem. Chem. Phys.*,
2018, 20, 9938**The effect of alkyl chain length on the structure and thermodynamics of protic–aprotic ionic liquid mixtures: a molecular dynamics study†**Borja Docampo-Álvarez,^a Víctor Gómez-González,^a Trinidad Méndez-Morales,^a Julio R. Rodríguez,^a Oscar Cabeza,^b Mireille Turmine,^b Luis J. Gallego^a and Luis M. Varela^{b,*}**Effect of Alkyl Chain Length on the Structure and Thermodynamics of Protic-Aprotic Ionic Liquid Mixtures: A Molecular Dynamics Study***Phys. Chem. Chem. Phys.* 2018, 20, 9938.Borja Docampo-Álvarez,^a Víctor Gómez-González,^a Trinidad Méndez-Morales,^a Julio R. Rodríguez,^a Oscar Cabeza,^b Mireille Turmine,^c Luis J. Gallego,^a and Luis M. Varela^a

^aGrupo de Nanomateriales, Fotónica y Materia Blanda. Departamento de Física de Partículas, Facultade de Física, Universidade de Santiago de Compostela, Campus Vida s/n, E-15782 Santiago de Compostela, Spain

^bDepartamento de Física e Ciencias da Terra, Facultade de Ciencias, Universidade da Coruña, Campus A Zapateira s/n, E-15071 A Coruña, Spain

^cSorbonne Université, CNRS, Laboratoire Interfaces et Systèmes Electrochimiques, LISE, 75005, Paris, France

2.6 MOLECULAR DYNAMICS SIMULATIONS OF NOVEL ELECTROLYTES BASED ON MIXTURES OF PROTIC AND APROTIC IONIC LIQUIDS AT THE ELECTROCHEMICAL INTERFACE: STRUCTURE AND CAPACITANCE OF THE ELECTRIC DOUBLE LAYER

In this section, the behavior of the systems studied in Sections 2.4 and 2.5 near graphene electrodes is investigated, looking into possible practical applications of these novel IL mixtures. ILs are materials of special interest for electrochemical applications. Many of their electrochemical properties can be improved by means of mixtures with molecular cosolvents. However, this negatively impacts the electrochemical window of the mixture. IL-IL mixtures allow the tuning of specific properties, such as capacitance, while circumventing this limitation. Additionally, as shown previously in this thesis, ILs at graphene interfaces present a rich, complex lateral structure, that will present phase transitions under varying voltages^{52,53} or in the presence of cosolvents (Section 2.2). The question of how the lateral structure of these mixtures evolves with concentrations remained open. This final article presents results of MD simulations of PIL-AIL mixtures of the PILs EAN, PAN, and BAN and the AILs [EMIM][BF₄] and [BMIM][BF₄].

Hydrogen bonding is again shown to be a key property in the structure of the mixture. In this case, the preference of protic cations towards hydrogen bonding with the anions near the positively charged electrode leads to a depletion of these cations near the negatively charged electrode. The resulting differences in the lateral structure of the innermost layer of the EDL (with, rather than phase transitions, displayed segregation into protic and aprotic regions), as well as the impact on the structure of the EDL, are shown to lead to a nonlinear dependence of the integral capacitance with concentration.

Molecular dynamics simulations of novel electrolytes based on mixtures of protic and aprotic ionic liquids at the electrochemical interface: structure and capacitance of the electric double layer

Borja Docampo-Álvarez,^a Víctor Gómez-González,^a Oscar Cabeza,^b
Vladislav B. Ivaništšev,^c Luis J. Gallego,^a and Luis M. Varela^{a*}

^aGrupo de Nanomateriais, Fotónica e Materia Branda, Departamento de Física de Partículas, Universidade de Santiago de Compostela, Campus Vida s/n E-15782, Santiago de Compostela, Spain.

^bDepartamento de Física e Ciencias da Terra, Facultade de Ciencias, Universidade da Coruña, Campus A Zapateira s/n, E-15071 A Coruña, Spain

^cInstitute of Chemistry, University of Tartu, Ravila 14a, 50411 Tartu, Estonia

Molecular dynamics simulations of novel electrolytes based on mixtures of protic and aprotic ionic liquids at the electrochemical interface: structure and capacitance of the electric double layer

Electrochimica Acta. Submitted for publication.

Borja Docampo-Álvarez,^a Víctor Gómez-González,^a Oscar Cabeza,^b
Vladislav B. Ivaništšev,^c Luis J. Gallego,^a and Luis M. Varela^a

^aGrupo de Nanomateriais, Fotónica e Materia Branda, Departamento de Física de Partículas, Universidade de Santiago de Compostela, Campus Vida s/n E-15782, Santiago de Compostela, Spain.

^bDepartamento de Física e Ciencias da Terra, Facultade de Ciencias, Universidade da Coruña, Campus A Zapateira s/n, E-15071 A Coruña, Spain

^cInstitute of Chemistry, University of Tartu, Ravila 14a, 50411 Tartu, Estonia



3 Conclusions and future perspectives

The main conclusions drawn from the work presented on this thesis are as follows:

- MD simulations of mixtures of PILs and water, methanol and ethanol have been performed in order to analyze the solvation mechanisms in these liquids. Results show that water molecules homogeneously accommodate themselves inside the polar regions of the liquid, integrating with the hydrogen bond network of the IL. This contrasts to the clustering behavior that has been observed for water in AILs. Amphiphilic alcohol molecules, on the other hand, place themselves at the border between polar and apolar regions. These results, which were also confirmed experimentally and tied to changes in magnitudes such as surface tension, have contributed to a better understanding of the nanostructured solvation paradigm.
- We have pioneeringly considered the structure of mixtures of water and ILs under high nanoconfinement, and introduced a simple, general statistical model to describe preferential adsorption. Specifically, we show that water is predominantly adsorbed near positively charged electrodes due to their preference for solvating anions. This effect is more pronounced under increasing nanoconfinement, where the blueshift of the vibrational states of water molecules reveals stronger caging in the interfacial region.
- The structure and single-particle dynamics and transport properties of mixtures containing a PIL and an AIL have been described for the first time by means of both MD simulations and experimental studies. As with water in AILs, the formation of

an hydrogen bonded PIL network happens at low PIL concentrations, between 20 and 30%, and dominates many structural and transport properties of the mixtures. In particular, it leads to a markedly non-ideal electrical conductivity curve, which had not previously been reported for any other IL mixture. This example shows how mixing two dissimilar ILs can lead to interesting, nontrivial phenomena not present in common-ion IL mixtures.

- The relative size of the polar/apolar parts of the IL molecules of the component ILs critically determines the way in which the polar/apolar network of the latter can possibly integrate. This process is the result of a delicate interplay between several interactions and has been shown to be a source of nonideal behavior in these mixtures. For mixtures of AILs in the longer chained PILs studied (PAN and BAN), this leads to the formation of intermolecular complexes where polar regions of AIL cations surround the apolar PIL tails, disrupting the polar-apolar ordering present in the pure liquid.
- Finally, and most notably, composition-induced surface phase transitions for the interfacial structure of ILs near graphene electrodes were reported and described for the first time. The discovery of this previously unknown complex behavior, triggered by changes in ionic mobility, opens a new line of research into the properties and tunability of confined ILs. Also in this thesis, it was shown that changes in the lateral structure of the first ionic layer influence the capacitance of the cell and, more generally, the structure of the EDL itself, through the modification of the surface charge density.

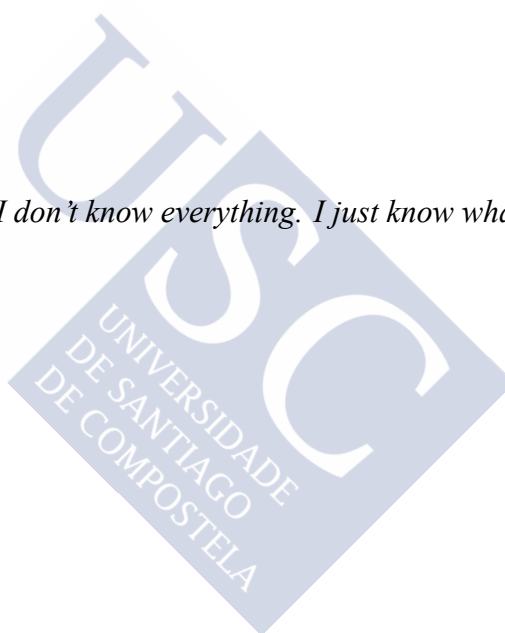
As for future perspectives, mixtures of ILs will remain the subject of active research for the foreseeable future. In particular, research in the structure of these and other compound-forming mixtures and their relation to nanostructured solvation mechanisms is a line of research

with applications in e.g. electrochemical devices. Additionally, the precise structure of ILs at the electrochemical interface, specifically of the innermost layer of the EDL and its influence on the 3D structure of this region, remains an open line of research, with potential applications such as the eventual possibility of designing IL mixtures with complex, heterogeneous solvent interfaces for complex chemical processes. Finally, the study of IL in contact with two-dimensional materials beyond graphene is expected to lead to interesting results in the field of electrochemistry.





"I don't know everything. I just know what I know."





Bibliography

- [1] M. J. Earle and K. R. Seddon, "Ionic liquids. green solvents for the future," *Pure Appl. Chem.*, vol. 72, no. 7, pp. 1391–1398, 2000.
- [2] N. V. Plechkova and K. R. Seddon, "Applications of ionic liquids in the chemical industry," *Chem. Soc. Rev.*, vol. 37, no. 1, pp. 123–150, 2008.
- [3] R. L. Vekariya, "A review of ionic liquids: applications towards catalytic organic transformations," *J. Mol. Liq.*, vol. 227, pp. 44–60, 2017.
- [4] R. D. Rogers and K. R. Seddon, *Ionic liquids: Industrial Applications for Green Chemistry*, vol. 818 of *A. C. S. Symposium Series*. American Chemical Society, 2002.
- [5] E. Rynkowska, K. Fatyeyeva, and W. Kujawski, "Application of polymer-based membranes containing ionic liquids in membrane separation processes: a critical review," *Rev. Chem. Eng.*, vol. 34, no. 3, pp. 341–363, 2018.
- [6] P. H. Shetty, S. K. Poole, and C. F. Poole, "Applications of ethylammonium and propylammonium nitrate solvents in liquid-liquid extraction and chromatography," *Anal. Chim. Acta*, vol. 236, pp. 51–62, 1990.
- [7] H. Zhao and S. V. Malhotra, "Applications of ionic liquids in organic synthesis," *Aldrichim. Acta.*, 2002.
- [8] S. Menne, J. Pires, M. Anouti, and A. Balducci, "Protic ionic liquids as electrolytes for lithium-ion batteries," *Electrochem. Commun.*, vol. 31, pp. 39–41, 2013.
- [9] R. D. Rogers and K. R. Seddon, "Ionic liquids—solvents of the future?," *Science*, vol. 302, no. 5646, pp. 792–793, 2003.

- [10] K. Marsh, J. Boxall, and R. Lichtenthaler, "Room temperature ionic liquids and their mixtures—a review," *Fluid Phase Equilibr.*, vol. 219, no. 1, pp. 93–98, 2004.
- [11] K. N. Marsh, A. Deev, A. C. Wu, E. Tran, and A. Klamt, "Room temperature ionic liquids as replacements for conventional solvents—a review," *Korean J. Chem. Eng.*, vol. 19, no. 3, pp. 357–362, 2002.
- [12] L. Cammarata, S. Kazarian, P. Salter, and T. Welton, "Molecular states of water in room temperature ionic liquids," *Phys. Chem. Chem. Phys.*, vol. 3, no. 23, pp. 5192–5200, 2001.
- [13] K. R. Seddon, A. Stark, and M.-J. Torres, "Influence of chloride, water, and organic solvents on the physical properties of ionic liquids," *Pure Appl. Chem.*, vol. 72, no. 12, pp. 2275–2287, 2000.
- [14] K. E. Gutowski, G. A. Broker, H. D. Willauer, J. G. Huddleston, R. P. Swatloski, J. D. Holbrey, and R. D. Rogers, "Controlling the aqueous miscibility of ionic liquids: aqueous biphasic systems of water-miscible ionic liquids and water-structuring salts for recycle, metathesis, and separations," *J. Am. Chem. Soc.*, vol. 125, no. 22, pp. 6632–6633, 2003.
- [15] T. Méndez-Morales, J. Carrete, O. Cabeza, L. J. Gallego, and L. M. Varela, "Molecular dynamics simulation of the structure and dynamics of water–1-alkyl-3-methylimidazolium ionic liquid mixtures," *J. Phys. Chem. B*, vol. 115, no. 21, pp. 6995–7008, 2011.
- [16] M. Allen, D. F. Evans, and R. Lumry, "Thermodynamic properties of the ethylammonium nitrate + water system: partial molar volumes, heat capacities, and expansivities," *J. Sol. Chem.*, vol. 14, no. 8, pp. 549–560, 1985.
- [17] T. J. V. Findlay and M. C. R. Symons, "Solvation spectra. part 50.—spectrophotometric studies of the solvation of nitrate ions

- in protic and aprotic media,” *J. Chem. Soc., Faraday Trans. 2*, vol. 72, pp. 820–826, 1976.
- [18] R. G. Horn, D. F. Evans, and B. W. Ninham, “Double-layer and solvation forces measured in a molten salt and its mixtures with water,” *J. Phys. Chem.*, vol. 92, no. 12, pp. 3531–3537, 1988.
- [19] I. B. Malham, P. Letellier, A. Mayaffre, and M. Turmine, “Part I: Thermodynamic analysis of volumetric properties of concentrated aqueous solutions of 1-butyl-3-methylimidazolium tetrafluoroborate, 1-butyl-2,3-dimethylimidazolium tetrafluoroborate, and ethylammonium nitrate based on pseudo-lattice theory,” *J. Chem. Thermodyn.*, vol. 39, no. 8, pp. 1132–1143, 2007.
- [20] S. Bouguerra, I. B. Malham, P. Letelliera, and M. T. A. Mayaffre and, “Part 2: Limiting apparent molar volume of organic and inorganic 1:1 electrolytes in (water + ethylammonium nitrate) mixtures at 298 k – thermodynamic approach using bahe–varela pseudo-lattice theory,” *J. Chem. Thermodyn.*, vol. 40, no. 2, pp. 146–154, 2008.
- [21] T. Heimburg, S. Z. Mirzaev, and U. Kaatz, “Heat capacity behavior in the critical region of the ionic binary mixture ethylammonium nitrate-n-octanol,” *Phys. Rev. E*, vol. 62, no. 4, pp. 4963–4967, 2000.
- [22] A. Chagnes, A. Tougui, B. Carre, N. Ranganathan, and D. Lemordant, “Abnormal temperature dependence of the viscosity of ethylammonium nitrate–methanol ionic mixtures,” *J. Sol. Chem.*, vol. 33, no. 3, pp. 247–255, 2004.
- [23] T. L. Greaves, D. F. Kennedy, A. Weerawardena, N. M. K. Tse, N. Kirby, and C. J. Drummond, “Nanostructured protic ionic liquids retain nanoscale features in aqueous solution while precursor brønsted acids and bases exhibit different behavior,” *J. Phys. Chem. B*, vol. 115, no. 9, pp. 2055–2066, 2011.

- [24] T. L. Greaves, D. F. Kennedy, N. Kirbyb, and C. J. Drummond, "Nanostructure changes in protic ionic liquids (PILs) through adding solutes and mixing PILs," *Phys. Chem. Chem. Phys.*, vol. 13, no. 30, pp. 13501–13509, 2011.
- [25] S. Perkin, "Ionic liquids in confined geometries," *Phys. Chem. Chem. Phys.*, vol. 14, no. 15, pp. 5052–5062, 2012.
- [26] M. P. Singh, R. K. Singh, and S. Chandra, "Ionic liquids confined in porous matrices: Physicochemical properties and applications," *Prog. Mat. Sci.*, vol. 64, pp. 73 – 120, 2014.
- [27] C. Merlet, B. Rotenberg, P. A. Madden, P.-L. Taberna, P. Simon, Y. Gogotsi, and M. Salanne, "On the molecular origin of supercapacitance in nanoporous carbon electrodes," *Nat. Mater.*, vol. 11, pp. 306—310, 2012.
- [28] P. Niga, D. Wakeham, A. Nelson, G. G. Warr, M. Rutland, and R. Atkin, "Structure of the ethylammonium nitrate surface: an x-ray reflectivity and vibrational sum frequency spectroscopy study," *Langmuir*, vol. 26, no. 11, pp. 8282–8288, 2010.
- [29] R. Wen, B. Rahn, and O. M. Magnussen, "Potential-dependent adlayer structure and dynamics at the ionic liquid/Au (111) interface: A molecular-scale in situ video-STM study," *Angew. Chem.*, vol. 54, no. 20, pp. 6062–6066, 2015.
- [30] S. A. Kislenko, I. S. Samoylov, and R. H. Amirov, "Molecular dynamics simulation of the electrochemical interface between a graphite surface and the ionic liquid [BMIM][PF₆]," *Phys. Chem. Chem. Phys.*, vol. 11, no. 27, pp. 5584–5590, 2009.
- [31] M. V. Fedorov and R. M. Lynden-Bell, "Probing the neutral graphene–ionic liquid interface: insights from molecular dynamics simulations," *Phys. Chem. Chem. Phys.*, vol. 14, pp. 2552–2556, 2012.

- [32] R. M. Lynden-Bell, A. I. Frolov, and M. V. Fedorov, "Electrode screening by ionic liquids," *Phys. Chem. Chem. Phys.*, vol. 14, no. 8, pp. 2693–2701, 2012.
- [33] C. Pinilla, M. G. Del Pópolo, R. M. Lynden-Bell, and J. Kohanoff, "Structure and dynamics of a confined ionic liquid. Topics of relevance to dye-sensitized solar cells," *J. Phys. Chem. B*, vol. 109, no. 38, pp. 17922–17927, 2005.
- [34] A. A. Kornyshev, "Double-layer in ionic liquids: Paradigm change?," *J. Phys. Chem. B*, vol. 111, no. 20, pp. 5545–5557, 2007.
- [35] M. V. Fedorov and A. A. Kornyshev, "Towards understanding the structure and capacitance of electrical double layer in ionic liquids," *Electrochim. Acta*, vol. 111, no. 23, pp. 6835–6840, 2008.
- [36] S. Maolin, Z. Fuchun, W. Guozhong, F. Haiping, W. Chunlei, C. Shimou, Z. Yi, and H. Jun, "Ordering layers of [BMIM][PF₆] ionic liquid on graphite surfaces: Molecular dynamics simulation," *J. Chem. Phys.*, vol. 128, no. 13, p. 134504, 2008.
- [37] G. Feng, J. S. Zhang, and R. Qiao, "Microstructure and capacitance of the electrical double layers at the interface of ionic liquids and planar electrodes," *J. Phys. Chem. C*, vol. 113, no. 11, pp. 4549–4559, 2009.
- [38] S. Wang, S. Li, Z. Cao, and T. Yan, "Molecular dynamic simulations of ionic liquids at graphite surface," *J. Phys. Chem. C*, vol. 114, no. 2, pp. 990–995, 2010.
- [39] Q. Dou, M. L. Sha, H. Y. Fu, and G. Z. Wu, "Molecular dynamics simulation of the interfacial structure of [C_nMIM][PF₆] adsorbed on a graphite surface: effects of temperature and alkyl chain length," *J. Phys. Condens. Matter*, vol. 23, no. 17, pp. 175001(1)–175001(8), 2011.

- [40] R. S. Payal and S. Balasubramanian, "Orientational ordering of ionic liquids near a charged mica surface," *Chem. Phys. Chem.*, vol. 13, no. 7, pp. 1764–1771, 2012.
- [41] M. V. Fedorov and A. A. Kornyshev, "Ionic liquids at electrified interfaces," *Chem. Rev.*, vol. 114, no. 5, pp. 2978–3036, 2014.
- [42] V. Ivaništšev, S. O'Connor, and M. V. Fedorov, "Poly(a)morphic portrait of the electrical double layer in ionic liquids," *Electrochem. Commun.*, vol. 48, pp. 61–64, 2014.
- [43] V. Ivaništšev, K. Kirchner, T. Kirchner, and M. V. Fedorov, "Restructuring of the electrical double layer in ionic liquids upon charging," *J. Phys. Condens. Matter*, vol. 27, no. 10, p. 102101, 2015.
- [44] N. N. Rajput, J. Monk, and F. R. Hung, "Ionic liquids confined in a realistic activated carbon model: A molecular simulation study," *J. Phys. Chem. C*, vol. 118, no. 3, pp. 1540–1553, 2014.
- [45] T. Méndez-Morales, J. Carrete, M. Pérez-Rodríguez, Ó. Cabeza, L. J. Gallego, R. M. Lynden-Bell, and L. M. Varela, "Molecular dynamics simulations of the structure of the graphene–ionic liquid/alkali salt mixtures interface," *Phys. Chem. Chem. Phys.*, vol. 16, no. 26, pp. 13271–13278, 2014.
- [46] V. Ivanistsev, T. Mendez-Morales, R. M. Lynden-Bell, O. Cabeza, L. J. Gallego, L. M. Varela, and M. V. Fedorov, "Molecular origin of high free energy barriers for alkali metal ion transfer through ionic liquid-graphene electrode interfaces," *Phys. Chem. Chem. Phys.*, vol. 18, no. 2, pp. 1302–1310, 2016.
- [47] V. Gómez-González, B. Docampo-Álvarez, O. Cabeza, M. Fedorov, R. M. Lynden-Bell, L. J. Gallego, and L. M. Varela, "Molecular dynamics simulations of the structure and single-particle dynamics of mixtures of divalent salts and ionic liquids," *J. Chem. Phys.*, vol. 143, no. 12, p. 124507, 2015.

- [48] V. Gómez-González, B. Docampo-Álvarez, T. Méndez-Morales, O. Cabeza, V. B. Ivaništšev, M. V. Fedorov, L. J. Gallego, and L. M. Varela, “Molecular dynamics simulation of the structure and interfacial free energy barriers of mixtures of ionic liquids and divalent salts near a graphene wall,” *Phys. Chem. Chem. Phys.*, vol. 19, no. 1, pp. 846–853, 2017.
- [49] Y. Chen, Y. Cao, X. Lu, C. Zhao, C. Yan, and T. Mu, “Water sorption in protic ionic liquids: correlation between hygroscopicity and polarity,” *New J. Chem.*, vol. 37, no. 7, pp. 1959–1967, 2013.
- [50] S. Cuadrado-Prado, M. Domínguez-Pérez, E. Rilo, S. García-Garabal, L. Segade, C. Franjo, and O. Cabeza, “Experimental measurement of the hygroscopic grade on eight imidazolium based ionic liquids,” *Fluid Phase Equil.*, vol. 278, no. 1–2, pp. 36–40, 2009.
- [51] G. Feng, X. Jiang, R. Qiao, and A. A. Kornyshev, “Water in ionic liquids at electrified interfaces: The anatomy of electrosorption,” *ACS Nano*, vol. 8, no. 11, pp. 11685–11694, 2014.
- [52] C. Merlet, D. T. Limmer, M. Salanne, R. Van Roij, P. A. Madden, D. Chandler, and B. Rotenberg, “The electric double layer has a life of its own,” *J. Phys. Chem. C*, vol. 118, no. 32, pp. 18291–18298, 2014.
- [53] B. Rotenberg and M. Salanne, “Structural transitions at ionic liquid interfaces,” *J. Phys. Chem. Lett.*, pp. 4978–4985, 2015.
- [54] H. Montes-Campos, J. M. Otero-Mato, T. Méndez-Morales, O. Cabeza, L. J. Gallego, A. Ciach, and L. M. Varela, “Two-dimensional pattern formation in ionic liquids confined between graphene walls,” *Phys. Chem. Chem. Phys.*, vol. 19, no. 36, pp. 24505–24512, 2017.

- [55] H. Niedermeyer, J. P. Hallett, I. J. Villar-Garcia, P. A. Hunt, and T. Welton, "Mixtures of ionic liquids," *Chem. Soc. Rev.*, vol. 41, no. 23, pp. 7780–7802, 2012.
- [56] G. Chatel, J. F. Pereira, V. Debbeti, H. Wang, and R. D. Rogers, "Mixing ionic liquids—"simple mixtures" or "double salts"?", *Green Chem.*, vol. 16, no. 4, pp. 2051–2083, 2014.
- [57] D. Xiao, J. R. Rajian, S. Li, R. A. Bartsch, and E. L. Quitevis, "Additivity in the optical Kerr effect spectra of binary ionic liquid mixtures: implications for nanostructural organization," *J. Phys. Chem. B*, vol. 110, no. 33, pp. 16174–16178, 2006.
- [58] D. Xiao, J. R. Rajian, L. G. Hines Jr, S. Li, R. A. Bartsch, and E. L. Quitevis, "Nanostructural organization and anion effects in the optical kerr effect spectra of binary ionic liquid mixtures," *J. Phys. Chem. B*, vol. 112, no. 42, pp. 13316–13325, 2008.
- [59] M. Brüssel, M. Brehm, T. Voigt, and B. Kirchner, "Ab initio molecular dynamics simulations of a binary system of ionic liquids," *Phys. Chem. Chem. Phys.*, vol. 13, no. 30, pp. 13617–13620, 2011.
- [60] M. Brüssel, M. Brehm, A. S. Pensado, F. Malberg, M. Ramzan, A. Stark, and B. Kirchner, "On the ideality of binary mixtures of ionic liquids," *Phys. Chem. Chem. Phys.*, vol. 14, no. 38, pp. 13204–13215, 2012.
- [61] A. Stoppa, R. Buchner, and G. Hefter, "How ideal are binary mixtures of room-temperature ionic liquids?," *J. Mol. Liq.*, vol. 153, no. 1, pp. 46–51, 2010.
- [62] K. Shimizu, M. Tariq, L. P. Rebelo, and J. N. C. Lopes, "Binary mixtures of ionic liquids with a common ion revisited: A molecular dynamics simulation study," *J. Mol. Liq.*, vol. 153, no. 1, pp. 52–56, 2010.

- [63] H. Every, A. Bishop, M. Forsyth, and D. MacFarlane, "Ion diffusion in molten salt mixtures," *Electrochim. Acta*, vol. 45, no. 8, pp. 1279–1284, 2000.
- [64] C. Lian, K. Liu, K. L. Van Aken, Y. Gogotsi, D. J. Wesolowski, H. Liu, D. Jiang, and J. Wu, "Enhancing the capacitive performance of electric double-layer capacitors with ionic liquid mixtures," *ACS Energy Lett.*, vol. 1, no. 1, pp. 21–26, 2016.
- [65] L. Shi and L. Zheng, "Aggregation behavior of surface active imidazolium ionic liquids in ethylammonium nitrate: effect of alkyl chain length, cations, and counterions," *J. Phys. Chem. B*, vol. 116, no. 7, pp. 2162–2172, 2012.
- [66] S. Thomaier and W. Kunz, "Aggregates in mixtures of ionic liquids," *J. Mol. Liq.*, vol. 130, no. 1, pp. 104–107, 2007.
- [67] O. Russina, F. Lo Celso, N. V. Plechkova, and A. Triolo, "Emerging evidences of mesoscopic-scale complexity in neat ionic liquids and their mixtures," *J. Phys. Chem. Lett.*, vol. 8, no. 6, pp. 1197–1204, 2017.
- [68] P. Wasserscheid and W. Keim, "Ionic liquids—new "solutions" for transition metal catalysis," *Angew. Chem. Int. Ed.*, vol. 39, no. 21, pp. 3772–3789, 2000.
- [69] I. Krossing, J. M. Slattery, C. Daguinet, P. J. Dyson, A. Oleinikova, and H. Weingärtner, "Why are ionic liquids liquid? a simple explanation based on lattice and solvation energies," *J. Am. Chem. Soc.*, vol. 128, no. 41, pp. 13427–13434, 2006.
- [70] J. N. Canongia Lopes and A. A. Pádua, "Nanostructural organization in ionic liquids," *J. Phys. Chem. B*, vol. 110, no. 7, pp. 3330–3335, 2006.
- [71] A. Triolo, O. Russina, H.-J. Bleif, and E. Di Cola, "Nanoscale segregation in room temperature ionic liquids," *J. Phys. Chem. B*, vol. 111, no. 18, pp. 4641–4644, 2007.

- [72] R. Atkin and G. G. Warr, "The smallest amphiphiles: Nanostructure in protic room-temperature ionic liquids with short alkyl groups," *J. Phys. Chem. B*, vol. 112, no. 14, pp. 4164–4166, 2008.
- [73] D. R. MacFarlane, J. M. Pringle, K. M. Johansson, S. A. Forsyth, and M. Forsyth, "Lewis base ionic liquids," *Chem. Comm.*, no. 18, pp. 1905–1917, 2006.
- [74] J.-P. Belieres and C. A. Angell, "Protic ionic liquids: preparation, characterization, and proton free energy level representation," *J. Phys. Chem. B*, vol. 111, no. 18, pp. 4926–4937, 2007.
- [75] M. A. Susan, A. Noda, S. Mitsushima, and M. Watanabe, "Brönsted acid–base ionic liquids and their use as new materials for anhydrous proton conductors," *Chem. Commun.*, no. 8, pp. 938–939, 2003.
- [76] H. Nakamoto and M. Watanabe, "Brönsted acid–base ionic liquids for fuel cell electrolytes," *Chem. Commun.*, no. 24, pp. 2539–2541, 2007.
- [77] S.-Y. Lee, A. Ogawa, M. Kanno, H. Nakamoto, T. Yasuda, and M. Watanabe, "Nonhumidified intermediate temperature fuel cells using protic ionic liquids," *J. Am. Chem. Soc.*, vol. 132, no. 28, pp. 9764–9773, 2010.
- [78] T. L. Greaves and C. J. Drummond, "Protic ionic liquids: properties and applications," *Chem. Rev.*, vol. 108, no. 1, pp. 206–237, 2008.
- [79] T. Sato, T. Maruo, S. Marukane, and K. Takagi, "Ionic liquids containing carbonate solvent as electrolytes for lithium ion cells," *J. Power Sources*, vol. 138, no. 1-2, pp. 253–261, 2004.
- [80] L. Varela, J. Carrete, M. García, L. Gallego, M. Turmine, E. Rilo, and O. Cabeza, "Pseudolattice theory of charge transport in ionic solutions: Corresponding states law for the

- electric conductivity,” *Fluid Phase Equilibr*, vol. 298, no. 2, pp. 280–286, 2010.
- [81] E. Rilo, J. Vila, S. García-Garabal, L. Varela, and O. Cabeza, “Electrical conductivity of seven binary systems containing 1-ethyl-3-methyl imidazolium alkyl sulfate ionic liquids with water or ethanol at four temperatures,” *J. Phys. Chem. B*, vol. 117, no. 5, pp. 1411–1418, 2013.
- [82] O. Russina, R. Caminiti, T. Méndez-Morales, J. Carrete, O. Cabeza, L. Gallego, L. Varela, and A. Triolo, “How does lithium nitrate dissolve in a protic ionic liquid?,” *J. Mol. Liq.*, vol. 205, pp. 16–21, 2015.
- [83] T. Méndez-Morales, J. Carrete, O. Cabeza, O. Russina, A. Triolo, L. J. Gallego, and L. M. Varela, “Solvation of lithium salts in protic ionic liquids: a molecular dynamics study,” *J. Phys. Chem. B*, vol. 118, no. 3, pp. 761–770, 2014.
- [84] L. Varela, T. Méndez-Morales, J. Carrete, V. Gómez-González, B. Docampo-Álvarez, L. Gallego, O. Cabeza, and O. Russina, “Solvation of molecular cosolvents and inorganic salts in ionic liquids: a review of molecular dynamics simulations,” *J. Mol. Liq.*, vol. 210, pp. 178–188, 2015.
- [85] L. Segade, M. Cabanas, M. Domínguez-Pérez, E. Rilo, S. García-Garabal, M. Turmine, L. M. Varela, V. Gómez-González, B. Docampo-Alvarez, and O. Cabeza, “Surface and bulk characterisation of mixtures containing alkylammonium nitrates and water or ethanol: Experimental and simulated properties at 298.15 k,” *J. Mol. Liq.*, vol. 222, pp. 663–670, 2016.
- [86] H. Rodríguez and J. F. Brennecke, “Temperature and composition dependence of the density and viscosity of binary mixtures of water+ ionic liquid,” *J. Chem. Eng. Data*, vol. 51, no. 6, pp. 2145–2155, 2006.

- [87] S. Zhang, N. Sun, X. He, X. Lu, and X. Zhang, “Physical properties of ionic liquids: database and evaluation,” *J. Phys. Chem. Ref. Data*, vol. 35, no. 4, pp. 1475–1517, 2006.
- [88] S. B. Capelo, T. Méndez-Morales, J. Carrete, E. López Lago, J. Vila, O. Cabeza, J. Rodríguez, M. Turmine, and L. Varela, “Effect of temperature and cationic chain length on the physical properties of ammonium nitrate-based protic ionic liquids,” *J. Phys. Chem. B*, vol. 116, no. 36, pp. 11302–11312, 2012.
- [89] L. Martínez, R. Andrade, E. G. Birgin, and J. M. Martínez, “Packmol: a package for building initial configurations for molecular dynamics simulations,” *J. Comput. Chem.*, vol. 30, no. 13, pp. 2157–2164, 2009.
- [90] H. J. Berendsen and W. F. Van Gunsteren, *Practical algorithms for dynamic simulations*. North-Holland, Amsterdam, 1986.
- [91] M. Abraham, D. van der Spoel, E. Lindahl, and B. Hess, “GROMACS 2016 user manual,”
- [92] W. L. Jorgensen, “Optimized intermolecular potential functions for liquid alcohols,” *J. Phys. Chem.*, vol. 90, no. 7, pp. 1276–1284, 1986.
- [93] W. F. van Gunsteren, X. Daura, and A. E. Mark, “GROMOS force field,” *Enc. Comp. Chem.*, vol. 2, 2002.
- [94] J. Wang, R. M. Wolf, J. W. Caldwell, P. A. Kollman, and D. A. Case, “Development and testing of a general amber force field,” *J. Comp. Chem.*, vol. 25, no. 9, pp. 1157–1174, 2004.
- [95] K. Vanommeslaeghe, E. Hatcher, C. Acharya, S. Kundu, S. Zhong, J. Shim, E. Darian, O. Guvench, P. Lopes, I. Vorobyov, *et al.*, “CHARMM general force field: A force field for drug-like molecules compatible with the CHARMM all-atom additive biological force fields,” *J. Comp. Chem.*, vol. 31, no. 4, pp. 671–690, 2010.

- [96] T. Méndez-Morales, J. Carrete, J. R. Rodríguez, O. Cabeza, L. J. Gallego, O. Russina, and L. M. Varela, "Nanostructure of mixtures of protic ionic liquids and lithium salts: effect of alkyl chain length," *Phys. Chem. Chem. Phys.*, vol. 17, no. 7, pp. 5298–5307, 2015.
- [97] M. Armand, F. Endres, D. R. MacFarlane, H. Ohno, and B. Scrosati, "Ionic-liquid materials for the electrochemical challenges of the future," *Nat. Mater.*, vol. 8, no. 8, pp. 621–629, 2009.
- [98] M. Freemantle, *An Introduction to Ionic Liquids*. RSC Publishing, 2009.
- [99] P. Wasserscheid and T. Welton, eds., *Ionic Liquids in Synthesis*. Wiley-VCH, 2003.
- [100] S. Zhang, X. Lu, Q. Zhou, X. Li, X. Zhang, and S. Li, *Ionic liquids. Physicochemical properties*. Elsevier, 2009.
- [101] M. Yoshizawa, W. Xu, and C. A. Angell, "Ionic liquids by proton transfer: Vapor pressure, conductivity, and the relevance of ΔpK_a from aqueous solutions," *J. Am. Chem. Soc.*, vol. 125, no. 50, pp. 15411–15419, 2003.
- [102] C. A. Angell, N. Byrne, and J.-P. Belieres, "Parallel developments in aprotic and protic ionic liquids: Physical chemistry and applications," *Acc. Chem. Res.*, vol. 40, no. 11, pp. 1228–1236, 2007.
- [103] T. L. Greaves, A. Weerawardena, C. Fong, I. Krodkiewska, and C. J. Drummond, "Protic ionic liquids: solvents with tunable phase behavior and physicochemical properties," *J. Phys. Chem. B*, vol. 110, no. 45, pp. 22479–22487, 2006.
- [104] L. Timperman, P. Skowron, A. Boisset, H. Galiano, D. Lemordant, E. Frackowiak, F. Béguin, and M. Anouti, "Triethylammonium bis (tetrafluoromethylsulfonyl) amide protic ionic

- liquid as an electrolyte for electrical double-layer capacitors,” *Phys. Chem. Chem. Phys.*, vol. 14, no. 22, pp. 8199–8207, 2012.
- [105] M. Anouti and L. Timperman, “A pyrrolidinium nitrate protic ionic liquid-based electrolyte for very low-temperature electrical double-layer capacitors,” *Phys. Chem. Chem. Phys.*, vol. 15, no. 17, pp. 6539–6548, 2013.
- [106] P. Walden *et al.*, “Molecular weights and electrical conductivity of several fused salts,” *Bull. Acad. Imper. Sci. (St. Petersburg)*, vol. 8, pp. 405–422, 1914.
- [107] V. H. Alvarez, N. Dosil, R. Gonzalez-Cabaleiro, S. Mattedi, M. Martin-Pastor, M. Iglesias, and J. M. Navaza, “Brønsted ionic liquids for sustainable processes: Synthesis and physical properties,” *J. Chem. Eng. Data*, vol. 55, no. 2, pp. 625–632, 2010.
- [108] B. Fernández-Castro, T. Méndez-Morales, J. Carrete, E. Fazer, O. Cabeza, J. R. Rodríguez, M. Turmine, and L. M. Varela, “Surfactant self-assembly nanostructures in protic ionic liquids,” *J. Phys. Chem. B*, vol. 115, no. 25, pp. 8145–8154, 2011.
- [109] R. Atkin, S. M. C. Bobillier, and G. G. Warr, “Propylammonium nitrate as a solvent for amphiphile self-assembly into micelles, lyotropic liquid crystals, and microemulsions,” *J. Phys. Chem. B*, vol. 114, no. 3, pp. 1350–1360, 2010.
- [110] R. Hayes, S. Imberti, G. G. Warr, and R. Atkin, “Pronounced sponge-like nanostructure in propylammonium nitrate,” *Phys. Chem. Chem. Phys.*, vol. 13, no. 30, pp. 13544–13551, 2011.
- [111] J. Hunger, T. Sonnleitner, L. Liu, R. Buchner, M. Bonn, and H. J. Bakker, “Hydrogen-bond dynamics in a protic ionic liquid: Evidence of large-angle jumps,” *J. Phys. Chem. Lett.*, vol. 3, no. 20, pp. 3034–3038, 2012.

- [112] R. Hayes, S. Imberti, G. G. Warr, and R. Atkin, "Amphiphilicity determines nanostructure in protic ionic liquids," *Phys. Chem. Chem. Phys.*, vol. 13, no. 8, pp. 3237–3247, 2011.
- [113] D. F. Kennedy and C. J. Drummond, "Large aggregated ions found in some protic ionic liquids," *J. Phys. Chem. B*, vol. 113, no. 17, pp. 5690–5693, 2009.
- [114] X. C. X. Wang, Q. Li and Z. Li, "Effects of structure dissymmetry on aggregation behaviors of quaternary ammonium gemini surfactants in a protic ionic liquid EAN," *Langmuir*, vol. 28, no. 48, pp. 16547–16554, 2012.
- [115] C. Zhao, G. Burrell, A. A. J. Torriero, F. Separovic, N. F. Dunlop, D. R. MacFarlane, and A. M. Bond, "Electrochemistry of room temperature protic ionic liquids," *J. Phys. Chem. B*, vol. 112, no. 23, pp. 6923–6936, 2008.
- [116] T. L. Greaves, A. Weerawardena, I. Krodkiewska, and C. J. Drummond, "Protic ionic liquids: Physicochemical properties and behavior as amphiphile self-assembly solvents," *J. Phys. Chem. B*, vol. 112, no. 3, pp. 896–905, 2008.
- [117] T. L. Greaves, A. Weerawardena, C. Fong, and C. J. Drummond, "Formation of amphiphile self-assembly phases in protic ionic liquids," *J. Phys. Chem. B*, vol. 111, no. 16, pp. 4082–4088, 2007.
- [118] E. Bodo, P. Postorino, S. Mangialardo, G. Piacente, F. Ramondo, F. Bosi, P. Ballirano, and R. Caminiti, "Structure of the molten salt methyl ammonium nitrate explored by experiments and theory," *J. Phys. Chem. B*, vol. 115, no. 45, pp. 13149–13161, 2011.
- [119] H. Markusson, J.-P. Belieres, P. Johansson, C. A. Angell, and P. Jacobsson, "Prediction of macroscopic properties of protic ionic liquids by ab initio calculations," *J. Phys. Chem. A*, vol. 111, no. 35, pp. 8717–8723, 2007.

- [120] E. Bodo, S. Mangialardo, F. Ramondo, F. Ceccacci, and P. Postorino, "Unravelling the structure of protic ionic liquids with theoretical and experimental methods: Ethyl, propyl- and butylammonium nitrate explored by Raman spectroscopy and DFT calculations," *J. Phys. Chem. B*, vol. 116, no. 47, pp. 13878–13888, 2012.
- [121] X. Song, H. Hamano, B. Minofar, R. Kanzaki, K. Fujii, Y. Kameda, S. Kohara, M. Watanabe, S. Ishiguro, and Y. Umebayashi, "Structural heterogeneity and unique distorted hydrogen bonding in primary ammonium nitrate ionic liquids studied by high-energy X-ray diffraction experiments and MD simulations," *J. Phys. Chem. B*, vol. 116, no. 9, pp. 2801–2813, 2012.
- [122] Y. Umebayashi, W.-L. Chung, T. Mitsugi, S. Fukuda, M. Takeuchi, K. Fujii, T. Takamuku, R. Kanzaki, and S. Ishiguro, "Liquid structure and the ion-ion interactions of ethylammonium nitrate ionic liquid studied by large angle X-ray scattering and molecular dynamics simulations," *J. Comput. Chem. Jpn.*, vol. 7, no. 4, pp. 125–134, 2008.
- [123] S. Zahn, J. Thar, and B. Kirchner, "Structure and dynamics of the protic ionic liquid monomethylammonium nitrate ($[\text{CH}_3\text{NH}_3][\text{NO}_3]$) from ab initio molecular dynamics simulations," *J. Chem. Phys.*, vol. 132, no. 12, pp. 124506–124506, 2010.
- [124] K. Fumino, A. Wulf, and R. Ludwig, "Hydrogen bonding in protic ionic liquids: reminiscent of water," *Angew. Chem. Int. Ed.*, vol. 48, no. 17, pp. 3184–3186, 2009.
- [125] A. Luzar and D. Chandler, "Effect of environment on hydrogen bond dynamics in liquid water," *Phys. Rev. Lett.*, vol. 76, no. 6, pp. 928–931, 1996.
- [126] F. H. Stillinger, "Water revisited," *Science*, vol. 209, no. 4455, pp. 451–457, 1980.

- [127] L. Saiz, J. A. Padro, and E. Guardia, "Structure and dynamics of liquid ethanol," *J. Phys. Chem. B*, vol. 101, no. 1, pp. 78–86, 1997.
- [128] M. Haughney, M. Ferrario, and I. R. McDonald, "Molecular-dynamics simulation of liquid methanol," *J. Phys. Chem.*, vol. 91, no. 19, pp. 4934–4940, 1987.
- [129] T. Yamaguchi, H. Hidaka, and A. K. Soper, "The structure of liquid methanol revisited: A neutron diffraction experiment at -80 C and 25 C," *Mol. Phys.*, vol. 96, no. 8, pp. 1159–1168, 1999.
- [130] M. Matsumoto and K. E. Gubbins, "Hydrogen bonding in liquid methanol," *J. Chem. Phys.*, vol. 93, no. 3, pp. 1981–1994, 1990.
- [131] R. Hayes, S. Imberti, G. G. Warr, and R. Atkin, "How water dissolves in protic ionic liquids," *Angew. Chem. Int. Ed.*, vol. 51, no. 30, pp. 7468–7471, 2012.
- [132] D. V. D. Spoel, E. Lindahl, B. Hess, A. R. V. Buuren, E. Apol, P. J. Meulenhoff, D. P. Tieleman, A. L. T. M. Sijbers, K. A. Feenstra, R. V. Drunen, and H. J. C. Berendsen, *GROMACS User Manual version 4.0*. <http://www.Gromacs.org>, 2005.
- [133] S. V. Sambasivarao and O. Acevedo, "Development of OPLS-AA force field parameters for 68 unique ionic liquids," *J. Chem. Theory Comput.*, vol. 5, no. 4, pp. 1038–1050, 2009.
- [134] M. W. Mahoney and W. L. Jorgensen, "A five-site model for liquid water and the reproduction of the density anomaly by rigid, nonpolarizable potential functions," *J. Chem. Phys.*, vol. 112, no. 20, p. 8910–8922, 2000.
- [135] W. L. Jorgensen, D. S. Maxwell, and J. Tirado-Rives, "Development and testing of the opls all-atom force field on conformational energetics and properties of organic liquids," *J. Am. Chem. Soc.*, vol. 118, no. 45, pp. 11225–11236, 1996.

- [136] T. Méndez-Morales, J. Carrete, S. Bouzón-Capelo, M. Pérez-Rodríguez, O. Cabeza, L. J. Gallego, and L. M. Varela, “Molecular dynamics simulations of the formation of stable clusters in mixtures of alkaline salts and imidazolium-based ionic liquids,” *J. Phys. Chem. B*, vol. 117, no. 11, pp. 3207–3220, 2013.
- [137] S. Feng and G. A. Voth, “Molecular dynamics simulations of imidazolium-based ionic liquid/water mixtures: Alkyl side chain length and anion effects,” *Fluid Phase Equilibr.*, vol. 294, no. 1, pp. 148–156, 2010.
- [138] G. Raabe and J. Köhler, “Thermodynamical and structural properties of binary mixtures of imidazolium chloride ionic liquids and alcohols from molecular simulation,” *J. Chem. Phys.*, vol. 129, no. 14, p. 144503, 2008.
- [139] W. Jiang, Y. Wang, and G. A. Voth, “Molecular dynamics simulation of nanostructural organization in ionic liquid/water mixtures,” *J. Phys. Chem. B*, vol. 111, no. 18, pp. 4812–4818, 2007.
- [140] T. Méndez-Morales, J. Carrete, O. Cabeza, L. Gallego, and L. Varela, “Molecular dynamics simulations of the structural and thermodynamic properties of imidazolium-based ionic liquid mixtures,” *J. Phys. Chem. B*, vol. 115, no. 38, pp. 11170–11182, 2011.
- [141] J. N. Canongia Lopes, M. F. Costa Gomes, and A. A. Pádua, “Nonpolar, polar, and associating solutes in ionic liquids,” *J. Phys. Chem. B*, vol. 110, no. 34, pp. 16816–16818, 2006.
- [142] J. H. Guo, Y. Luo, A. Augustsson, J. Rubensson, C. Sånne, H. Ågren, H. Siegbahn, and J. Nordgren, “X-ray emission spectroscopy of hydrogen bonding and electronic structure of liquid water,” *Phys. Rev. Lett.*, vol. 89, no. 13, pp. 137402(1)–137402(4), 2002.

- [143] I. Harsányi, L. Pusztai, J. C. Soetens, and P. A. Bopp, “Molecular dynamics simulations of aqueous rbbr-solutions over the entire solubility range at room temperature,” *J. Mol. Liq.*, vol. 129, pp. 80–85, 2006.
- [144] M. Sokol, A. Dawid, Z. Dendzik, and Z. Gburski, “Structure and dynamics of water—molecular dynamics study,” *J. Mol. Struct.*, vol. 704, no. 1–3, pp. 341–345, 2004.
- [145] T. Méndez-Morales, J. Carrete, M. García, O. Cabeza, L. J. Gallego, and L. M. Varela, “Dynamical properties of alcohol+1-hexyl-3-methylimidazolium ionic liquid mixtures: a computer simulation study,” *J. Phys. Chem. B*, vol. 115, no. 51, pp. 15313–15322, 2011.
- [146] J. Vatamanu, Z. Hu, D. Bedrov, C. Perez, and Y. Gogotsi, “Increasing energy storage in electrochemical capacitors with ionic liquid electrolytes and nanostructured carbon electrodes,” *J. Phys. Chem. Lett.*, pp. 2829–2837, 2013.
- [147] D. R. MacFarlane, N. Tachikawa, M. Forsyth, J. M. Pringle, P. C. Howlett, G. D. Elliott, J. H. Davis, M. Watanabe, P. Simon, and C. A. Angell, “Energy applications of ionic liquids,” *Energy Environ. Sci.*, vol. 7, pp. 232–250, 2014.
- [148] H. Ohno, ed., *Electrochemical Aspects of Ionic Liquids*. Wiley & Sons, 2005.
- [149] D. R. MacFarlane, M. Forsyth, P. C. Howlett, J. M. Pringle, J. Sun, G. Annat, W. Neil, and E. I. Izgorodina, “Ionic liquids in electrochemical devices and processes: Managing interfacial electrochemistry,” *Acc. Chem. Res.*, vol. 40, no. 11, pp. 1165–1173, 2007.
- [150] Y. Zhai, Y. Dou, D. Zhao, P. F. Fulvio, R. T. Mayes, and S. Dai, “Carbon materials for chemical capacitive energy storage,” *Adv. Mater.*, vol. 23, no. 42, p. 4828–4850, 2011.

- [151] L. L. Zhang and X. S. Zhao, "Carbon-based materials as supercapacitor electrodes," *Chem. Soc. Rev.*, vol. 38, no. 9, pp. 2520–2531, 2009.
- [152] P. Simon and Y. Gogotsi, "Capacitive energy storage in nanostructured Carbon–Electrolyte systems," *Acc. Chem. Res.*, vol. 46, no. 5, pp. 1094–1103, 2013.
- [153] F. Béguin, V. Presser, A. Balducci, and E. Frackowiak, "Carbons and electrolytes for advanced supercapacitors," *Adv. Mater.*, vol. 26, no. 14, pp. 2219–2251, 2014.
- [154] G. Feng, S. Li, V. Presser, and P. T. Cummings, "Molecular insights into carbon supercapacitors based on room-temperature ionic liquids," *J. Phys. Chem. Lett.*, vol. 4, no. 19, pp. 3367–3376, 2013.
- [155] H. Kurig, M. Russina, I. Tallo, M. Siebenbürger, T. Romann, and E. Lust, "The suitability of infinite slit-shaped pore model to describe the pores in highly porous carbon materials," *Carbon*, vol. 100, pp. 617–624, 2016.
- [156] J. Britton, N. E. A. Cousens, S. W. Coles, C. D. van Engers, V. Babenko, A. T. Murdock, A. Koós, S. Perkin, and N. Grobert, "A graphene surface force balance," *Langmuir*, vol. 30, no. 38, pp. 11485–11492, 2014.
- [157] J. A. Widegren, A. Laesecke, and J. W. Magee, "The effect of dissolved water on the viscosities of hydrophobic room-temperature ionic liquids," *Chem. Commun.*, no. 12, pp. 1610–1612, 2005.
- [158] E. Rilo, J. Pico, S. García-Garabal, L. Varela, and O. Cabeza, "Density and surface tension in binary mixtures of $[C_n\text{MIM}][\text{BF}_4]$ ionic liquids with water and ethanol," *Fluid Phase Equilib.*, vol. 285, no. 1-2, pp. 83–89, 2009.

- [159] E. Rilo, J. Vila, S. García-Garabal, L. M. Varela, and O. Cabeza, “Electrical conductivity of seven binary systems containing 1-ethyl-3-methyl imidazolium alkyl sulfate ionic liquids with water or ethanol at four temperatures,” *J. Phys. Chem. B*, vol. 117, no. 5, pp. 1411–1418, 2013.
- [160] A. M. O’Mahony, D. S. Silvester, L. Aldous, C. Hardacre, and R. G. Compton, “Effect of water on the electrochemical window and potential limits of room-temperature ionic liquids,” *J. Chem. Eng. Data*, vol. 53, no. 12, pp. 2884–2891, 2008.
- [161] M. D. Fayer and N. E. Levinger, “Analysis of water in confined geometries and at interfaces,” *Annu. Rev. Anal. Chem.*, vol. 3, p. 89–107, 2010.
- [162] H. Zhou, P. Ganesh, V. Presser, M. C. F. Wander, P. Fenter, P. R. C. Kent, D. E. Jiang, A. A. Chialvo, J. McDonough, K. L. Shuford, and Y. Gogotsi, “Understanding controls on interfacial wetting at epitaxial graphene: Experiment and theory,” *Phys. Rev. B*, vol. 85, no. 3, p. 035406, 2012.
- [163] R. M. Espinosa-Marzal, A. Arcifa, A. Rossi, and N. D. Spencer, “Ionic liquids confined in hydrophilic nanocontacts: Structure and lubricity in the presence of water,” *J. Phys. Chem. C*, vol. 118, no. 12, pp. 6491–6503, 2014.
- [164] B. Hess, C. Kutzner, D. Van Der Spoel, and E. Lindahl, “GROMACS 4: algorithms for highly efficient, load-balanced, and scalable molecular simulation,” *J. Chem. Theory Comput.*, vol. 4, no. 3, pp. 435–447, 2008.
- [165] S. Pronk, S. Páll, R. Schulz, P. Larsson, P. Bjelkmar, R. Apostolov, M. R. Shirts, J. C. Smith, P. M. Kasson, D. v. d. Spoel, B. Hess, and E. Lindahl, “GROMACS 4.5: a high-throughput and highly parallel open source molecular simulation toolkit,” *Method. Biochem Anal.*, vol. 29, no. 7, pp. 845–854, 2013.

- [166] D. van der Spoel, E. Lindahl, B. Hess, A. R. van Buuren, E. Apol, P. J. Meulenhoff, D. P. Tieleman, A. L. T. M. Sijbers, K. A. Feenstra, R. van Drunen, and H. J. C. Berendsen, *GROMACS User Manual version 4.5*. www.gromacs.org, 2010.
- [167] E. Lindahl, B. Hess, and D. Van Der Spoel, “GROMACS 3.0: a package for molecular simulation and trajectory analysis,” *J. Mol. Model.*, vol. 7, no. 8, pp. 306–317, 2001.
- [168] H. J. Berendsen, D. van der Spoel, and R. van Drunen, “GROMACS: a message-passing parallel molecular dynamics implementation,” *Comput. Phys. Commun.*, vol. 91, no. 1, pp. 43–56, 1995.
- [169] G. Bussi, D. Donadio, and M. Parrinello, “Canonical sampling through velocity rescaling,” *J. Chem. Phys.*, vol. 126, no. 1, pp. 014101(1)–014101(7), 2007.
- [170] D. v. d. Spoel, E. Lindahl, B. Hess, A. R. v. Buuren, E. Apol, P. J. Meulenhoff, D. P. Tieleman, A. L. T. M. Sijbers, K. A. Feenstra, R. v. Drunen, and H. J. C. Berendsen, *GROMACS Users’ Manual version 3.3*. 2005.
- [171] W. Humphrey, A. Dalke, and K. Schulten, “VMD: visual molecular dynamics,” *J. Mol. Graph.*, vol. 14, no. 1, pp. 33–38, 27–28, 1996.
- [172] D. Frenkel and B. Smit, *Understanding molecular simulation*. Academic Press, 2002.
- [173] N. Michaud-Agrawal, E. J. Denning, T. B. Woolf, and O. Beckstein, “MDAnalysis: a toolkit for the analysis of molecular dynamics simulations,” *J. Comput. Chem.*, vol. 32, no. 10, pp. 2319–2327, 2011.
- [174] H. Li, R. J. Wood, F. Endres, and R. Atkin, “Influence of alkyl chain length and anion species on ionic liquid structure at the graphite interface as a function of applied potential,” *J. Phys. Condens. Matter*, vol. 26, no. 28, p. 284115, 2014.

- [175] V. Ivaništšev, M. V. Fedorov, and R. M. Lynden-Bell, "Screening of Ion–Graphene electrode interactions by ionic liquids: The effects of liquid structure," *J. Phys. Chem. C*, vol. 118, no. 11, pp. 5841–5847, 2014.
- [176] H. Ye, H. Zhang, Z. Zhang, and Y. Zheng, "Water sheared by charged graphene sheets," *J. Adhes. Sci. Technol.*, vol. 26, no. 12-17, pp. 1897–1908, 2012.
- [177] D. J. Bozym, B. Uralcan, D. T. Limmer, M. A. Pope, N. J. Szamreta, P. G. Debenedetti, and I. A. Aksay, "Anomalous capacitance maximum of the glassy Carbon–Ionic liquid interface through dilution with organic solvents," *J. Phys. Chem. Lett.*, vol. 6, no. 13, pp. 2644–2648, 2015.
- [178] J. Ding, D. Zhou, G. Spinks, G. Wallace, S. Forsyth, M. Forsyth, and D. MacFarlane, "Use of ionic liquids as electrolytes in electromechanical actuator systems based on inherently conducting polymers," *Chem. Mater.*, vol. 15, no. 12, pp. 2392–2398, 2003.
- [179] D. S. Silvester and L. Aldous, "Electrochemical detection using ionic liquids," in *RSC Detection Science* (D. W. M. Arrigan, ed.), pp. 341–386, Cambridge: Royal Society of Chemistry, 2015.
- [180] I. Must, U. Johanson, F. Kaasik, I. Põldsalu, A. Punning, and A. Aabloo, "Charging a supercapacitor-like laminate with ambient moisture: from a humidity sensor to an energy harvester," *Phys. Chem. Chem. Phys.*, vol. 15, no. 24, p. 9605, 2013.
- [181] I. Must, V. Vunder, F. Kaasik, I. Põldsalu, U. Johanson, A. Punning, and A. Aabloo, "Ionic liquid-based actuators working in air: The effect of ambient humidity," *Sens. Actuator B-Chem.*, vol. 202, pp. 114–122, 2014.
- [182] R. D. Rogers, K. R. Seddon, and S. Volkov, *Green industrial applications of ionic liquids*, vol. 92. Springer Science & Business Media, 2012.

- [183] A. P. De Los Rios and F. J. H. Fernandez, *Ionic Liquids in Separation Technology*. Elsevier, 2014.
- [184] J. Vila, P. Gines, J. Pico, C. Franjo, E. Jimenez, L. Varela, and O. Cabeza, “Temperature dependence of the electrical conductivity in emim-based ionic liquids: evidence of Vogel–Tamman–Fulcher behavior,” *Fluid Phase Equilib*, vol. 242, no. 2, pp. 141–146, 2006.
- [185] J. Vila, L. Varela, and O. Cabeza, “Cation and anion sizes influence in the temperature dependence of the electrical conductivity in nine imidazolium based ionic liquids,” *Electrochim Acta*, vol. 52, no. 26, pp. 7413–7417, 2007.
- [186] O. Cabeza, S. García-Garabal, L. Segade, M. Domínguez-Pérez, E. Rilo, and L. M. Varela, “Physical properties of binary mixtures of ILs with water and ethanol. A review.,” in *Ionic Liquids: Theory, Properties, New Approaches*, InTech, 2011.
- [187] E. Rilo, M. Domínguez-Pérez, J. Vila, L. Segade, M. García, L. Varela, and O. Cabeza, “Easy prediction of the refractive index for binary mixtures of ionic liquids with water or ethanol,” *J. Chem. Thermodyn*, vol. 47, pp. 219–222, 2012.
- [188] O. Cabeza, J. Vila, E. Rilo, M. Domínguez-Pérez, L. Otero-Cernadas, E. López-Lago, T. Méndez-Morales, and L. Varela, “Physical properties of aqueous mixtures of the ionic 1-ethyl-3-methyl imidazolium octyl sulfate: A new ionic rigid gel,” *J. Chem. Thermodyn*, vol. 75, pp. 52–57, 2014.
- [189] T. L. Greaves and C. J. Drummond, “Protic ionic liquids: evolving structure–property relationships and expanding applications,” *Chem. Rev.*, vol. 115, no. 20, pp. 11379–11448, 2015.
- [190] L. J. Moore, M. D. Summers, and G. A. Ritchie, “Optical trapping and spectroscopic characterisation of ionic li-

- quid solutions,” *Phys. Chem. Chem. Phys.*, vol. 15, no. 32, pp. 13489–13498, 2013.
- [191] X. Lu and C. Zhao, “Controlled electrochemical intercalation, exfoliation and in situ nitrogen doping of graphite in nitrate-based protic ionic liquids,” *Phys. Chem. Chem. Phys.*, vol. 15, no. 46, pp. 20005–20009, 2013.
- [192] N. Byrne and C. A. Angell, “The solubility of hen lysozyme in ethylammonium nitrate/h₂O mixtures and a novel approach to protein crystallization,” *Molecules*, vol. 15, no. 2, pp. 793–803, 2010.
- [193] S. Gottesfeld, *Fuel Cell Science: theory, fundamentals, and biocatalysis*, vol. 9. John Wiley & Sons, 2011.
- [194] J. H. Gladstone, T. Dale, *et al.*, “Xiv. researches on the refraction, dispersion, and sensitiveness of liquids,” *Philosophical Transactions of the Royal Society of London*, vol. 153, pp. 317–343, 1863.
- [195] J. A. Riddick, W. B. Bunger, and T. K. Sakano, “Organic solvents: physical properties and methods of purification,” 1986.
- [196] G. Vazquez, E. Alvarez, and J. M. Navaza, “Surface tension of alcohol water + water from 20 to 50 C,” *J. Chem. Eng. Data*, vol. 40, no. 3, pp. 611–614, 1995.
- [197] M. Haddad, A. Mayaffre, and P. Letellier, “Tensions superficielles des solutions idéales: application aux solvants binaires constitués de méthanol et de nitrate d’éthylammonium fondu à 298 k,” *J. Chim. Phys.*, vol. 86, pp. 525–537, 1989.
- [198] S. Porcedda, B. Marongiu, M. Schirru, D. Falconieri, and A. Piras, “Excess enthalpy and excess volume for binary systems of two ionic liquids+ water,” *J. Therm. Anal. Calorim.*, vol. 103, no. 1, pp. 29–33, 2010.

- [199] M. Haddad, H. Bahri, and P. Letellier, "Tensions superficielles des mélanges binaires eau-nitrate d'éthylammonium à 298 K," *J. Chim. Phys.*, vol. 83, pp. 419–426, 1986.
- [200] M. Usula, E. Matteoli, F. Leonelli, F. Mocchi, F. C. Marincola, L. Gontrani, and S. Porcedda, "Thermo-physical properties of ammonium-based ionic liquid+n-methyl-2-pyrrolidone mixtures at 298.15 K," *Fluid Phase Equilib*, vol. 383, pp. 49–54, 2014.
- [201] Y. Xu, B. Chen, W. Qian, and H. Li, "Properties of pure n-butylammonium nitrate ionic liquid and its binary mixtures of with alcohols at T=(293.15 to 313.15) K," *J. Chem. Thermodyn*, vol. 58, pp. 449–459, 2013.
- [202] R. Miller, A. Hofmann, R. Hartmann, A. Halbig, and K.-H. Schano, "Measuring dynamic surface and interfacial tensions," *Adv. Mater.*, vol. 4, no. 5, pp. 370–374, 1992.
- [203] T. Méndez-Morales, J. Carrete, S. Bouzón-Capelo, M. Perez-Rodríguez, O. Cabeza, L. J. Gallego, and L. M. Varela, "MD simulations of the formation of stable clusters in mixtures of alkaline salts and imidazolium-based ionic liquids," *J. Phys. Chem. B*, vol. 117, no. 11, pp. 3207–3220, 2013.
- [204] O. Redlich and A. Kister, "Algebraic representation of thermodynamic properties and the classification of solutions," *Industrial & Engineering Chemistry*, vol. 40, no. 2, pp. 345–348, 1948.
- [205] P. R. Bevington and D. K. Robinson, "Data reduction and error analysis for the physical sciences," 1992.
- [206] E. Bodo, S. Mangialardo, F. Capitani, L. Gontrani, F. Leonelli, and P. Postorino, "Interaction of a long alkyl chain protic ionic liquid and water," *J. Chem. Phys.*, vol. 140, no. 20, p. 204503, 2014.

- [207] B. Docampo-Álvarez, V. Gómez-González, T. Méndez-Morales, J. Carrete, J. R. Rodríguez, O. Cabeza, L. J. Gallego, and L. M. Varela, "Mixtures of protic ionic liquids and molecular cosolvents: A molecular dynamics simulation," *J. Chem. Phys.*, vol. 140, no. 21, p. 214502, 2014.
- [208] M. Hadded, M. Biquard, P. Letellier, and R. Schaal, "Propriétés volumiques du nitrate d'éthylammonium fondu à 298 K et de ses mélanges avec l'eau," *Can. J. Chemistry*, vol. 63, no. 3, pp. 565–570, 1985.
- [209] R. Zarrougui, M. Dhahbi, and D. Lemordant, "Transport and thermodynamic properties of ethylammonium nitrate–water binary mixtures: effect of temperature and composition," *J. Solution Chem.*, vol. 44, no. 3-4, pp. 686–702, 2015.
- [210] Y. Xu, "Volumetric, viscosity, and electrical conductivity properties of aqueous solutions of two n-butylammonium-based protic ionic liquids at several temperatures," *J. Chem. Thermodyn.*, vol. 64, pp. 126–133, 2013.
- [211] A.-L. Rollet, P. Porion, M. Vaultier, I. Billard, M. Deschamps, C. Bessada, and L. Jouvensal, "Anomalous diffusion of water in [bmim][tfsi] room-temperature ionic liquid," *J. Phys. Chem. B*, vol. 111, no. 41, pp. 11888–11891, 2007.
- [212] T. Welton, "Ionic liquids in catalysis," *Coord. Chem. Rev.*, vol. 248, no. 21, pp. 2459–2477, 2004.
- [213] J. L. Anthony, J. L. Anderson, E. J. Maginn, and J. F. Brennecke, "Anion effects on gas solubility in ionic liquids," *J. Phys. Chem. B*, vol. 109, no. 13, pp. 6366–6374, 2005.
- [214] R. Hayes, S. Imberti, G. G. Warr, and R. Atkin, "The nature of hydrogen bonding in protic ionic liquids," *Angew. Chem. Int. Ed.*, vol. 52, no. 17, pp. 4623–4627, 2013.

- [215] H. Bekker, H. Berendsen, E. Dijkstra, S. Achterop, R. Van Drunen, D. Van der Spoel, A. Sijbers, H. Keegstra, B. Reitsma, and M. Renardus, "GROMACS: A parallel computer for molecular dynamics simulations," in *Phys. Comput.*, vol. 92, pp. 252–256, 1993.
- [216] D. Van Der Spoel, E. Lindahl, B. Hess, G. Groenhof, A. E. Mark, and H. J. Berendsen, "GROMACS: fast, flexible, and free," *J. Comput. Chem.*, vol. 26, no. 16, pp. 1701–1718, 2005.
- [217] J. Choe, K. Kim, and S. Chang, "Computer simulations on molecular recognition of alkylamines by ester derivatives of p-tert-butylcalix[6]arene," *Bull. Korean Chem. Soc.*, vol. 21, no. 2, pp. 200–206, 2000.
- [218] M. Parrinello and A. Rahman, "Polymorphic transitions in single crystals: A new molecular dynamics method," *J. Appl. Phys.*, vol. 52, no. 12, pp. 7182–7190, 1981.
- [219] M. Bamdad, S. Alavi, B. Najafi, and E. Keshavarzi, "A new expression for radial distribution function and infinite shear modulus of Lennard-Jones fluids," *Chem. Phys.*, vol. 325, no. 2, pp. 554–562, 2006.
- [220] J. Souto, M. Alemany, L. Gallego, L. González, and D. González, "Ab initio molecular dynamics study of the static, dynamic, and electronic properties of liquid Bi near melting using real-space pseudopotentials," *Phys. Rev. B*, vol. 81, no. 13, p. 134201, 2010.
- [221] R. P. Matthews, T. Welton, and P. A. Hunt, "Competitive pi interactions and hydrogen bonding within imidazolium ionic liquids," *Phys. Chem. Chem. Phys.*, vol. 16, no. 7, pp. 3238–3253, 2014.
- [222] M. Brehm and B. Kirchner, "TRAVIS - a free analyzer and visualizer for Monte Carlo and molecular dynamics trajectories," *J. Chem. Inf. Model.*, vol. 51, no. 8, pp. 2007–2023, 2011.

- [223] A. Luzar and D. Chandler, "Structure and hydrogen bond dynamics of water–dimethyl sulfoxide mixtures by computer simulations," *J. Chem. Phys.*, vol. 98, no. 10, pp. 8160–8173, 1993.
- [224] S. M. Urahata and M. C. Ribeiro, "Single particle dynamics in ionic liquids of 1-alkyl-3-methylimidazolium cations," *J. Chem. Phys.*, vol. 122, no. 2, p. 024511, 2005.
- [225] M. Ferrario, M. Haughney, I. R. McDonald, and M. L. Klein, "Moleculardynamics simulation of aqueous mixtures: Methanol, acetone, and ammonia," *J. Chem. Phys.*, vol. 93, no. 7, pp. 5156–5166, 1990.
- [226] L. Varela, J. Carrete, M. García, L. Gallego, M. Turmine, E. Rilo, and O. Cabeza, "Pseudolattice theory of charge transport in ionic solutions: Corresponding states law for the electric conductivity," *Fluid Phase Equilib.*, vol. 298, no. 2, pp. 280–286, 2010.
- [227] M. Egashira, S. Okada, and J.-i. Yamaki, "The effect of the coexistence of anion species in imidazolium cation-based molten salt systems," *Solid State Ion.*, vol. 148, no. 3, pp. 457–461, 2002.
- [228] A. Easteal and I. Hodge, "The electrical conductance of molten lead chloride and its mixtures with potassium chloride," *J. Phys. Chem.*, vol. 74, no. 4, pp. 730–735, 1970.
- [229] J. Picalek and J. Kolafa, "Molecular dynamics study of conductivity of ionic liquids: The Kohlrausch law," *J. Mol. Liq.*, vol. 134, no. 1, pp. 29–33, 2007.
- [230] K. R. Harris, "Relations between the fractional Stokes- Einstein and Nernst- Einstein equations and velocity correlation coefficients in ionic liquids and molten salts," *J. Phys. Chem. B*, vol. 114, no. 29, pp. 9572–9577, 2010.

- [231] Y.-C. Lee, J. Kolafa, L. A. Curtiss, M. A. Ratner, and D. F. Shriver, "Molten salt electrolytes. I. experimental and theoretical studies of LiI/AlCl₃," *J. Chem. Phys.*, vol. 114, no. 22, pp. 9998–10009, 2001.
- [232] B. Kirchner, F. Malberg, D. S. Firaha, and O. Hollóczki, "Ion pairing in ionic liquids," *J. Phys. Condens. Matter*, vol. 27, no. 46, p. 463002, 2015.
- [233] M. Salanne, C. Simon, P. Turq, and P. A. Madden, "Conductivity-viscosity-structure: unpicking the relationship in an ionic liquid," *J. Phys. Chem. B*, vol. 111, no. 18, pp. 4678–4684, 2007.
- [234] C. Schröder, M. Haberler, and O. Steinhauser, "On the computation and contribution of conductivity in molecular ionic liquids," *J. Chem. Phys.*, vol. 128, no. 13, p. 134501, 2008.
- [235] C. Schröder and O. Steinhauser, "On the dielectric conductivity of molecular ionic liquids," *J. Chem. Phys.*, vol. 131, no. 11, p. 114504, 2009.
- [236] R. Ren, Y. Zuo, Q. Zhou, H. Zhang, and S. Zhang, "Density, excess molar volume and conductivity of binary mixtures of the ionic liquid 1, 2-dimethyl-3-hexylimidazolium bis (trifluoromethylsulfonyl) imide and dimethyl carbonate," *J. Chem. Eng. Data*, vol. 56, no. 1, pp. 27–30, 2010.
- [237] J. Wang, A. Zhu, Y. Zhao, and K. Zhuo, "Excess molar volumes and excess logarithm viscosities for binary mixtures of the ionic liquid 1-butyl-3-methylimidazolium hexafluorophosphate with some organic compounds," *J. Solution Chem.*, vol. 34, no. 5, pp. 585–596, 2005.
- [238] J. Wang, H. Wang, S. Zhang, H. Zhang, and Y. Zhao, "Conductivities, volumes, fluorescence, and aggregation behavior of ionic liquids [C₄MIM][BF₄] and [C_nMIM]Br (n= 4, 6, 8, 10,

- 12) in aqueous solutions,” *J. Phys. Chem. B*, vol. 111, no. 22, pp. 6181–6188, 2007.
- [239] T. Singh and A. Kumar, “Aggregation behavior of ionic liquids in aqueous solutions: effect of alkyl chain length, cations, and anions,” *J. Phys. Chem. B*, vol. 111, no. 27, pp. 7843–7851, 2007.
- [240] Y. Zhao, S. Gao, J. Wang, and J. Tang, “Aggregation of ionic liquids [C_nMIM]Br (n= 4, 6, 8, 10, 12) in D₂O: A NMR study,” *J. Phys. Chem. B*, vol. 112, no. 7, pp. 2031–2039, 2008.
- [241] S. Dorbritz, W. Ruth, and U. Kragl, “Investigation on aggregate formation of ionic liquids,” *Adv. Synth. Catal.*, vol. 347, no. 9, pp. 1273–1279, 2005.
- [242] W. Zhao, F. Leroy, B. Heggen, S. Zahn, B. Kirchner, S. Balasubramanian, and F. Müller-Plathe, “Are there stable ion-pairs in room-temperature ionic liquids? Molecular dynamics simulations of 1-n-butyl-3-methylimidazolium hexafluorophosphate,” *J. Am. Chem. Soc.*, vol. 131, no. 43, pp. 15825–15833, 2009.
- [243] B. Docampo-Álvarez, V. Gómez-González, T. Méndez-Morales, J. R. Rodríguez, E. López-Lago, O. Cabeza, L. J. Gallego, and L. M. Varela, “Molecular dynamics simulations of mixtures of protic and aprotic ionic liquids,” *Phys. Chem. Chem. Phys.*, vol. 18, no. 34, pp. 23932–23943, 2016.
- [244] O. Hollóczki, F. Malberg, T. Welton, and B. Kirchner, “On the origin of ionicity in ionic liquids. ion pairing versus charge transfer,” *Phys. Chem. Chem. Phys.*, vol. 16, no. 32, pp. 16880–16890, 2014.
- [245] M. T. Clough, C. R. Crick, J. Gräsvik, P. A. Hunt, H. Niedermeyer, T. Welton, and O. P. Whitaker, “A physicochemical investigation of ionic liquid mixtures,” *Chem. Sci.*, vol. 6, no. 2, pp. 1101–1114, 2015.

- [246] K. Fumino, A.-M. Bonsa, B. Golub, D. Paschek, and R. Ludwig, "Non-ideal mixing behaviour of hydrogen bonding in mixtures of protic ionic liquids," *ChemPhysChem*, vol. 16, no. 2, pp. 299–304, 2015.
- [247] R. P. Matthews, I. J. Villar-Garcia, C. C. Weber, J. Griffith, F. Cameron, J. P. Hallett, P. A. Hunt, and T. Welton, "A structural investigation of ionic liquid mixtures," *Phys. Chem. Chem. Phys.*, vol. 18, no. 12, pp. 8608–8624, 2016.
- [248] R. Hayes, G. G. Warr, and R. Atkin, "Structure and nanostructure in ionic liquids," *Chem. Rev.*, vol. 115, no. 13, pp. 6357–6426, 2015.
- [249] J. H. Hildebrand, "A quantitative treatment of deviations from Raoult's law," *Proc. Natl. Acad. Sci. U.S.A.*, vol. 13, no. 5, pp. 267–272, 1927.
- [250] J. H. Hildebrand, "Solubility. XII. Regular solutions 1," *J. Am. Chem. Soc.*, vol. 51, no. 1, pp. 66–80, 1929.
- [251] J. Hildebrand and R. Scott, "Solutions of nonelectrolytes," *Annu. Rev. Phys. Chem.*, vol. 1, no. 1, pp. 75–92, 1950.
- [252] O. Kleppa and L. Hersh, "Heats of mixing in liquid alkali nitrate systems," *J. Chem. Phys.*, vol. 34, no. 2, pp. 351–358, 1961.
- [253] E. Guggenheim, "The theoretical basis of Raoult's law," *Trans. Far. Soc.*, vol. 33, pp. 151–156, 1937.
- [254] A. Bhatia and W. Hargrove, "Concentration fluctuations and thermodynamic properties of some compound forming binary molten systems," *Phys. Rev. B*, vol. 10, no. 8, p. 3186, 1974.
- [255] O. Akinlade and R. Singh, "Bulk and surface properties of liquid In–Cu alloys," *J Alloys Compd.*, vol. 333, no. 1, pp. 84–90, 2002.

- [256] J. C. Araque, J. J. Hettige, and C. J. Margulis, "Modern room temperature ionic liquids, a simple guide to understanding their structure and how it may relate to dynamics," *J. Phys. Chem. B*, vol. 119, no. 40, pp. 12727–12740, 2015.
- [257] A. A. Freitas, K. Shimizu, and J. N. Canongia Lopes, "Complex structure of ionic liquids. molecular dynamics studies with different cation–anion combinations," *J. Chem. Eng. Data*, vol. 59, no. 10, pp. 3120–3129, 2014.
- [258] M. G. Del Pópolo and G. A. Voth, "On the structure and dynamics of ionic liquids," *J. Phys. Chem. B*, vol. 108, no. 5, pp. 1744–1752, 2004.
- [259] B. Docampo-Álvarez, V. Gómez-González, H. Montes-Campos, J. M. Otero-Mato, T. Méndez-Morales, O. Cabeza, L. Gallego, R. M. Lynden-Bell, V. B. Ivaništšev, M. V. Fedorov, *et al.*, "Molecular dynamics simulation of the behaviour of water in nano-confined ionic liquid–water mixtures," *J. Phys. Condens. Matter*, vol. 28, no. 46, p. 464001, 2016.
- [260] G. Feng, X. Jiang, R. Qiao, and A. A. Kornyshev, "Water in ionic liquids at electrified interfaces: The anatomy of electrosorption," *ACS Nano*, vol. 8, no. 11, pp. 11685–11694, 2014.
- [261] V. Gómez-González, B. Docampo-Álvarez, J. M. Otero-Mato, O. Cabeza, L. J. Gallego, and L. M. Varela, "Molecular dynamics simulations of the structure of mixtures of protic ionic liquids and monovalent and divalent salts at the electrochemical interface," *Phys. Chem. Chem. Phys.*, vol. 20, no. 18, pp. 12767–12776, 2018.
- [262] V. Gómez-González, B. Docampo-Álvarez, H. Montes-Campos, J. C. Otero, E. L. Lago, O. Cabeza, L. J. Gallego, and L. M. Varela, "Solvation of Al^{3+} cations in bulk and confined protic ionic liquids: a computational study," *Phys. Chem. Chem. Phys.*, vol. 20, no. 28, pp. 19071–19081, 2018.

- [263] S. W. Coles, A. M. Smith, M. V. Fedorov, F. Hausen, and S. Perkin, "Interfacial structure and structural forces in mixtures of ionic liquid with a polar solvent," *Faraday Discuss.*, vol. 206, pp. 427–442, 2018.
- [264] J. Friedl, I. I. Markovits, M. Herpich, G. Feng, A. A. Kornyshev, and U. Stimming, "Interface between an Au (111) surface and an ionic liquid: The influence of water on the double-layer capacitance," *ChemElectroChem*, vol. 4, no. 1, pp. 216–220, 2017.
- [265] L. Timperman, F. Béguin, E. Frackowiak, and M. Anouti, "Comparative study of two protic ionic liquids as electrolyte for electrical double-layer capacitors," *J. Electrochem. Soc.*, vol. 161, no. 3, pp. A228–A238, 2014.
- [266] M. T. Alam, M. M. Islam, T. Okajima, and T. Ohsaka, "Electrical double layer in mixtures of room-temperature ionic liquids," *J. Phys. Chem. C*, vol. 113, no. 16, pp. 6596–6601, 2009.
- [267] R. Costa, C. M. Pereira, and F. Silva, "Electric double layer studies at the interface of mercury–binary ionic liquid mixtures with a common anion," *RSC Adv.*, vol. 3, pp. 11697–11706, 2013.
- [268] L. Siinor, J. Poom, C. Siimenson, K. Lust, and E. Lust, "Electrochemical characteristics pyrolytic graphite | mixture of 1-ethyl-3-methylimidazolium tetrafluoroborate and 1-ethyl-3-methylimidazolium iodide interface," *J. Electroanal. Chem.*, vol. 719, p. 133–137, 2014.
- [269] R. Costa, C. M. Pereira, and A. F. Silva, "Structural ordering transitions in ionic liquids mixtures," *Electrochem. Commun.*, vol. 57, pp. 10–13, 2015.
- [270] C. Siimenson, M. Lembinen, O. Oll, L. Läll, M. Tarkanovskaja, V. Ivaništšev, L. Siinor, T. Thomberg, K. Lust,

- and E. Lust, "Electrochemical investigation of 1-ethyl-3-methylimidazolium bromide and tetrafluoroborate mixture at bi(111) electrode interface," *J. Electrochem. Soc.*, vol. 163, no. 9, pp. H723–H730, 2016.
- [271] L. Siinor, C. Siimenson, K. Lust, and E. Lust, "Mixture of 1-ethyl-3-methylimidazolium tetrafluoroborate and 1-ethyl-3-methylimidazolium iodide: A new potential high capacitance electrolyte for EDLCs," *Electrochem. Commun.*, vol. 35, pp. 5–7, 2013.
- [272] T. Tooming, T. Thomberg, L. Siinor, K. Tõnurist, A. Jänes, and E. Lust, "A type high capacitance supercapacitor based on mixed room temperature ionic liquids containing specifically adsorbed iodide anions," *J. Electrochem. Soc.*, vol. 161, no. 3, pp. A222–A227, 2014.
- [273] Z. Lin, P.-L. Taberna, and P. Simon, "Graphene-based supercapacitors using eutectic ionic liquid mixture electrolyte," *Electrochim. Acta.*, vol. 206, pp. 446–451, 2016.
- [274] K. L. Van Aken, M. Beidaghi, and Y. Gogotsi, "Formulation of ionic-liquid electrolyte to expand the voltage window of supercapacitors," *Angew. Chem.*, vol. 127, no. 16, pp. 4888–4891, 2015.
- [275] B. Docampo-Álvarez, V. Gómez-González, T. Méndez-Morales, J. R. Rodríguez, O. Cabeza, M. Turmine, L. J. Gallego, and L. M. Varela, "The effect of alkyl chain length on the structure and thermodynamics of protic–aprotic ionic liquid mixtures: a molecular dynamics study," *Phys. Chem. Chem. Phys.*, vol. 20, no. 15, pp. 9938–9949, 2018.
- [276] R. J. Gowers, M. Linke, J. Barnoud, T. J. Reddy, M. N. Melo, S. L. Seyler, D. L. Dotson, J. Domanski, S. Buchoux, I. M. Kenney, *et al.*, "MDAnalysis: a python package for the rapid analysis of molecular dynamics simulations," in *Proceedings*

- of the 15th Python in Science Conference*, pp. 98–105, SciPy, 2016.
- [277] A. J. Bard, L. R. Faulkner, J. Leddy, and C. G. Zoski, *Electrochemical methods: fundamentals and applications*. Wiley New York, 1980.
- [278] J. Vatamanu, O. Borodin, and G. D. Smith, “Molecular dynamics simulations of atomically flat and nanoporous electrodes with a molten salt electrolyte,” *Phys. Chem. Chem. Phys.*, vol. 12, no. 1, pp. 170–182, 2010.
- [279] A. J. Page, A. Elbourne, R. Stefanovic, M. A. Addicoat, G. G. Warr, K. Voitchovsky, and R. Atkin, “3-dimensional atomic scale structure of the ionic liquid–graphite interface elucidated by AM-AFM and quantum chemical simulations,” *Nanoscale*, vol. 6, no. 14, pp. 8100–8106, 2014.
- [280] A. Elbourne, K. Voitchovsky, G. G. Warr, and R. Atkin, “Ion structure controls ionic liquid near-surface and interfacial nanostructure,” *Chem. Sci.*, vol. 6, no. 1, pp. 527–536, 2015.
- [281] M. Z. Bazant, B. D. Storey, and A. A. Kornyshev, “Double layer in ionic liquids: Overscreening versus crowding,” *Phys. Rev. Lett.*, vol. 106, no. 4, p. 046102, 2011.
- [282] N. Otsu, “A threshold selection method from gray-level histograms,” *IEEE Trans. Syst. Man Cyber.*, vol. 9, no. 1, pp. 62–66, 1979.
- [283] H. Montes-Campos, J. M. Otero-Mato, T. Méndez-Morales, E. López-Lago, O. Russina, O. Cabeza, L. J. Gallego, and L. M. Varela, “Nanostructured solvation in mixtures of protic ionic liquids and long-chained alcohols,” *J. Chem. Phys.*, vol. 146, no. 12, p. 124503, 2017.
- [284] K. Mecke, “Morphological characterization of patterns in reaction-diffusion systems,” *Phys. Rev. E*, vol. 53, no. 5, p. 4794, 1996.

- [285] L. M. Varela, M. García, and V. Mosquera, “Exact mean-field theory of ionic solutions: non-Debye screening,” *Phys. Rep.*, vol. 382, no. 1-2, pp. 1–111, 2003.



List of Tables

2.1	Simulation box width (in nm) and number of IL pairs, water molecules, and electrode C atoms.	52
2.2	Average energies for anions and cations ($\langle E_{\text{ion}} \rangle$) in the first surface layer along the z -axis for the non-confined ($L = 11.42$ nm) pure IL and 5% IL-water mixture.	57
2.3	Fitted values for the depth of the potential energy well (ΔE) near neutral and charged surfaces in Figure 2.16. The mean integral value of the water PMF near each graphene sheet (E_{PMF}) for $L = 11.42$ nm is provided for comparison.	63
2.4	Provenance, mass fraction purity and impurities of PILs .	71
2.5	Physical properties of pure materials at 298.15 K and 101 kPa. ^a	72
2.6	Densities and refractive indexes of binary mixtures of $\{x_1$ ionic liquid + x_2 water} and $\{x_1$ ionic liquid + x_2 ethanol} at 298.15 K and 101 kPa. ^a	74
2.7	Fitted coefficients and standard deviation for Redlich-Kister equation.	76
2.8	Percentile standard deviation, s%, given by equation (5) obtained with the model Gladstone-Dale to reproduce values of the refractive index.	79
2.9	Surface tension (in $N \cdot m^{-1}$) of binary mixtures of $\{x_1$ ionic liquid + x_2 water} and $\{x_1$ ionic liquid + x_2 ethanol} at 298.15 K and 101 kPa. ^a	80

2.10	[EA] ⁺ -[NO ₃] ⁻ hydrogen bonds per EAN pair for different concentrations and the corresponding percentages of the pure EAN value.	106
2.11	Experimental values of electrical conductivity of the studied mixtures at 298.15 K.	115
2.12	Data on the simulation boxes prepared for each system. Calculated diffusion coefficients, in 10 ⁻⁸ cm ² /s, are also included for each of the ionic species.	122
2.13	Minkowski parameters for the anion surface maps found near neutral surfaces with pure [BMIM] [BF ₄] and its mixtures with EAN.	160



List of Figures

1.1	Examples of commonly found IL cations and anions. Figure taken from Ref. 5.	8
1.2	Diagram with different commonly employed simulation methods showing the size and time scales they are commonly used for.	13
1.3	Depiction of the leap-frog integration method. Figure taken from Ref. 91	16
2.1	Simulated (solid symbols) and experimental (open symbols) densities at $T = 298.15$ K of EAN mixed with water (circles), ethanol (triangles) and methanol (squares).	28
2.2	Water concentration dependence of water-water (a), water-cation (b) and water-anion (c) rdfs in aqueous EAN mixtures at 298.15 K and 1 atm.	29
2.3	Cosolvent concentration dependence of anion-cation rdfs for EAN at 298.15 K and 1 atm.	30
2.4	Water concentration dependence of the relative heights of water-water (circles) and cation-anion (squares) in mixtures with EAN at 298.15 K and 1 atm.	31
2.5	Alcohol concentration dependence of alcohol-anion (a,b), alcohol-cation (c,d) and alcohol-alcohol (e,f) rdfs in ethanol and methanol mixtures with EAN at 298.15 K and 1 atm.	33

2.6	Coordination numbers of water (a), ethanol (b) and methanol (c) in mixtures with EAN at 298.15 K. The lines are guides to the eye.	37
2.7	Concentration dependence of the average number of cosolvent-cosolvent (a), cation-anion (b), cosolvent-cation (c) and cosolvent-anion (d) hydrogen bonds per molecule for mixtures with EAN at 298.15 K. The lines are guides to the eye.	38
2.8	Spatial distribution functions of water (a,b), ethanol (c,d) and methanol (e,f) around anions in mixtures with EAN at 298.15 K. The pictures on the left column correspond to a concentration of 25% and those on the right to 85% .	40
2.9	Concentration dependence of water (a), ethanol (b) and methanol (c) vacfs in solutions with EAN. The insets show the evolution of the collision time with the concentration of cosolvent molecules. The statistical uncertainties of $C(t)$ in the time intervals of the insets are expected to be less than 10^{-4}	41
2.10	Snapshot showing the 10.04 nm simulation box with charged walls; red: cation atoms; blue: anion atoms; green: water molecules. The latter are slightly enlarged for clarity purposes.	52
2.11	Density profiles for anion (offset by 20 nm^{-3}), cation (offset by 20 nm^{-3}), cation tail and water molecule (solid curve, magnified by 5) in systems with different distance between the graphene sheets (L). (A) system with neutral graphene sheet situated as $z = 0$ and $z = L = 1.70 \text{ nm}$; (B)–(D) systems with a positively charged graphene sheet situated at $z = 0 \text{ nm}$ and a negatively charged graphene sheet situated at $z = L$	53

- 2.12 PMF profiles of water molecules as a function of distance from the positively, neutral and negatively charged surfaces, for confined ($L = 3.06$ nm) and non-confined ($L = 11.42$ nm) cases. The background represent the number density profiles for anion and cation represented as gradients of semi-transparent blue (darker) and red (lighter) colours, respectively. 55
- 2.13 Density map of anions (blue, darker) and cations (red, lighter) within 0.5 nm of a positively charged surface in absence of and with 5% of water (green, light). The overlaid hexagons highlight the change in the ions arrangement at the interface. 58
- 2.14 Frequency distribution for $\cos \theta$ of water orientation in the first layer near charged surfaces for $L = 3.06$ nm. The angle θ is taken as the one between the molecular dipole moment and the surface's normal vector. Bars represent 0.1 wide intervals of cosine values. 59
- 2.15 Vibrational density of states for water molecules near the graphene sheets, with solid lines for the confined ($L = 3.06$ nm) and dashed lines for the non-confined ($L = 11.42$ nm) IL–water mixtures. Lines with filled area represent the data for water molecules in the non-confined bulk. The arrow indicates the blue shift in the vibrational density of states. 60
- 2.16 Difference in the interfacial water fraction vs. distance between the graphene sheets (L). Higher values indicate adsorption. The lines show the respective fit to Eq. 2.8. 62
- 2.17 Experimental density data, ρ , at $T = 298.15$ K of the binary systems composed of: a) $\blacklozenge \{x_1 \text{ EAN} + x_2 \text{ water}\}$, $\bullet \{x_1 \text{ PAN} + x_2 \text{ water}\}$ and $\blacktriangle \{x_1 \text{ BAN} + x_2 \text{ water}\}$. b) $\diamond \{x_1 \text{ EAN} + x_2 \text{ ethanol}\}$, $\circ \{x_1 \text{ PAN} + x_2 \text{ ethanol}\}$ and $\triangle \{x_1 \text{ BAN} + x_2 \text{ ethanol}\}$. The black symbols correspond to experimental densities and the blue ones correspond to the simulated densities at 298.15 K. 75

- 2.18 Excess molar volumes data, V_m^E at $T = 298.15$ K of the binary systems composed of, \blacklozenge $\{x_1 \text{ EAN} + x_2 \text{ water}\}$, \bullet $\{x_1 \text{ PAN} + x_2 \text{ water}\}$, \blacktriangle $\{x_1 \text{ BAN} + x_2 \text{ water}\}$, \diamond $\{x_1 \text{ EAN} + x_2 \text{ ethanol}\}$, \circ $\{x_1 \text{ PAN} + x_2 \text{ ethanol}\}$ and \triangle $\{x_1 \text{ BAN} + x_2 \text{ ethanol}\}$. Lines represent the fittings obtained by the Redlich-Kister equation. 77
- 2.19 Experimental refractive index, n_D , at $T = 298.15$ K of the binary systems composed of: a) \diamond $\{x_1 \text{ EAN} + x_2 \text{ water}\}$, \circ $\{x_1 \text{ PAN} + x_2 \text{ water}\}$, \triangle $\{x_1 \text{ BAN} + x_2 \text{ water}\}$, and b) \diamond $\{x_1 \text{ EAN} + x_2 \text{ ethanol}\}$, \circ $\{x_1 \text{ PAN} + x_2 \text{ ethanol}\}$, \triangle $\{x_1 \text{ BAN} + x_2 \text{ ethanol}\}$. The solid symbols correspond to the values obtained using Gladstone-Dale model. 79
- 2.20 Experimental surface tension data, ρ , at $T = 298.15$ K of, \blacklozenge $\{x_1 \text{ EAN} + x_2 \text{ water}\}$, \bullet $\{x_1 \text{ PAN} + x_2 \text{ water}\}$, \blacktriangle $\{x_1 \text{ BAN} + x_2 \text{ water}\}$, \diamond $\{x_1 \text{ EAN} + x_2 \text{ ethanol}\}$, \circ $\{x_1 \text{ PAN} + x_2 \text{ ethanol}\}$ and \triangle $\{x_1 \text{ BAN} + x_2 \text{ ethanol}\}$ 81
- 2.21 Radial distribution functions for EAN (left column), PAN (central column), and BAN (right column) in mixtures with water (blue) and ethanol (red). Dashed lines show values for a 25% molar percentage of cosolvent, while continuous lines correspond to 75% concentrations. Figures (a,b,c) show anion-solvent distribution functions; (d,e,f) the solvent and the terminal carbon of the cation alkyl chain; and (g,h,i) solvent-solvent pairs. 83
- 2.22 Snapshot of MD simulations of BAN + ethanol mixture. $[\text{BA}]^+$ head is shown in red, $[\text{BA}]^+$ organic tail in green, $[\text{NO}_3]^-$ in blue, OH group in cyan and tail of ethanol in grey. 84
- 2.23 Schematic figure of the surface structure of the mixtures: orientation of the alkyl chains as a function of the mole fraction in PIL. On the left, the region rich in water is shown in blue and the region rich in PIL is in green. On the right, the region rich in ethanol is shown in yellow and the region rich in PIL is in green. 85
- 2.24 (a) $[\text{EMIM}][\text{BF}_4]$, (b) EAN. 93

2.25	Comparison of the MD simulated (red) and experimental (black) densities of the studied mixtures. The inset shows the corresponding excess molar volumes calculated by means of Eq. 2.16. The dotted line represents ideal mixture behaviour and is included as a guide to the eye.	96
2.26	[EMIM] ⁺ -[BF ₄] ⁻ radial distribution function at different EAN concentrations.	99
2.27	[EA] ⁺ -[NO ₃] ⁻ radial distribution function at different EAN concentrations.	100
2.28	Partial structure factors for [EMIM] ⁺ -[BF ₄] ⁻ (top) and [EA] ⁺ -[NO ₃] ⁻ (bottom) for mixtures with different EAN concentrations.	101
2.29	Atomic radial distribution functions for the hydrogen atoms in the [EMIM] ⁺ ring as shown in Figure 2.24: (a) shows the hydrogen between both nitrogen atoms in the ring (H1), (b) H2, (c) H3. In each case, solid lines correspond to [BF ₄] ⁻ fluorine atoms and dashed lines to [NO ₃] ⁻ oxygen atoms. EAN concentrations shown are 20% (blue), 50% (black) and 80% (red).	102
2.30	Spatial distribution functions around imidazolium rings, highlighting high occupancy regions for [EMIM] ⁺ (red), BF ₄ ⁻ (light and dark blue) and NO ₃ ⁻ (green) for EAN concentrations of 10% (a), 50% (b), and 90% (c). Red regions and light blue regions correspond to local densities 2.5 times higher than their average values in the bulk for the corresponding species, while dark blue and green show those regions with densities 5 times higher than the corresponding bulk averages.	103
2.31	Coordination numbers for anions around both cations. Dashed lines represent the total averaged number of anions around [EA] ⁺ (black) and [EMIM] ⁺ (red).	105
2.32	Vibrational density of states of [EMIM] ⁺ cations for different EAN concentrations.	108
2.33	Vibrational density of states of [EA] ⁺ cations for different EAN concentrations.	109

2.34	Mean squared displacement (MSD) curves for [EMIM] ⁺ ions at different EAN concentrations. The dotted line represents the unit slope line.	110
2.35	Diffusion coefficients for the different ionic species in the mixtures. Error bars correspond to two standard deviations.	111
2.36	Experimental conductivity measurements at 298.15 K (black) of [EMIM]-EAN mixtures and conductivity data obtained from MD simulation using Eq. 2.22 (red) and a fit to current data (blue). All sets of data have been normalized with respect to the values for pure [EMIM][BF ₄]. The dashed line represents the simple, linear mixing rule $\sigma = x_{EAN}\sigma_{EAN} + (1 - x_{EAN})\sigma_{[EMIM][BF_4]}$	113
2.37	Densities for mixtures studied along the entire concentration range. Dashed lines represent simulation data, while points correspond to experimental measurements. Below, excess molar volumes, with their corresponding error bars.	124
2.38	Excess enthalpies for the studied mixtures. Dashed lines show the corresponding fit to the subregular mixture model.	125
2.39	Radial distribution functions of [BF ₄] ⁻ anions around the terminal carbon atom of [EA] ⁺ and [BA] ⁺ cations for selected concentrations of each of the different systems. .	126
2.40	Spatial distribution functions for different species around alkylammonium cations for [EMIM][BF ₄] + EAN (top) and [EMIM][BF ₄] + BAN (bottom), for the pure protic liquid (left) and at concentrations of 90% (right). Imidazolia are represented in red, [EA] ⁺ and [BA] ⁺ in orange, [BF ₄] ⁻ in blue, and [NO ₃] ⁻ in purple.	128
2.41	Spatial distribution functions for different species around imidazolium cations for [EMIM][BF ₄] + EAN (top) and [BMIM][BF ₄] + EAN (bottom), at concentrations of 20% (left) and 50% (right). Imidazolia are represented in red, [EA] ⁺ in orange, [BF ₄] ⁻ in blue, and [NO ₃] ⁻ in purple. .	129
2.42	Hydrogen bonds between ions of the protic component in each mixture.	132

- 2.43 Coordination numbers of all anions around each of the protic cations, with each mixture shown in a different colour: [EMIM][BF₄] + EAN in black, [EMIM][BF₄] + PAN in green and [EMIM][BF₄] + BAN in blue. 133
- 2.44 Total structure factor for selected [EMIM][BF₄] - EAN, [BMIM][BF₄] - EAN and [EMIM][BF₄] - BAN mixtures. 134
- 2.45 Polar-polar, polar-apolar and apolar-apolar partial structure factors for [EMIM][BF₄] - EAN, [BMIM][BF₄] - EAN and [EMIM][BF₄] - BAN mixtures. 135
- 2.46 Percentage of protic cations (top) and aprotic cations (bottom) located in small clusters (less than half the total number of cations of the respective species). 138
- 2.47 Velocity autocorrelation functions of [EA]⁺ and [BA]⁺ cations in EAN - [EMIM][BF₄] (left), EAN - [BMIM][BF₄] (centre) and BAN - [EMIM][BF₄] (right) mixtures for selected concentrations. 139
- 2.48 Mean squared displacement of [EMIM]⁺ and [BMIM]⁺ cations in EAN - [EMIM][BF₄] (left), EAN - [BMIM][BF₄] (centre) and BAN - [EMIM][BF₄] (right) mixtures for selected concentrations. 142
- 2.49 Experimental conductivity results at 298.15 K for the studied systems as well as simulation predictions using Kohlrausch's law (dashed line). Both sets have been normalized to the values for pure [EMIM][BF₄]. 144
- 2.50 Number densities for the different species in [BMIM][BF₄]+BAN mixtures near neutral graphene surfaces (left), and positively and negatively charged surfaces (middle and right, respectively). 155
- 2.51 Cumulative number density of both anion species near negatively charged surfaces for different [BMIM][BF₄] + BAN mixtures. $z = 0$ corresponds to the position of the negative electrode. 157

2.52	Surface distribution of ions in pure [EMIM] [BF ₄] (left) and its mixture with 10% EAN (right) near the positive electrode. [EMIM] ⁺ in red, [BF ₄] ⁻ in blue, [EA] ⁺ in orange, and [NO ₃] ⁻ in sky blue.	160
2.53	Surface distribution of ions in pure [BMIM] [BF ₄] (left) and its mixture with 10% EAN (right) near a neutral surface. [BMIM] ⁺ in red, [BF ₄] ⁻ in blue, [EA] ⁺ in orange, and [NO ₃] ⁻ in sky blue.	161
2.54	Surface distribution of polar (yellow) and apolar (green) domains in pure BAN (left) and its mixture with 10% [EMIM] [BF ₄] (right) near neutral surfaces.	162
2.55	Surface distribution of ions in equimolar mixtures of [EMIM] [BF ₄] and EAN (top) and BAN (bottom) near positively charged electrodes. The color codes in the left column are the same used in Fig. 2.53. The middle column highlights, for the same picture, anions (blue) and cations (red), while the right column shows protic/aprotic components (green and red).	163
2.56	Integral capacitance curves as a function of PIL concentration for positively (top) and negatively (bottom) charged electrodes in all systems studied.	164



List of publications related to this thesis

- **Mixtures of protic ionic liquids and molecular cosolvents: A molecular dynamics simulation**, Borja Docampo-Álvarez, Víctor Gómez-González, Trinidad Méndez-Morales, Jesús Carrete, Julio R. Rodríguez, Oscar Cabeza, Luis J. Gallego, & Luis M. Varela, *J. Chem. Phys.*, **140**(21), 214502 (2014).
- **Solvation of molecular cosolvents and inorganic salts in ionic liquids: a review of molecular dynamics simulations**, L.M. Varela, T. Méndez-Morales, J. Carrete, V. Gómez-González, B. Docampo-Álvarez, L.J. Gallego, O. Cabeza, & O. Russina, *J. Mol. Liq.*, **210**, 178 (2015).
- **Molecular dynamics simulations of mixtures of protic and aprotic ionic liquids**, Borja Docampo-Álvarez, Víctor Gómez-González, Trinidad Méndez-Morales, Julio R. Rodríguez, Elena López-Lago, Oscar Cabeza, Luis J. Gallego, & Luis M. Varela, *Phys. Chem. Chem. Phys.*, **18**(34), 23932 (2016).
- **Molecular dynamics simulation of the behaviour of water in nano-confined ionic liquid–water mixtures**, Borja Docampo-Álvarez, Víctor Gómez-González, Hadrián Montes-Campos, José M. Otero-Mato, Trinidad Méndez-Morales, Oscar Cabeza, L.J. Gallego, Ruth M. Lynden-Bell, Vladislav B. Ivaništšev, Maxim V. Fedorov, & Luis M. Varela, *J. Phys. Condens. Matter*, **28**(46), 464001 (2016).
- **Surface and bulk characterisation of mixtures containing alkylammonium nitrates and water or ethanol: Experimental and simulated properties at 298.15 K**, Luisa Segade, Manuel Cabanas, Montserrat Domínguez-Pérez, Esther Rilo, Sandra García-Garabal, Mireille Turmine, Luis M. Varela, Víctor Gómez-González, Borja Docampo-Alvarez, & Oscar Cabeza, *J. Mol. Liq.*, **222**, 663 (2016).

- **The effect of alkyl chain length on the structure and thermodynamics of protic–aprotic ionic liquid mixtures: a molecular dynamics study**, Borja Docampo-Álvarez, Víctor Gómez-González, Trinidad Méndez-Morales, Julio R. Rodríguez, Oscar Cabeza, Mireille Turmine, Luis J. Gallego, & Luis M. Varela, *Phys. Chem. Chem. Phys.*, **20**(15), 9938 (2018).
- **Langevin behavior of the dielectric decrement in ionic liquid water mixtures**, Esther Heid, Borja Docampo-Álvarez, Luis M Varela, Konstantin Prosenz, Othmar Steinhauser, Christian Schröder, *Phys. Chem. Chem. Phys.*, **20**(22), 15106-15117 (2018).
- **Molecular dynamics simulations of the structure and single-particle dynamics of mixtures of divalent salts and ionic liquids**, Víctor Gómez-González, Borja Docampo-Álvarez, Oscar Cabeza, Maxim Fedorov, Ruth M. Lynden-Bell, Luis J. Gallego, & Luis M. Varela, *J. Chem. Phys.*, **143**(12), 124507 (2015).
- **Molecular dynamics simulation of the structure and interfacial free energy barriers of mixtures of ionic liquids and divalent salts near a graphene wall**, Víctor Gómez-González, Borja Docampo-Álvarez, Trinidad Méndez-Morales, Oscar Cabeza, Vladislav B. Ivaništšev, Maxim V. Fedorov, Luis J. Gallego, & Luis M. Varela, *Phys. Chem. Chem. Phys.*, **19**(1), 846 (2017).
- **Molecular dynamics simulations of the structure of mixtures of protic ionic liquids and monovalent and divalent salts at the electrochemical interface**, Víctor Gómez-González, Borja Docampo-Álvarez, J. Manuel Otero-Mato, Oscar Cabeza, Luis J. Gallego, & Luis M. Varela, *Phys. Chem. Chem. Phys.*, **20**(18), 12767 (2018).
- **Solvation of Al³⁺ cations in bulk and confined protic ionic liquids: a computational study**, Víctor Gómez-González, Bor-

ja Docampo-Álvarez, Hadrián Montes-Campos, Juan Carlos Otero, Elena López Lago, Oscar Cabeza, Luis J. Gallego, & Luis M. Varela, *Phys. Chem. Chem. Phys.*, **20** 19071, (2018).





